



Interim Report

IR-03-009

The Radioactive Legacy of the Russian Pacific Fleet Operations and its Potential Impact on Neighboring Countries

Edited by:

K. L. Compton (compton@iiasa.ac.at)
V. M. Novikov (novikov@iiasa.ac.at)
F. L. Parker (parkerfl@vuse.vanderbilt.edu)
Yu. V. Sivintsev (yury@quest.net.kiae.su)

Contributing Authors:

T. Banba
K. L. Compton
V. A. Danilyan
V. I. Kobzev
S. A. Lavkovsky
N. I. Lysenko
A. Mahura
A. A. Maksimov
V. Mordashov
V. M. Novikov
F. L. Parker
A. Pechkurov
B. G. Pologich
V. Romanova
Yu. V. Sivintsev
M. Takano
V. L. Visotsky

Approved by

Frank L. Parker (parkerfl@vuse.vanderbilt.edu)
Project Leader, Radiation Safety of the Biosphere Project

June 2003

Contents

List of Figures.....	iv
List of Tables.....	vi
1 Introduction	1
2 Background: Facilities and Source Terms.....	4
2.1 Primorye Territory.....	4
2.1.1 Pavlovsk Bay Naval Base.....	4
2.1.2 Bolshoi Kamen and the Far Eastern Plant Zvezda	15
2.1.3 Chazhma Bay Ship Repair Facility	21
2.1.4 Razboinik Bay Naval Station	21
2.1.5 Cape Sysoeva Naval Waste Facility.....	22
2.2 Kamchatka Oblast.....	24
2.2.1 Seldevaya Bay Naval Shipyard	26
2.2.2 Kamchatka Refuelling and Waste Management Facility	26
2.2.3 Rybachy Naval Base.....	29
2.3 Spent Fuel Storage Characteristics	30
2.3.1 Shore Based Storage in Transport Casks.....	30
2.3.2 Project 326 Class Floating Workshops.....	31
2.3.3 Project 326M Class Floating Workshops	32
2.3.4 Project 2020 (“Malina”) Class Floating Workshops	32
2.4 Conclusions	33
3 Transboundary Atmospheric Transport.....	35
3.1 Climactic Settings.....	35
3.2 Probability of Transport: Trajectory Analyses	39
3.2.1 Methodology.....	40
3.2.2 Results And Discussion.....	43
3.2.3 Conclusions	54
3.3 Case Study: Atmospheric Transport and Deposition to Japan from an Accident in Southern Primorye Territory	55

3.3.1	Brief Description of WSPEEDI.....	55
3.3.2	Wind Field Analysis for January 1997	56
3.3.3	Analysis of the Results	57
3.3.4	Parametric Study	62
3.3.5	Dose Assessment	63
3.3.6	Conclusions and Discussions	65
4	Consequence Assessment.....	66
4.1	Methodology.....	67
4.1.1	Selection of Critical Deposition Level	68
4.1.2	Selection of Atmospheric Transfer Factor.....	69
4.1.3	Critical Release and Critical Release Factor	71
4.2	Release Fractions from Severe Accidents	72
4.2.1	Identification of Potential Accidents	74
4.3	Data.....	77
4.3.1	Selection of Target Region	77
4.3.2	Critical Deposition Level.....	77
4.3.3	Determination of Atmospheric Transfer Coefficient	78
4.4	Results	79
5	Conclusions and Recommendations.....	84
5.1	Conclusions	84
5.1.1	Source Term	84
5.1.2	Transport and Consequence Analysis	86
5.2	Recommendations	87
6	References	88

List of Figures

Figure 1-1: Naval nuclear facilities in the Russian Far East (from OTA, 1995).....	2
Figure 2-1: Primorye Territory (inset shows naval facilities) Map source: www.expedia.com	5
Figure 2-2: Pavlovsk Bay Naval Base (adapted from Danilyan et al, 2000b).....	6
Figure 2-3: Three-compartment unit alongside a decommissioned Victor Class SSN at Pavlovsk Bay. The vessels are now stored at Razboinik Bay. (Handler, 1995. Photo credit: J. Handler).....	6
Figure 2-4: TNT-27 underway in the Sea of Japan in October 1993 (Handler, 1995. Photo credit: J. Handler).....	14
Figure 2-5: Far Eastern Plant Zvezda(adapted from Danilyan et al., 2000b).....	15
Figure 2-6: Project 2020 (“Malina”) Class Floating Workshop (Bellona, 1996).....	17
Figure 2-7: The Project 11510 class technological tanker "Amur", sister ship to the "Pinega" (Bellona, 1996).....	18
Figure 2-8: PEK-50 floating LRW storage at the Far Eastern Plant Zvezda (Handler, 1995. Photo credit: J. Handler).....	20
Figure 2-9: Cape Sysoeva Waste Management Facility (adapted from Danilyan et al, 2000b).....	22
Figure 2-10: Map of Kamchatka Oblast (inset shows naval facilities) (map source: www.expedia.com).....	25
Figure 3-1a: January Sea Surface Pressure (image source: http://www.cdc.noaa.gov/cgi-bin/DataMenu.pl?stat=mon.ltm&dataset=NCEP). 36	
Figure 3-1b: July Sea Surface Pressure (image source: http://www.cdc.noaa.gov/cgi-bin/DataMenu.pl?stat=mon.ltm&dataset=NCEP)	37
Figure 3-2: Geographical impact regions	41
Figure 3-3: Examples of trajectories	42
Figure 3-4: Monthly variations in the average atmospheric transport time (in days) to specified regions based on the forward trajectories during 1987-1996.....	46
Figure 3-5: Monthly variations in the number of trajectories originating at lower altitudes within the boundary layer in Kamchatka Oblast and reaching the specified regions during 1987-1996.....	47
Figure 3-6: Monthly variations in the number of trajectories originating at lower altitudes within the boundary layer in southern Primorye Territory and reaching the specified regions during 1987-1996	48
Figure 3-7: Atmospheric transport pathways (cluster mean trajectories) from the Kamchatka NRS region based on the forward trajectories during 1987-1996.....	49

Figure 3-8: Atmospheric transport pathways (cluster mean trajectories) from the Vladivostok NRS region based on the forward trajectories during 1987-1996	49
Figure 3-9: Airflow probability field within the boundary layer for the trajectories during 1987-1996 (isolines are shown every 5 units)	51
Figure 3-10: Typical atmospheric transport time fields for the trajectories during 1987-1996	52
Figure 3-11: Fast boundary layer transport (one day) probability field for trajectories during 1987-1996 (isolines are shown every 10 units)	54
Figure 3-12: Typical Wind Patterns in January 1997	57
Figure 3-13: Atmospheric Concentrations under Strong North Wind Conditions	59
Figure 3-14: Atmospheric Concentrations under Weak North Wind Conditions	60
Figure 3-15: Atmospheric Concentrations under Cyclonic Wind Conditions	61
Figure 3-16: Total Ground Deposition for a Unit Release (Bq/m ² per Bq released) ...	62

List of Tables

Table 2-1: Isotopic inventory of typical submarine reactor core three years after shutdown (assumed burnup 42 GWd) (<i>Lysenko et al. (2002)</i>).....	7
Table 2-2: Estimated radioactive inventory (Bq) onboard the Project 675 (Echo II) SSGN Factory Number 541 as of August 1998 (<i>Kobzev and Lavkovsky, 2001</i>)	8
Table 2-3: Estimated radioactive inventory (Bq) onboard the Project 671 (Victor I) SSN Factory Number 610 as of August 1998 (<i>Kobzev and Lavkovsky, 2001</i>).	9
Table 2-4: Radioactive inventory (Bq) in spent fuel assemblies onboard the PM-80 as of August 1998 (<i>Kobzev and Lavkovsky, 2001</i>)	10
Table 2-5: Radioactive inventory in liquid radioactive waste onboard the PM-80 as of April 2000 (<i>Kobzev and Lavkovsky, 2001</i>).....	11
Table 2-6: Radioactive inventory (Bq) in spent fuel assemblies onboard the PM-125 as of August 1998 (<i>Kobzev and Lavkovsky, 2001</i>)	12
Table 2-7: Radioactive inventory in liquid radioactive waste onboard the PM-125 as of April 2000 (<i>Kobzev and Lavkovsky, 2001</i>).....	12
Table 2-8: Radioactive inventory (Bq) in spent fuel assemblies onboard the PM-133 as of August 1998 (<i>Kobzev and Lavkovsky, 2001</i>)	13
Table 2-9: Radioactive inventory in liquid radioactive waste onboard the PM-133 as of April 2000 (<i>Kobzev and Lavkovsky, 2001</i>).....	13
Table 2-10: Radioactive inventory in liquid radioactive waste onboard the TNT-27 (<i>Kobzev and Lavkovsky, 2001</i>)	14
Table 2-11: Radioactive Waste Inventories in Shore Storage at Pavlovsk Bay (<i>Danilyan et al, 2000b</i>).....	15
Table 2-12: Radioactive inventory in spent fuel assemblies onboard the PM-74 (<i>Kobzev and Lavkovsky, 2001</i>)	16
Table 2-13: Radioactive inventory in liquid radioactive waste onboard the PM-74 as of April 2000 (<i>Kobzev and Lavkovsky, 2001</i>).....	16
Table 2-14: Radioactive inventory in liquid radioactive waste onboard the "Pinega" as of April 2000 (<i>Kobzev and Lavkovsky, 2001</i>)	18
Table 2-15: Radioactive Waste Inventories at Razboinik Bay (<i>Danilyan et al. (2000b)</i>)	22
Table 2-16: Information on Waste Inventories at Cape Sysoeva as of Jan 2000 (<i>Lavkovsky (2000), Danilyan et al. (2000a)</i>).....	24
Table 2-17: Inventory of the LRW on the PKDS-60 as of April 2000 (<i>Lavkovsky (2000)</i> and <i>Kobzev and Lavkovsky (2001)</i>).....	26
Table 2-18: Assessment of activity in spent fuel on the PM-32.....	28
Table 2-19: LRW on the PM-32 (<i>Kobzev and Lavkovsky, 2001</i>).....	28

Table 2-20: LRW onboard the TNT-23 (<i>Kobzev and Lavkovsky (2001)</i>).....	28
Table 2-21: LRW onboard the TNT-42 (<i>Kobzev and Lavkovsky (2001)</i>).....	29
Table 2-22: RW at the Rybachy Naval Base (adapted from <i>Danilyan et al, 2000b</i>)....	30
Table 2-23: Estimated isotopic inventory (Bq) of a TUK-18 fully loaded with spent fuel	30
Table 2-24: Permissible levels for liquid radioactive waste storage on PM-326 floating workshops.....	32
Table 3-1: Summary of atmospheric transport from the Kamchatka NRS to geographical regions during 1987-1996.....	44
Table 3-2: Summary of atmospheric transport from the Vladivostok NRS to geographical regions during 1987-1996.....	44
Table 3-3: Maximum Radionuclide Concentration in Air 25 m over the ground (Bq/m ³ per Bq released).....	57
Table 3-4: Maximum External and Internal Dose (mSv per Bq released).....	57
Table 3-5: Structure of the simulations modeled using WSPEEDI.....	62
Table 3-6: Maximum concentration of ¹³⁷ Cs (Bq/m ³) at different heights of the point release.....	63
Table 3-7: Source Terms used for estimation of accident scenarios (after <i>NATO, 1998</i>)	64
Table 3-8: Total Dose in Areas of Maximum Impact in Japan and Korea (mSv).....	64
Table 4-1: Estimated Release Fractions of Main Elements During a High-Temperature Fire in Spent Nuclear Fuel Storage Facilities (after <i>Banba, 2001</i>).	73
Table 4-2: Estimated Release Fractions of Main Elements From Heated Spent Fuel (after <i>Restrepo, 1991</i>).	74
Table 4-3: Estimated Release Fractions of Main Elements During a Low-Temperature Fire in Spent Nuclear Fuel Storage Facilities (after <i>Banba, 2001</i>).	74
Table 4-4: Nuclide-Specific Parameters for Facility Screening Analysis.....	79
Table 4-5: Estimated Radionuclide Inventories (Bq) in Spent Fuel Storage Facilities and Waste Management Facilities Based upon Analogy with Spent Fuel Stored on the PM-74 (based on Table 3 of <i>Lavkovsky, 2000</i>)	80
Table 4-6: Isotopic Inventories (Bq) in Major Facilities in Southern Primorye Territory (Based On Table 3 of <i>Lavkovsky, 2000</i> , and Table 1 of <i>Lysenko Et Al., 2002</i>)	80
Table 4-7: Critical release fractions under dry deposition conditions.....	81
Table 4-8: Critical release fraction under wet deposition conditions.....	81
Table 4-9: Airborne Release Fractions under different accident conditions.....	82

Acknowledgments

The work was undertaken jointly by the members of the IIASA Radiation Safety of the Biosphere, Russian specialists from the Ministries of Defense and Atomic Energy, Japanese scientists from the Japan Atomic Energy Research Institute, and graduate students from the Russian and Bulgarian Academies of Science. Although this summary report is being issued by IIASA, the work has been a joint effort and would not have been possible without the contributions of scientists and administrators from many different countries.

Among those participating were Valery Danilyan, A. A. Maksimov, and V. L. Visotsky of the Russian Pacific Fleet; N. I. Lysenko, V. Mordashev, A. Pechkurov, and B. G. Pologich of the Russian Research Centre "Kurchatov Institute"; and S.A. Lavkovsky and V.I. Kobzev of the Central Design Bureau "Lazurit". Working at IIASA were Makoto Takano and Tsunetaka Banba of the Japan Atomic Energy Research Institute, Alexander Mahura of the Institute of the Northern Environmental Problems (INEP) of the Russian Academy of Sciences and Vanya Romanova of the Space Research Institute of the Bulgarian Academy of Sciences. We would also like to acknowledge the work of the many organizations of the Russian Federation and of the former Soviet Union which have contributed to the current store of knowledge about these sites.

We are grateful to the many people who contributed to the development of this research, including Hiromi Yamazwa (Japan Atomic Energy Research Institute) for supplying the WSPEEDI model and Ginger Caldwell (Scientific Computing Division, National Center for Atmospheric Research) for the collaboration, computer assistance, and advice. Thanks to Drs. William Hamilton (Department of Civil and Environmental Engineering, Vanderbilt University, Nashville, TN, USA) and Ann Clarke (ANC Associates, Inc., Brentwood, TN, USA) for running the cluster analysis at the Vanderbilt University computer facilities. A special acknowledgement is due to the support staff at IIASA, and particularly to Mrs. Ulrike Neudeck for taking care of the administrative issues.

Financial support for the work described herein was provided by the United States Department of Energy and the Japanese Atomic Energy Research Institute. Funding for graduate student research at IIASA as a part of the Young Scientists Summer Program was provided by the Swedish Council for Planning and Coordination of Research. Portions of this analysis were performed under a computing grant from the Scientific Computing Division of the US National Center for Atmospheric Research in Boulder, Colorado. The views and opinions of the authors expressed here do not necessarily state or reflect those of the sponsoring agencies or their institutions.

The Radioactive Legacy of the Russian Pacific Fleet Operations and Its Potential Impact on Neighboring Countries

1 Introduction

Frank L. Parker

Study background, statement of need, goals

The impact of the operation and decommissioning of the world's nuclear navies is an environmental concern because of the ecologically sensitive nature of the oceans and their cultural and religious significance to many people. This is evidenced by the enactment of the London Convention that prohibits dumping of hazardous materials into the seas. Much of the interest on nuclear contamination of the oceans has been centered in the operation of Russia's nuclear navy. Although Russia has five regional fleets (Northern, Pacific, Baltic, Black and Caspian), only the Northern Fleet and the Pacific Fleet sustain nuclear operations. The Russian Northern Fleet has 84 operating nuclear submarines with 161 nuclear reactors and two nuclear powered battle cruisers. In addition, there are 71 inactive nuclear submarines with 135 reactors at its bases. In addition to the naval vessels, there are eight nuclear icebreakers and one nuclear container ship as of 1996. In the Pacific Fleet, there are 42 operating nuclear submarines, one nuclear powered battle cruiser and one nuclear powered communications ship. An additional 55 inactive nuclear submarines of the Russian Pacific Fleet are laid up at various bases in the Far East (*Bradley, 1997*).

The interest in the West about the legacy of the Russian nuclear fleet has been unequally divided despite the fact that the Russian Navy was reported to have stored more radioactive waste in the Far East than in the Northwest (630 vs. 54 TBq) (*Egorov et al, 2000*). Most of the interest has been concentrated on the activities of the Northern Fleet as evidenced by the activities of the Arctic Military Environmental Cooperation group (AMEC), the Contact Expert Group (CEG) of the International Atomic Energy Agency, and the Arctic Monitoring and Assessment Program (AMAP). For example, the Russian Ministry of Atomic Energy (MINATOM) suggested 20 high-priority remediation projects to the CEG in April 1998. Ten dealt expressly with the Northern fleet and four dealt with submarine problems that were based on conditions in the Northern fleet. Not one proposal dealt with the Pacific Fleet. Further, *Bradley (1997)* devotes 17 pages to the Northern fleet but only 5½ pages to the Pacific fleet. Of additional interest in the Far East is that a number of nuclear accidents have already taken place in this area. An accident on a nuclear submarine in the Chazhma Bay (near the Sea of Japan) on August 10, 1985, resulted in the release of 200,000 TBq (5 MCi) of radioactive substances, and a radioisotope thermal generator containing 13,000 TBq (350 kCi) of activity was lost during transport near Sakhalin Island. One could say that conditions, a priori, are worse in the Far East because of a lack of infrastructure to move some of the spent fuel and ships' hulls from their present locations to more centralized sites or even sites where treatment can take place. Relatively little is known in the West about conditions in the Far East despite their obvious similarity to conditions in the Russian Northwest. Therefore, after consultation with our Russian colleagues, we at IIASA decided to study the problems of the Russian Pacific Fleet.

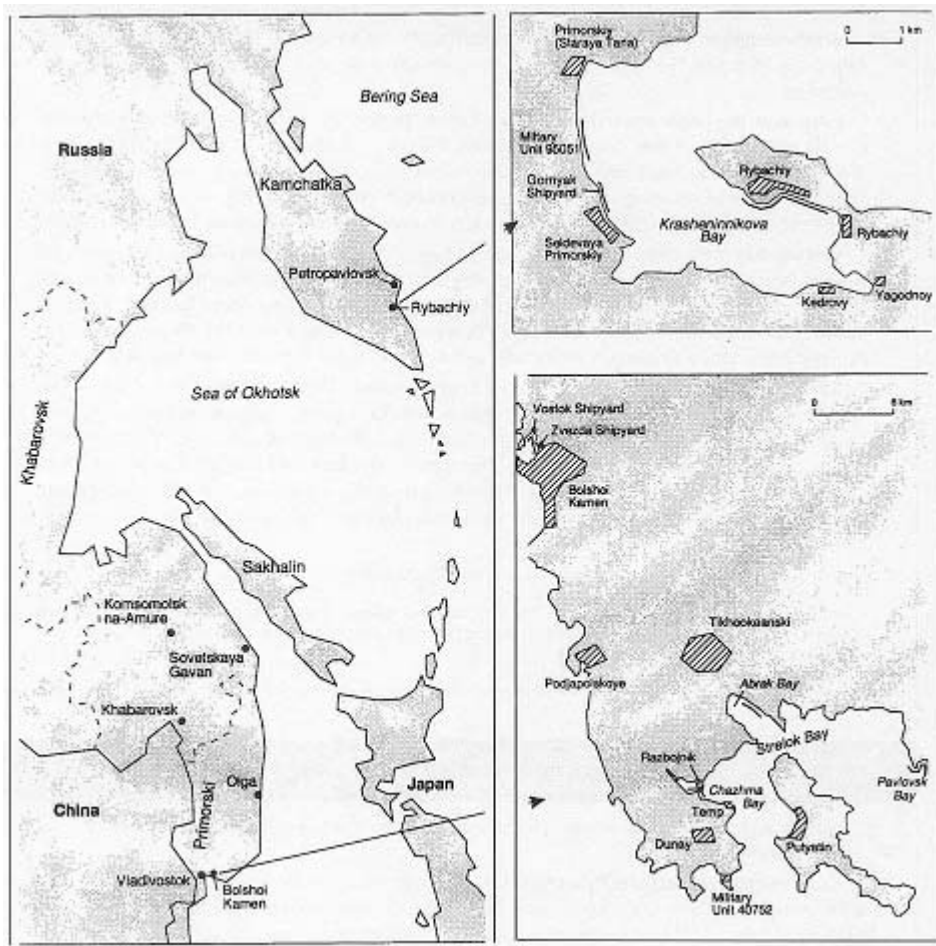


Figure 1-1: Naval nuclear facilities in the Russian Far East (from OTA, 1995)

The nuclear legacy in the Russian Far East has been derived mainly from the operations of the Soviet Pacific Fleet and its Pacific coastal bases. The radioactivity is stored at land-based nuclear waste storage sites, in submarines awaiting decommissioning, in spent nuclear fuel, onboard nuclear service ships, and at shipyards and submarine repair facilities. The decommissioned nuclear submarines of the Russian Pacific Fleet are distributed in many places of the Russian Far East. The nuclear facilities are concentrated mainly in two groups near Vladivostok in southern Primorye Territory and near Petropavlovsk at the southern part of the Kamchatka peninsula (*cf.* Figure 1-1). The first group, in the Primorye Region, comprises an assortment of naval bases together with the Far Eastern Plant Zvezda ("Star") on the Dunai Peninsula opposite to Vladivostok across Ussuri Bay. The second major group comprises the naval bases in Krasheninnikov Bay together with the Kamchatka Marine Plant near Petropavlovsk on south of the Kamchatka Peninsula. Currently, decommissioning of Pacific fleet nuclear submarines occurs only in Primorye Region at the civilian Far Eastern Plant Zvezda. Decommissioning activities at the Kamchatka Marine Plant in Vilyuchinsk are limited.

A fraction of the radioactive waste produced in the Far East was dumped in ten officially sanctioned areas in the Far East seas (with the last dumping occurring in 1993). The dumped wastes included both liquid and solid wastes, including two reactors without spent nuclear fuel. It should be noted only one of these ten sea disposal sites meets the IAEA depth and location requirements for dumping radioactive waste at sea. The total activity discarded in the Far Eastern seas (excluding the radioisotope thermal generator which was lost in 1987 in the Sea of Okhotsk near Sakhalin

Island, which contained approximately 25 PBq of ^{90}Sr was around 430 TBq (*Sivintsev and Kiknadze, 1998b*).

The necessity to quickly decommission a large number of Russian nuclear submarines that have reached, or are close to, the end of their service life creates a potentially serious problem. Russia has a backlog of more than fifty nuclear submarines in the Far East awaiting final disposal. There is also a risk associated with the large amount of spent fuel that is still on board decommissioned submarines.

In general, the radiation situation in the Russian Far East resulting from radioactive waste disposal, nuclear accidents, and any potential threats due to hypothetical accidents at land-based nuclear waste storage sites, has not been examined in detail and has not been subject to the same scrutiny as radioactively contaminated sites in the rest of Russia.

Recently, two articles have appeared in the Russian Journal of Atomic Energy (“Atomnaya Energiya”) which provide a comprehensive view of the land and water contamination surrounding the naval bases of the Pacific Fleet (*Danilyan et al. 2000a, 2000b*). In the second paper it is stated that:

The results of investigations performed over many years make it possible to conclude in general that the influence of accident-free operation and utilization of nuclear powered submarines from the Pacific Ocean fleet on the radiological conditions on the marine water areas used is negligible (less than 1% the activity of global fallout)...At the same time, it should be noted that the probability of a reactivity accident during offloading of spent nuclear fuel from reactors in a nuclear powered submarine has not been ruled out. For the existing technology, it is considered to be $5 \cdot 10^{-5}$ events/(reactor-yr). This is a high level and it does not correspond to the target safety criterion.

This is consistent with our initial evaluation that the atmospheric transport of accidental releases has the potential to cause greater transboundary impact than the hydrospheric transport. We began with studying the possibility of accidental releases reaching and affecting parts of Japan and have recently extended these analyses to other nations around the Russian nuclear naval sites in the Far East.

2 Background: Facilities and Source Terms

Main Contributors: V.A. Danilyan, V. I Kobzev, S.A. Lavkovsky, A.A. Maksimov, Yu. V. Sivintsev, and V.L. Visotsky

Edited by K. L. Compton

The information presented in Chapter Two is based largely on work conducted by Russian institutes who were partners in the Far East Study. The bulk of the work is derived from six reports: two reports prepared for the Far East Study by the Central Design Bureau "Lazurit" based on data from ISTC Project 101 referenced as *Lavkovsky (2000)* and *Kobzev and Lavkovsky (2001)*; project reports prepared for the Far East study under the direction of Yuri Sivintsev (*Sivintsev et al. 2000, Lysenko et al. 2002*); and two journal articles which appeared in the Russian Journal of Atomic Energy ("Atomnaya Energiya") in 2000 (*Danilyan et al. 2000a, 2000b*). Data in this chapter is based on these reports and is therefore not cited unless there is a need to identify the specific source of information. In addition, a literature review was carried out to identify other possible sources of information and to compare the previously reported information with the information made available during the study. Information derived from these outside sources of information is referenced when used. A final section provides some technical details regarding the ships and casks used to store spent nuclear fuel in the Russian Pacific Fleet.

2.1 Primorye Territory

Primorye Territory, covering an mostly forested area of approximately 161 thousand km², lies at the extreme southeastern end of Russia in East Asia between 42°N-48°N and 130°E-139°E (Figure 2-1). The major naval facilities in Primorye Territory comprise a naval base at Pavlovsk Bay, a shipyard at Bolshoi Kamen, a ship repair facility at Chazhma Bay, a naval facility at Razboinik Bay, and a fuel management and waste management facility at Cape Sysoeva. Each will be considered in more detail below.

2.1.1 Pavlovsk Bay Naval Base

The Pavlovsk Bay Naval Base is located on the eastern side of Strelok Bay (see Figures 2-1 and 2-2). The base is home to decommissioned submarines, including three submarines with cores that have been damaged during accidents. Pavlovsk Bay is also the current berth for several major support ships, including the floating workshops PM-80, PM-125, PM-133, and technological tankers TNT-27 and TNT-5. The PM-80 contains damaged spent nuclear fuel. According to the Inspection of State Supervision for Nuclear and Radiation Safety of Nuclear Power Plants of the Administration of State Supervision, Defense Ministry of the RF, neither the PM-125 nor the PM-133 are usable for defueling or refueling of nuclear submarines.

Decommissioned Submarines

As of January 2000, 16 decommissioned non-defueled submarines were berthed at the Pavlovsk Bay facility. An estimate of the inventory of radioactivity in the decommissioned submarines has been provided by *Lysenko et al. (2002)* as a part of an evaluation of hypothetical accidents. Table 2-1 represents a conservative assessment of the estimated activity in one submarine reactor core three years after final shutdown. Because most first- and second-generation submarines have two reactors, the values from Table 2-1 should be multiplied by two to estimate the total inventory per submarine.



Figure 2-1: Primorye Territory (inset shows naval facilities)
 Map source: www.expedia.com

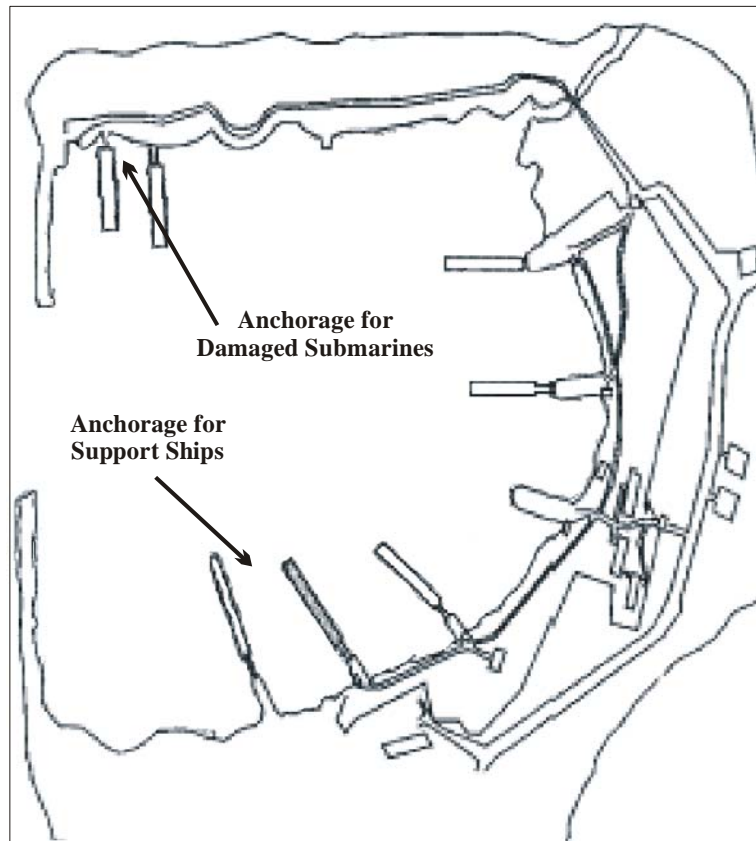


Figure 2-2: Pavlovsk Bay Naval Base (adapted from Danilyan et al, 2000b)

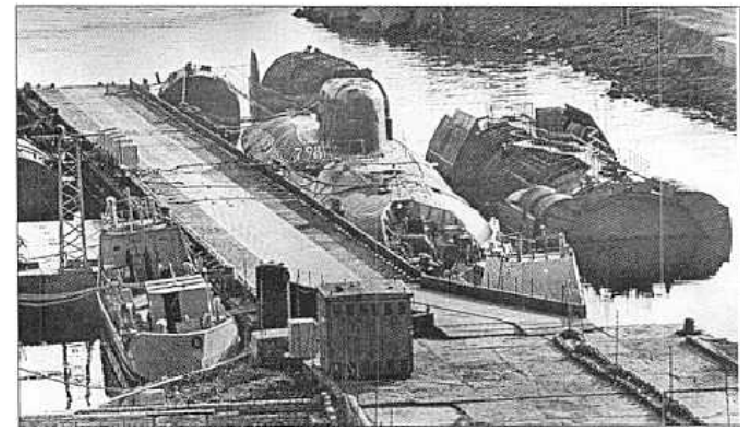
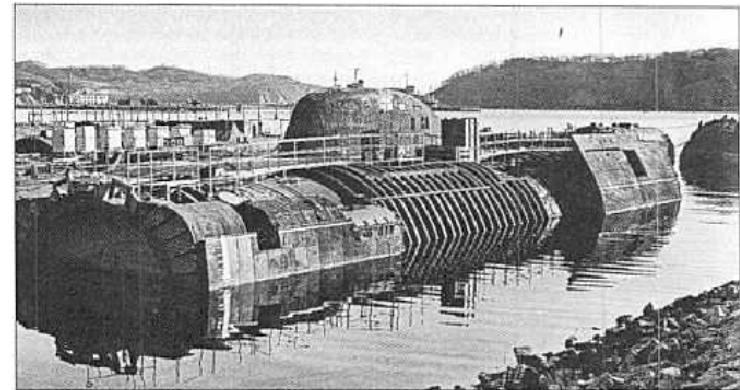


Figure 2-3: Three-compartment unit alongside a decommissioned Victor Class SSN at Pavlovsk Bay. The vessels are now stored at Razboinik Bay. (Handler, 1995. Photo credit: J. Handler).

Table 2-1: Isotopic inventory of typical submarine reactor core three years after shutdown (assumed burnup 42 GWd) (*Lysenko et al. (2002)*)

Radionuclide	T _{1/2} , years	Activity, Bq
¹³⁷ Cs	30	4.9x10 ¹⁵
⁹⁰ Sr	29.1	4.2x10 ¹⁵
¹⁴⁴ Ce	0.78	2.3x10 ¹⁵
¹³⁴ Cs	2.06	1.9x10 ¹⁵
²⁴¹ Pu	14.4	1.1x10 ¹⁵
¹⁰⁶ Ru	1.01	3.2x10 ¹⁴
²³⁸ Pu	87.7	4.1x10 ¹³
²⁴¹ Am	432	1.1x10 ¹³
²³⁹ Pu	24,100	6.5x10 ¹²
²⁴⁰ Pu	6,540	4.1x10 ¹²
⁶⁰ Co	5.27	2.6x10 ¹¹
⁵⁵ Fe	2.7	1.7x10 ¹¹

Damaged Submarines

Three major accidents resulting in core damage on submarines in the Russian Pacific Fleet have been reported. All three damaged submarines are stored afloat at Pavlovsk Bay. A short description of each accident is given below. A more extensive description of the accident in Chazhma Bay is given in *Sivintsev et al. (1994)*. Although several of these accidents had been described in by *Handler (1994a)*, there is one remaining unconfirmed report that refers to a Victor SSN (tactical number 371) that suffered a loss of coolant accident at Pavlovsk Bay in the summer of 1986. There are no references to such an accident on the K-371 in published Russian sources. However, *Bellona (1996)* reports that this submarine underwent a "critical underspace leakage" and is laid up at a Northern Fleet shipyard near Murmansk.

July 1979 Loss of Coolant Accident

According *Sivintsev et al. (2000a)* and *Kutcher et al. (1996)*, the submarine designated as factory number 541 (Tactical no. not reported) underwent a loss of coolant accident in 1979. This may be the submarine referred to by *Handler (1994a)* as the "K-116, an Echo I SSN, [Project no 659T] (order no 541), (that) suffered a meltdown due to operator error while the submarine was at sea near Russia...as of 1994, it was stored at the Pavlovsk submarine base awaiting the deployment of special decommissioning procedures". The ship is a Project 675 (NATO designation "Echo II") class guided missile submarine built in 1965 at the Severodvinsk Machine-building Enterprise. It is 115.4 m long and 9.3 m wide with draft of 7.8 m at a surface displacement of 4500 tons. It normally carries a crew of 90 and is powered by two VM-A reactors, each of which is rated at 70 MWt (*Bellona, 1996*). The ship was transferred in 1966 from the Northern Fleet to the Pacific Fleet. There is some inconsistency regarding the number of refuelings. According to information from *Lavkovsky (2000)*, the starboard¹ reactor had been defueled twice, and the port reactor three times. The starboard reactor began operations in 1971, and the port in 1978. However, according to *Kobzev and Lavkovsky (2001)*, the starboard reactor had been refueled in 1971 and again in 1979. The port reactor was reported to have been refueled in 1971 (during the same overhaul that the starboard reactor was refueled) and again in 1978. Both were permanently shut down at some point between July and August 1979. *Kobzev and Lavkovsky (2001)* reports that the total power generation of the core of the port reactor was approximately 0.17 GWd, and the starboard core had generated 8.3 GWd. The total power generation of the steam generating plant amounted to 18.7 GWd (port) and 19.8 GWd (starboard).

¹ It appears that reactors on Project 675 submarines are arranged fore-and-aft. The designation "port" denotes the forward reactor and the designation "starboard" denotes the aft reactor. On the Project 675 (Echo II) SSGNs the reactors are installed in the sixth compartment.

According to *Kutcher et al. (1996)*, a loss of coolant accident occurred in the port reactor in the summer of 1979. Existing reports conflict as to the exact time and location of the accident. *Sivintsev et al. (2000a)* reports that the accident took place in June alongside the pier in Pavlosky Bay, whereas *Kutcher et al. (1996)* reports that the accident took place during a surface transit on July 2 from Pavlovsk Bay to Vladimir Bay. Given that the port reactor had only approximately sixty hours of full power operation, it appears that the accident may have been related to improper procedures during the refueling of the port reactor. Major leakage along the port reactor cover resulted in a sharp pressure drop in the primary circuit. As a result, the primary coolant boiled and fuel assemblies were damaged, with a loss of cladding tightness. This resulted in the spread of gas and aerosol activity to all compartments. The leakage from the primary circuit entered the reactor shield and the hold of the reactor compartment. The equipment installed in the reactor compartment completely failed due to the flooding from leakage of the reactor. This also led to strong radioactive contamination of the reactor compartment. The nuclear submarine was decommissioned from the Navy as a result of the accident (*Kutcher et al., 1996*). The estimated radioactivity inventory of the spent fuel (in Bq) and activated reactor structures is given in Table 2-2. Additional information on the radiation conditions onboard the submarine is given in *Kobzev and Lavkovsky (2001)*.

Table 2-2: Estimated radioactive inventory (Bq) onboard the Project 675 (Echo II) SSGN Factory Number 541 as of August 1998 (*Kobzev and Lavkovsky, 2001*)

Isotope	Fuel	Internal Reactor Components	Reactor Pressure Vessel	Shield Tank	Reactor Compartment	Fuel	Internal Reactor Components	Reactor Pressure Vessel	Shield Tank	Reactor Compartment
	Starboard Reactor					Port (Damaged) Reactor				
²³⁹ Pu	2.0x10 ¹²					4.0x10 ¹⁰				
²⁴⁰ Pu	3.2x10 ¹¹					6.4x10 ⁹				
²⁴¹ Pu	3.0x10 ¹²					6.1x10 ¹⁰				
²⁴¹ Am	4.8x10 ¹¹					9.6x10 ⁹				
⁹⁰ Sr	5.5x10 ¹⁴					1.2x10 ¹³				
¹³⁴ Cs	n/r					n/r				
¹³⁷ Cs	5.9x10 ¹⁴					1.3x10 ¹³				
⁵⁵ Fe	4.4x10 ¹²	1.8x10 ¹³	8.2x10 ¹¹	2.0x10 ¹¹	7.6x10 ⁷	1.9x10 ¹¹	1.4x10 ¹³	6.4x10 ¹¹	1.5x10 ¹¹	6.0x10 ⁷
⁶⁰ Co	1.4x10 ¹³	5.1x10 ¹³	1.5x10 ¹²	5.8x10 ¹¹	6.3x10 ⁷	4.5x10 ¹¹	4.4x10 ¹³	1.3x10 ¹²	5.0x10 ¹¹	5.4x10 ⁷
⁶³ Ni	1.8x10 ¹³	8.9x10 ¹³	1.7x10 ¹²	1.1x10 ¹²	9.9x10 ⁷	3.6x10 ¹¹	8.4x10 ¹³	1.6x10 ¹²	1.0x10 ¹²	9.4x10 ⁷
¹⁵² Eu	8.9x10 ¹⁰					2.2x10 ⁹				
¹⁵⁴ Eu	7.8x10 ¹¹					2.1x10 ¹⁰				
Total	1.2x10¹⁵	1.6x10¹⁴	4.0x10¹²	1.9x10¹²	2.4x10⁸	2.6x10¹³	1.4x10¹⁴	3.5x10¹²	1.7x10¹²	2.1x10⁸

n/r: not reported

August 1985 Criticality Accident

On the morning of 10 August 1985, during completion of reactor refueling work on a Project 675 (NATO designation "Echo II") SSGN (Factory No. 175, Tactical No. K-431/B-431) at the Chazhma Bay Ship Repair Facility, a reactivity accident occurred in the port reactor as a result of violation of standard refueling procedures. The accident is described in greater detail elsewhere (*Sivintsev et al. (1994a)*, *Sivintsev (2000a, 2000b)*, *Takano et al. (2001)*). The resulting thermal explosion of the reactor destroyed the forward and aft machine enclosures and the forward enclosure of the control and protection system. The entire core consisting of freshly loaded nuclear fuel was blown out of the reactor. The fuelling shack was also partially destroyed, and its roof was blown off to a distance of 70 - 80 m where it fell into the water 30 m from shore. The submarine sustained damage to its pressure hull in the aft section of the reactor compartment. Immediately after the explosion in the reactor compartment, a fire broke out, which was brought under control after four hours. Combustion products, fission and activation products, and fine

particles of nuclear fuel fell out within a radius of 50-100 m around the damaged submarine. On the basis of a theoretical paper (*Romanov, 1993*), it is possible to estimate that the energy of the explosion was approximately 5×10^{18} fissions. This value is consistent with the results of activation measurements made immediately after the accident (*Sivintsev, 2000b*).

After the accident, the damaged submarine was towed from Chazhma Bay to Pavlovsk Bay, where it is currently berthed. A description of the current condition of the K-431 is provided in *Goriglejan (1999)*. The environmental contamination resulting from this accident is described in a number of publications, including *Sivintsev et al. (1994)* and *Chaikovskaya et al. (2001)*.

December 1985 Loss of Coolant Accident

The third reported submarine reactor accident in the Russian Far East also occurred in 1985. The Project 671 (NATO designation "Victor I") class nuclear submarine (Factory no. 610, tactical no. K-314/B-314) was built in 1972 by the Leningrad Admiralty Association and assigned to the Pacific Fleet in 1975. The submarine carries a crew of 90 and is 94.3 m long and 10.6 m wide, with a draft of 7.3 m at a surface displacement of 3500 tons. The submerged displacement is 6085 tons. The vessel is powered by a VM-4 nuclear power plant with two reactors located side-by-side in the third compartment. The reactors had both undergone two previous refuelings, the latest being completed in November 1979. Both were permanently shutdown on 31 Dec 1985. The power generation of the installed cores amounted to 6.3 GWd each, and the total power generation of the steam plants amounted to 16.7 GWd each.

The submarine suffered an accident to the port reactor while pierside in Pavlovsk Bay in December 1985. It is described as a primary coolant leak of the portside reactor resulting in core damage ("loss of cladding tightness") and flooding of the reactor compartment by primary coolant. The environmental contamination resulting from the accident is described in *Danilyan et al. (2000b)*. Damage of the portside reactor plant core made off-loading impossible. In addition, the elevated radiation levels in the reactor compartment hamper off-loading of the undamaged starboard core. The nuclear submarine is stored afloat with both cores still on board. This may be the submarine referred to by *Handler (1994a)* as "the K-314, a Charlie SSGN (order no 610) (or maybe a Victor I SSN), (*that*) suffered a reactor meltdown in the Pacific, reportedly in Russian waters." The estimated radioactivity inventory (in Bq) of the spent fuel and activation products in structural components is given in Table 2-3.

Table 2-3: Estimated radioactive inventory (Bq) onboard the Project 671 (Victor I) SSN Factory Number 610 as of August 1998 (*Kobzev and Lavkovsky, 2001*).

Isotope	Fuel	Internal Reactor Components	Reactor Pressure Vessel	Shield Tank	Reactor Compartment	Fuel	Internal Reactor Components	Reactor Pressure Vessel	Shield Tank	Reactor Compartment
	Starboard Reactor					Port (Damaged) Reactor				
²³⁹ Pu	6.8×10^{12}					6.8×10^{12}				
²⁴⁰ Pu	1.6×10^{12}					1.6×10^{12}				
²⁴¹ Pu	7.4×10^{13}					7.4×10^{13}				
²⁴¹ Am	2.0×10^{12}					2.0×10^{12}				
⁹⁰ Sr	1.0×10^{15}					1.0×10^{15}				
¹³⁴ Cs	1.4×10^{13}					1.4×10^{13}				
¹³⁷ Cs	1.1×10^{15}					1.1×10^{15}				
⁵⁵ Fe	n/r		4.3×10^{14}		1.6×10^{11}	n/r		4.3×10^{14}		1.6×10^{11}
⁶⁰ Co	n/r		2.9×10^{14}		6.2×10^{10}	n/r		2.9×10^{14}		6.2×10^{10}
⁶³ Ni	n/r		1.4×10^{14}		3.3×10^{10}	n/r		1.4×10^{14}		3.3×10^{10}
¹⁵² Eu	n/r									
¹⁵⁴ Eu										
Total	2.2×10^{15}		8.6×10^{14}		2.6×10^{11}	2.2×10^{15}		8.6×10^{14}		2.6×10^{11}

Floating Workshops

In addition to damaged and undamaged submarines awaiting decommissioning, there are also service ships berthed at Pavlovsk Bay. These include three PM-326 class floating workshops. Two of these (the PM-125 and the PM-133) were refitted to store spent fuel in ChT-4 canisters and are thus designated as PM-326M class support ships. All are in very poor condition and are not usable for their designated purpose of defuelling and/or refuelling nuclear submarines. The technical characteristics of fuel storage onboard PM-326 and PM-326M floating workshops is given in Section 2.3

The PM-80 is a Project 326 barge built in 1964 which had been reported to contain considerable amounts of wedged, damaged spent fuel (113 damaged spent fuel assemblies in 1995). The fuel appears to have been in storage for a considerable amount of time, as the date of last criticality is reported to be 1969. However, a technology has been developed to extract the damaged fuel (*Sarkisov, 1999*), and as of 1998, 90 spent fuel assemblies had been removed from the PM-80. As of 1 August 1998, the PM-80 held 23 damaged spent fuel assemblies from different first-generation cores with 430 TBq of radioactivity. Data on the inventory of spent fuel and radioactive waste on the PM-80 are given in Tables 2-4 and 2-5. According to Table 18 in *Danilyan et al. (2000b)*, the total LRW storage capacity of the PM-80 as of January 2000 was 319.4 m³, and it contained 5.6 TBq of radioactivity in 136 m³ of liquid radioactive waste in tanks 1-4 and montejes². This appears consistent with the 5.4 TBq of activity in 136 m³ reported by *Kobzev and Lavkovsky (2001)* in Table 2-5 below. In addition, the PM-80 was reported to contain four storage containers totalling 6 m³ with a total activity of 0.0074 TBq. However, Table 19 in *Danilyan et al. (2000b)* report 4.0 m³ of SRW containing 0.16 TBq of activity. The PM-80 is in critical condition. According to information from *Lavkovsky (2000)*, all of special systems to ensure nuclear and radiation safety and systems for loading and storage of spent fuel and liquid radioactive waste are defective. The drydocking that should have taken place in 1994 has not yet taken place. The inter-compartmental bulkheads, doors, hatches, and manholes are not watertight, making the vessel vulnerable to sinking in the case of flooding. The radiation monitoring systems are defective. Because there is no system for monitoring the spent fuel storage tanks, the possibility of water leakage from storage tanks cannot be excluded. The vessel has been decommissioned. The volumetric activity of water in the spent fuel storage tanks is 2.2x10⁵ kBq/L in the forward storage compartment and 1.4x10⁵ kBq/L in the aft storage compartment. Data on the estimated radioactive inventory in spent fuel assemblies as of August 1998, presuming that the fuel assemblies had reached their design power generation, is given in Table 2-4.

Table 2-4: Radioactive inventory (Bq) in spent fuel assemblies onboard the PM-80 as of August 1998 (*Kobzev and Lavkovsky, 2001*)

²³⁹ Pu	²⁴⁰ Pu	²⁴¹ Pu	²⁴¹ Am	⁹⁰ Sr	¹³⁴ Cs	¹³⁷ Cs	Total
1.6x10 ¹¹	1.8x10 ¹¹	6.8x10 ¹²	6.4x10 ¹¹	2.0x10 ¹⁴	1.0x10 ¹⁰	2.2X10 ¹⁴	4.3x10 ¹⁴

² A montejes is a type of sedimentation tank used for water treatment.

Table 2-5: Radioactive inventory in liquid radioactive waste onboard the PM-80 as of April 2000 (*Kobzev and Lavkovsky, 2001*)

Storage description	Designed capacity, m ³	Filled in volume, m ³	Activity, Bq	Specific activity, kBq/L
Forward spent fuel assembly storage tank	12.3	12	2.7x10 ¹²	222,000
Aft spent fuel assembly storage tank	12.3	12	2.4x10 ¹²	196,000
Sewage water tank No.1	23.5	23	3.0x10 ¹⁰	1,300
Sewage water tank No.2	23.5	23	1.9x10 ¹¹	8,100
Enclosure for high activity liquid waste	25	23	5.6x10 ¹⁰	2,400
Enclosure for low activity liquid waste	25	23	5.5x10 ¹⁰	2,400
Enclosure for low activity liquid waste	25	15	3.5x10 ¹⁰	2,300
Enclosure for spent fuel assembly storages	2	2	5.0x10 ⁹	2,500
Enclosure for filter washing No.1	3	3	5.0x10 ¹⁰	17,000

The PM-125 is a Project 326M barge built in 1960 and modified in 1982. As of August 1 1998, the vessel held approximately 360 fuel assemblies (*Kobzev and Lavkovsky, 2001*), representing two first-generation cores³. Based upon an assumed combined burnup for both cores of 5.2 GWd⁴ and a final criticality in 1985, the total activity as of August 1998 was estimated to be 3,900 TBq. Data on the inventory of spent fuel and radioactive waste on the PM-125 are given in Tables 2-6 and 2-7. According to Table 18 in *Danilyan et al. (2000b)*, the total LRW storage capacity of the PM-125 as of January 2000 was 359.2 m³, and it contained 0.34 TBq of radioactivity in 194.5 m³ of liquid radioactive waste in tanks 1-4 and montejes. This appears consistent with the 0.33 TBq of activity in 194 m³ reported by *Lavkovsky (2000)* and *Kobzev and Lavkovsky (2001)* in Table 2-7.⁵ In addition, the PM-125 was reported to contain four storage containers totalling 6 m³ with a total activity of 0.021 TBq. However, Table 19 in *Danilyan et al. (2000b)* report 16.5 m³ of SRW containing 0.33 TBq of activity in SRW containers in the zone of controlled radiation safety. The PM-125 is also in very poor condition. According to data from *Lavkovsky (2000)*, the last drydocking took place in May 1992. Hull corrosion is up to 18%. There is a pitting corrosion of the inner hull in the area of the third and fourth boiler fuel tanks, and the bottom framing is damaged by the pitting corrosion with corroded sections up to 30mm long and 3 to 5 mm deep near the waterline. The inter-compartmental bulkheads, doors, hatches, and manholes are not watertight, making the vessel vulnerable to sinking in the case of flooding. Most of the safety-related systems on the ship are defective, including the fire protection, drainage, spent fuel handling, water treatment, and refrigeration and heating systems. There is therefore a significant threat of fire, flooding, or of freezing of the water in the spent fuel storage compartments during the winter. The nuclear fuel handling cranes are missing small assemblies, and the use of nuclear fuel offloading gears is prohibited. Water quality in the tanks with spent fuel assembly does not meet the requirements to store spent nuclear fuel storage containers. Because of the poor condition of the vessel, the Inspection of State Supervision for Nuclear and Radiation Safety of Nuclear Power Plants of the Administration of State Supervision, Defense Ministry of the RF, has prohibited use of the PM-125 for defuelling and refuelling of nuclear submarines.

³ *Lavkovsky (2000)* reports that the spent fuel onboard the PM-125 is from two second generation cores. We use the later data from *Kobzev and Lavkovsky (2001)* as presumably the most current data.

⁴ This value seems low for a combined burnup when compared to the 42 GWd burnup per core used by *Lysenko et al. (2002)* or the values reported for the cores in storage on the PM-74, which are approximately 1550 MWh per SFA for both first- and second-generation submarines in contrast to the 350 MWh per SFA for the fuel on the PM-125 under the assumption of combined burnup.

⁵ In contrast, *Handler (1994a)* reports that the PM-125 contained 108 m³ of waste containing 0.8 TBq as of March 1994.

Table 2-6: Radioactive inventory (Bq) in spent fuel assemblies onboard the PM-125 as of August 1998 (*Kobzev and Lavkovsky, 2001*)

²³⁹ Pu	²⁴⁰ Pu	²⁴¹ Pu	²⁴¹ Am	⁹⁰ Sr	¹³⁴ Cs	¹³⁷ Cs	Total
5.7x10 ¹²	1.3x10 ¹²	6.2x10 ¹³	1.7x10 ¹²	1.9x10 ¹⁵	6.8x10 ¹²	1.9x10 ¹⁵	3.9x10 ¹⁵

Table 2-7: Radioactive inventory in liquid radioactive waste onboard the PM-125 as of April 2000 (*Kobzev and Lavkovsky, 2001*)

Storage description	Designed capacity, m ³	Filled in volume, m ³	Activity, Bq	Specific activity, kBq/L
Bow spent fuel assembly storage tank	12.3	10	2.5x10 ¹¹	25,000
Aft spent fuel assembly storage tank	12.3	10	3.0x10 ¹⁰	3000
Sewage water tank No.1	23.5	18	6.0x10 ⁶	0.33
Sewage water tank No.2	23.5	6	2.2x10 ⁷	3.7
Sewage water tank of special sanitary unit No.1	14.6	10	2.1x10 ⁶	0.21
Sewage water tank of special sanitary unit No.2	14.6	0.5	1.0x10 ⁵	0.21
Sewage water tank of special sanitary unit No.3	20.1	9	1.7x10 ⁷	1.9
Sewage water tank of special sanitary unit No.4	23.5	11	1.1x10 ⁷	0.96
Treated water tank No.1	46	45.6	8.8x10 ⁶	0.19
Enclosure for high activity liquid waste	25	24	2.0x10 ⁹	85
Enclosure for low activity liquid waste	25	24.8	1.0x10 ¹⁰	410
Enclosure for low activity liquid waste	25	24.8	1.5x10 ¹⁰	590
Enclosure for spent fuel assembly storages	2	1	2.5x10 ¹⁰	25,000

The third floating workshop in Pavlovsk Bay is the PM-133, a Project 326 barge built in 1962 and upgraded to PM-326M class in 1972. This is the floating workshop that was involved in the 1985 Chazhma Bay accident. The vessel currently holds two second-generation spent cores (560 spent fuel assemblies) with an estimated total activity of 9,200 TBq in storage (*Kobzev and Lavkovsky, 2001*). Data on the inventory of spent fuel and radioactive waste on the PM-133 is given in Table 2-8 and 2-9 based on a burnup of 10.4 GWd per core and a final shutdown in 1994. According to *Danilyan et al. (2000b)*, the total LRW storage capacity of the PM-133 as of January 2000 was 333.8 m³, and it contained 1.8 TBq of radioactivity in 68.0 m³ of liquid radioactive waste in tanks 1-4 and monteuses. This is consistent with the 1.8 TBq of activity in 68 m³ reported by *Lavkovsky (2000)* and *Kobzev and Lavkovsky (2001)* in Table 2-8. ⁶In addition, the PM-133 was reported to contain two storage containers totalling 3 m³ with a total activity of 0.0074 TBq. However, *Danilyan et al. (2000b)* report 6.25 m³ of SRW containing 0.21 TBq of activity in SRW containers in the zone of controlled radiation safety. The last routine overhaul was in 1987 after the radiation accident in Chazhma Bay. Additional individual repairs were carried out 1995. According to *Lavkovsky (2000)*, the prescribed service life of 30 years has been exceeded. Corrosion is ubiquitous. The bilge in the sewage room (eighth compartment) has been completely destroyed by corrosion, with holes up to 50 cm in diameter. In the ninth compartment there is maximum hull destruction by stratification corrosion. Like the PM-80, most of the systems are defective,

⁶ In contrast, *Handler (1994a)* reports that the PM-133 contained 46 m³ of waste containing 0.013 TBq as of March 1994.

including the drainage, heating, fire protection, and spent fuel handling systems. The Inspection of State Supervision for Nuclear and Radiation Safety of Nuclear Power Plants of the Administration of State Supervision, RF Defense Ministry, has prohibited use of the PM-133 for defuelling and refuelling of nuclear submarines.

Table 2-8: Radioactive inventory (Bq) in spent fuel assemblies onboard the PM-133 as of August 1998 (*Kobzev and Lavkovsky, 2001*)

²³⁹ Pu	²⁴⁰ Pu	²⁴¹ Pu	²⁴¹ Am	⁹⁰ Sr	¹³⁴ Cs	¹³⁷ Cs	Total
1.1x10 ¹³	2.7x10 ¹²	1.8x10 ¹⁴	1.2x10 ¹²	4.1x10 ¹⁵	4.6x10 ¹⁴	4.5x10 ¹⁵	9.2x10 ¹⁵

Table 2-9: Radioactive inventory in liquid radioactive waste onboard the PM-133 as of April 2000 (*Kobzev and Lavkovsky, 2001*)

Storage description	Designed capacity, m ³	Filled in volume, m ³	Activity, Bq	Specific activity, kBq/L
Bow spent fuel storage tank	12.3	10	1.1x10 ¹²	110,000
Aft spent fuel storage tank	12.3	10	3.6x10 ¹¹	36,000
Enclosure for low activity water	25	23	1.1x10 ¹⁰	480
Enclosure for low activity water	25	23	8.1x10 ¹⁰	3,500
Enclosure for spent fuel assembly storages	2	2	2.6x10 ¹¹	130,000

Technological Tankers and Miscellaneous Support Ships

In addition to the three floating workshops, the Project 1783A technological tankers TNT-5 and TNT-27⁷ are berthed at Pavlovsk Bay (*Danilyan et al. (2000b)*). According to data from *Kuzin and Nikolsky (1996)* and *Lavkovsky (2000)*, each of these vessels is 74.4 m long and 12 m wide, and displaces 2300 tons at a draft of 3.95 m. The vessels require a crew of 33, and can cruise for 1000 km at a speed of 9 knots. Top speed is 11 knots. The tanks of special-purpose tankers TNT-5, TNT-42, TNT-23 and TNT-27 are allowed to store LRW with specific activity less than 0.37 kBq/L.

The TNT-5, built in 1960, has a design LRW capacity of 969 m³ in a total of nine tanks. These comprise two 123 m³ tanks, four 120.1 m³ tanks, two 116.1 m³ tanks, and one 10 m³ tank. There is no detailed inventory data available for the TNT-5 provided by either *Lavkovsky (2000)* and *Kobzev and Lavkovsky (2001)* or *Danilyan et al. (2000b)*. However, *Handler (1994a, 1995)* reported that the TNT-5 was in such poor condition in 1994 that it was taking on water. It was therefore in the process of being emptied to avoid problems in the event that the vessel were to sink, and contained only 100 tons of LRW as of December 1994.

⁷ *Lavkovsky (2000)* and *Kobzev and Lavkovsky (2001)* reports that the TNT-27 is located at Krashenninikov Bay. However, *Handler (1994)* reports that the TNT-5 was towed from Bolshoi Kamen to Pavlovsk Bay on May 27 1994, and that the TNT-27 was moved to Pavlovsk Bay on 1 August 1994. Given that *Danilyan et al. (2000b)* also reports the location of the TNT-27 as "Pavlovskogo Bay", it seems likely that the TNT-27 is in Pavlovsk Bay.

The TNT-27, built in 1967 and shown in Figure 2-4, has a design LRW capacity of 905.7 m³ in nine tanks. Inventory data are shown in Figure 2-10. It appears that the tanks are holding waste with a considerably higher level of activity than permitted (cf Table 2-24).



Figure 2-4: TNT-27 underway in the Sea of Japan in October 1993
(Handler, 1995. Photo credit: J. Handler)

Table 2-10: Radioactive inventory in liquid radioactive waste onboard the TNT-27
(Kobzev and Lavkovsky, 2001)

Storage description	Designed capacity, m ³	Filled in volume, m ³	Activity, Bq	Specific activity, kBq/L
Tank No.1	104.3	80	2.9x10 ¹¹	3,630
Tank No.2	104.3	80	3.3x10 ¹⁰	410
Tank No.3	123.7	70	2.3x10 ¹¹	3,200
Tank No.4	123.7	70	2.3x10 ¹¹	3,300
Tank No.5	114	60	5.3x10 ⁹	89
Tank No.6	114	60	2.9x10 ⁹	48
Tank No.7	95.5	60	6.9x10 ⁸	12
Tank No.8	95.5	60	8.9x10 ⁸	15
Tank No.9	30.7	30	6.8x10 ¹⁰	2,300

According to *Danilyan et al. (2000b)*, the total LRW storage capacity of the TNT-27 as of January 2000 was 906.1 m³, very close to the figure reported by *Lavkovsky (2000)* and *Kobzev and Lavkovsky (2001)*. However, *Danilyan et al. (2000b)* reports a total activity of 0.033 TBq contained in 859 m³ on the TNT-27 in tanks 1-9 as of January 1, 2000. This is not consistent with the 0.86 TBq of activity in 570 m³ as of April 2000 reported by *Lavkovsky (2000)* and *Kobzev and Lavkovsky (2001)* in Table 2-10 above.⁸ In addition, the TNT-27 was reported to contain three storage containers totaling 4.5 m³ with a total activity of 0.026 TBq. However, *Danilyan et al. (2000b)* report 8 m³ of SRW containing 0.053 TBq of activity in SRW containers in the zone of controlled radiation safety in the form of filters and SRW containers.

⁸ In contrast, *Handler (1994a)* reports that the TNT-5 contained 794 m³ of waste containing 0.029 TBq and that the TNT-27 contained 905 m³ of waste containing 0.26 TBq as of March 1994.

Shore Facilities

There is no detailed information on radioactive waste inventories in shore facilities at Pavlovsk Bay. The only reported levels are found in *Danilyan et al. (2000b)*, summarized below.

Table 2-11: Radioactive Waste Inventories in Shore Storage at Pavlovsk Bay
(*Danilyan et al, 2000b*)

Object	Type of storage	Waste Type	Volume, m ³ (actual/capacity)	Aggregate activity, Bq
Dosimetric control service	Zone of controlled radiation safety	SRW	4/-	3.0x10 ¹⁰
Radiation safety service	Drainage tanks No 1,2	LRW	960 / 1000	7.1x10 ⁸

2.1.2 Bolshoi Kamen and the Far Eastern Plant Zvezda⁹

Bolshoi Kamen ("Big Rock") is a city of 80,000 which is centered on shipbuilding and repair works together with food industry and construction (see Figures 2-1 and 2-5). The town of Bolshoi Kamen adjoins closely to the territory of the Zvezda ("Star") shipyard. On the seacoast northeast from the town, there is a youth camp at a distance of 2.5 km from the territory of the shipyard. The central part of the town spreads along the seashore over the crest of a hill within the distance of 1.5 - 2 km from the sea. A reservoir is located to the east of the town about five kilometers from the shipyard. The land near the town is widely used by the city dwellers for agriculture, including for kitchen gardens and country houses.

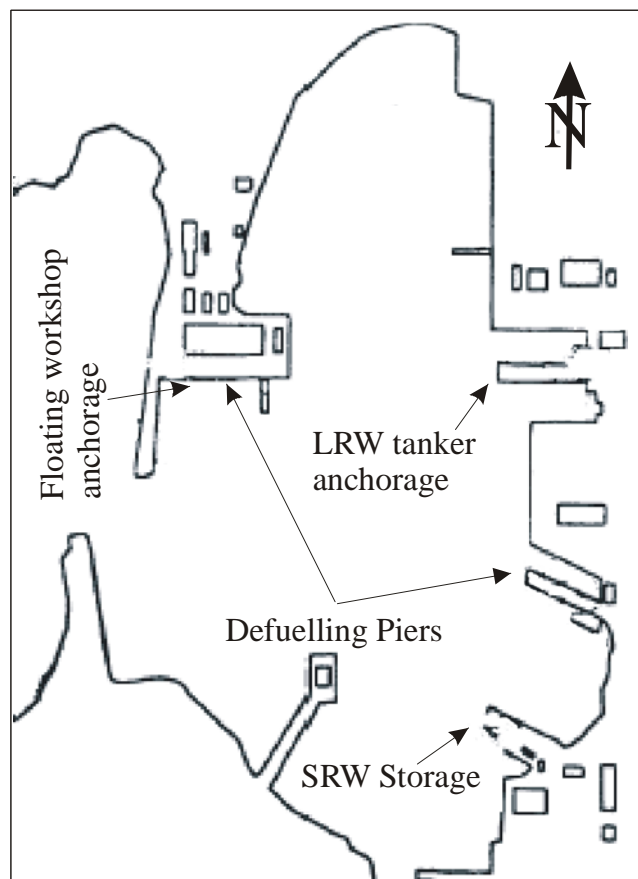


Figure 2-5: Far Eastern Plant Zvezda(adapted from Danilyan et al., 2000b)

⁹ The description of the surroundings of Bolshoi Kamen is taken from *Mordashev and Pechkurov (2000)*

The zone of the Far Eastern Plant Zvezda (Figure 2-5) comprises the bay of Bolshoi Kamen and the adjacent coastal area. The bay of Bolshoi Kamen is a part of the Ussury Gulf, located at 43°11' N, 132°20' E. The bay has a Ω-shaped form with a narrow inlet in the western side. The area of bay is 2.4 km² and the depth reaches 12 m in parts. The median tidal amplitude is 21 cm, but can range up to 60 cm. The exchange of water with the Ussury Gulf is limited. There is a weak (median speed 0.01 - 0.04 m/sec) and changeable counter-clockwise current in the bay. Bottom sediments are sandy and oozy. The shape and position of the bay make it a good shelter for vessels staying there even in the case of dangerous meteorological conditions near to the northwestern coast of the Sea of Japan. For region of the bay of Bolshoi Kamen southerly winds are prevailing in winter (October - March) and northeasterly winds are prevailing in summer (May - August). The median wind speed is 4 - 7 m/sec. In some areas, wind deflection from the prevailing direction is possible because of the local terrain. Strong gales in which the windspeed can exceed 14 m/sec are frequent, occurring more than seventy days per year. Recurrence of calm seas is less than 10% per year.

The terrain surrounding the bay of Bolshoi Kamen is ringed by small hills (50-70 m) which slope gently to the sea. The northern shore of the bay is higher than eastern, southern and southwestern shores. Main structures of the yard are located along the shores of the bay. The main part of industrial site is located on Cape Lagerny to the northwest of the bay. Before the beginning of construction works, the shores of Cape Lagerny were high and abrupt, with elevations of 20-25 m. There was a 34 m hill in the central part of the cape. These peaks have been leveled down to absolute marks of 2-3 m and the site has been occupied by industrial buildings.

Decommissioned Submarines

Bolshoi Kamen is the main site for decommissioning of nuclear submarines in the Russian Far East, and exact numbers of decommissioned submarines is thus subject to change depending upon the pace of decommissioning operations. As of 2000, six submarines and three three-compartment modules were located at the Zvezda Shipyard (*Danilyan et al, 2000b*). Of these, one was defueled, and the other eight were awaiting defueling. The estimated inventory in a typical submarine core was previously given in Table 2-1.

Floating Workshops

According to *Kuzin and Nikolsky (1996)*, the PM-74, a Project 2020 ("Malina" class) floating workshop designed by the "Iceberg" Central Design Bureau and built in 1985 by the 61 Communars Shipyard Production Association Nikolaev, is berthed at Bolshoi Kamen. A ship of the Project 2020 class is shown in Figure 2-6. According to *Zakharkin (1995)*, there were 1368 spent fuel assemblies in storage as of 1995. According to *Kobzev and Lavkovsky (2001)*, there were a total of 1368 fuel assemblies from two first generation cores and four second generation cores as of August 1998. There are 640 spent fuel assemblies (last criticality in 1991), comprising two first generation cores with a burnup of 10.4 GWd each and one second generation core with a burnup of 21 GWd. There were 728 spent fuel assemblies (last criticality in 1994) comprising three second generation cores with a burnup of 15.6 GWd. Based upon the preceding assumptions, data on the inventory of spent fuel and radioactive waste on the PM-74 is given in Table 2-12.

Table 2-12: Radioactive inventory in spent fuel assemblies onboard the PM-74 (*Kobzev and Lavkovsky, 2001*)

²³⁹ Pu	²⁴⁰ Pu	²⁴¹ Pu	²⁴¹ Am	⁹⁰ Sr	¹³⁴ Cs	¹³⁷ Cs	Total
3.8x10 ¹³	8.6x10 ¹²	5.3x10 ¹⁴	5.6x10 ¹²	1.4x10 ¹⁶	1.1x10 ¹⁵	1.5x10 ¹⁶	3x10 ¹⁶

Table 2-13: Radioactive inventory in liquid radioactive waste onboard the PM-74 as of April 2000 (*Kobzev and Lavkovsky, 2001*)

Storage description	Designed capacity, m ³	Filled in volume, m ³	Activity, Bq	Specific activity, kBq/L
Spent fuel assembly storage tank No. 1	40	32	4.1x10 ⁹	129
Spent fuel assembly storage tank No. 2	40	32	1.1x10 ⁹	3.44
Spent fuel assembly storage tank No. 3	40	32	6.6x10 ¹⁰	2,070
Spent fuel assembly storage tank No. 4	40	32	9.8x10 ⁹	307
Spent fuel assembly storage overflow tank	3.8	3.8	5.5x10 ¹⁰	14,400
Cooling water tank No. 1	82.6	4.6	1.0x10 ⁹	226
Cofferdam of cooling water tank No. 1		21	1.4x10 ¹¹	6,670

Danilyan et al. (2000b) reports a capacity of 637.2 m³ that contains 174.6 m³ of waste totalling 1.3 TBq in tanks and spent fuel storage compartments. This data is not consistent with *Kobzev and Lavkovsky (2001)*, who reports a capacity of 246.4 m³ and a total of 157.4 m³ of waste containing 0.28 TBq in all LRW storage tanks (*cf.* Table 2-13). As of April 2000, the vessel also contains 57 containers of SRW totalling 85.5 m³ with a total activity of 0.0047 TBq. However, *Danilyan et al. (2000b)* report a zone of controlled radiation safety containing 15.40 m³ with 14 TBq in containerized reactivity control rods.



Figure 2-6: Project 2020 ("Malina") Class Floating Workshop (Bellona, 1996)

According to *Lavkovsky (2000)*, the PM-74 is overdue for overhaul. The lifting cranes have been prohibited from use. Defective systems include radiation monitoring systems, the water shielding system, temperature monitoring system in spent fuel assembly Storage Tank № 2, sampling system, high pressure air system, and the vacuum-generating system. Operation has been prohibited by the Inspection of State Supervision for Nuclear Radiation Safety of Nuclear Power Plants of the Administration of State Supervision for Nuclear Radiation Safety, RF Defense Ministry.

Technological Tankers and Miscellaneous Support Ships

According to data from *Kuzin and Nikolsky (1996)* and *Lavkovsky (2000)*, the Project 11510 technological tanker (TNT) "Pinega", built in 1989, is also berthed at Bolshoi Kamen. The "Amur", a ship of the same class at the Pinega, is shown in Figure 2-7. The 122 m long, 17 m wide vessel displaces 8250 tons with a draft of 6.2 m. The vessel has a crew of 86 and can cruise for 4000 km at 14 knots, with a top speed of 15 knots. It can hold up to 685.6 m³ of LRW. The tanks of Pinega are allowed to store LRW with a specific activity of up to 370 kBq/L for low activity water and up to 370 MBq/L for high activity water. According to *Lavkovsky (2000)*, the LRW inventory, primarily composed of ⁹⁰Sr, ¹³⁷Cs, and ⁶⁰Co, is given in Table 2-14. Twelve tanks are installed for LRW storage on TNT "Pinega". In addition to the tanks listed below, there is also one 3.5m³ tank for high activity acidic wastes and one 5.1 m³ overflow tank.



Figure 2-7: The Project 11510 class technological tanker "Amur", sister ship to the "Pinega" (Bellona, 1996)

Table 2-14: Radioactive inventory in liquid radioactive waste onboard the "Pinega" as of April 2000 (*Kobzev and Lavkovsky, 2001*)

Storage description	Design capacity, m ³	Filled in volume, m ³	Activity, Bq	Specific activity, kBq/L
Tank No. 1 (low activity)	107.1	102	7.9x10 ⁹	78
Tank No. 2 (decontaminated water)	89.46	85.2	2.4x10 ⁹	29
Tank No. 4 (overflow)	11.24	10.7	6.7x10 ⁸	63
Tank No. 5 (low activity, alkaline)	203.7	194	3.1x10 ⁸	1.6
Tank No. 7 (high activity)	63.4	63	2.6x10 ⁹	41
Tank No. 9 (high activity, acid)	104.9	51	1.2x10 ⁹	23
Tank No. 12 (high activity, alkaline)	76.3	58	7.9x10 ⁸	14

Danilyan et al. (2000b) reports that the Pinega contains thirteen (instead of twelve) tanks for LRW with a capacity of 873.6 m³, and which contain 682.1m³ of LRW totalling 0.095 TBq of activity. This is in contrast with the twelve tanks with a total capacity of 656 m³, reported by *Kobzev and Lavkovsky (2001)*, which are reported to be filled with 564 m³ of LRW containing 0.016 TBq.¹⁰ In

¹⁰ *Handler (1994a)* reported that the Pinega contained 320 m³ of waste containing an unknown amount of radioactivity as of March 1994.

addition, *Danilyan et al. (2000b)* reports 42.6 m³ of solid radioactive waste containing 0.7 TBq of activity. This does not appear consistent with *Kobzev and Lavkovsky (2001)* who report a higher volume but a lower total activity. *Kobzev and Lavkovsky (2001)* reports that there is 46.3 m³ of solid radioactive waste containing 0.12 TBq of activity. It comprises twenty-five 1.5 m³ SRW containers containing a total of 0.078 TBq, four one m³ SRW containers containing a total of 0.00023 TBq, eleven 0.18 m³ compartmental radiation monitoring units containing a total of 0.00036 TBq, one 0.1 m³ mechanical filter and one 0.5 m³ decontamination tank each containing 37 MBq, two protective plugs containing a total of 2.2 MBq, four 0.1 m³ filtering device barriers containing a total of 0.0037 TBq, and nine filtering device barriers containing a total of 0.033 TBq.

According to *Kobzev and Lavkovsky (2001)* and *Shilgan (2001)*, three barges for LRW treatment or storage are berthed at Zvezda. These are the recently completed PZO-500 "Landysh", and two PE-50-Mr 002 floating cells (PEK-50), the PEK-50 No. 170 and the PEK-50 No. 171. The PZO-500 "Landysh" is intended for LRW processing. It is a single-deck non-self-propelled vessel with an ice-reinforced double hull and a three-layer deckhouse. The vessel was built in 2000 by Babcock and Wilcox Nuclear Environmental Services, Inc and the Amur Shipyard. It is capable of storing 1150 m³ of LRW in seven tanks of 50 m³ each (the tanks being equipped with a biological shielding made of reinforced concrete of 240-400 mm thickness) and four tanks of 200 m³ each. The barrels of solidified cement concentrate are stored in a special space in the cementation unit. PZO-500 tanks are allowed to store LRW provided that the specific activity does not exceed 370 kBq/L in the 200 m³ tanks and 370 MBq/L in the 50 m³ tanks. As of January 2001, the Landysh held 187 m³ of waste with a total activity of 0.032 TBq. The total specific activity of the waste was 170 kBq/L, comprising mainly ¹³⁷Cs (111 kBq/L), ⁹⁰Sr (12 kBq/L), and ⁶⁰Co (1.3 kBq/L).



Figure 2-8: PEK-50 floating LRW storage at the Far Eastern Plant Zvezda
(Handler, 1995. Photo credit: J. Handler)

The two floating cells PEK-50 No. 170 and PEK-50 No. 171, shown in Figure 2-8, were built in 1991 at the Zvezda Shipyard. The floating cells are non-self-propelled and unmanned floating structures with ice-reinforced hulls. Each PEK-50 is capable of storing 50 m³ of LRW at a full displacement of 131.2 tons. SRW storage on PEK was not intended. PEK tanks are allowed to store LRW with specific activity less than 370 kBq/L. As of January 2001, the PEK-50 No. 170 contained 50 m³ of LRW totalling 0.0082 TBq, with a specific activity of 163 kBq/L, comprising mainly ¹³⁷Cs (89 kBq/L), ⁹⁰Sr (16 kBq/L), and ⁶⁰Co (4.4 kBq/L). The PEK-50 No. 171 contained 40 m³ of waste with 0.033 TBq of activity, with a specific activity of 813 kBq/L (which exceeds the 370 kBq/L limit).¹¹ The majority of the waste is ¹³⁷Cs at 651 kBq/L.

Shore Facilities

According to *Kobzev and Lavkovsky (2001)*, the following shore facilities for radioactive waste storage are located at the Zvezda Shipyard. The launching slip (Object 103) contains a special tank section for LRW storage designed by the State Union Design Institute "Soyuzproektverf" that was commissioned in December 1975. It consists of two 20 m³ cells and one 3.2 m³ enclosure. The tanks are made of stainless steel, painted by oil paint, with no local protection. The enclosure is made of concrete covered by stainless steel. The special tank section is located in the cellar space one meter below ground level with 600mm thick concrete walls. As of April 2000, the two tanks contained 34 m³ of waste with an specific activity of 137 kBq/L and an aggregate activity of 0.0047 TBq, comprising mainly ¹³⁷Cs (100 kBq/L), ⁹⁰Sr (0.12 kBq/L), and ⁶⁰Co (4.8 kBq/L). The deactivation section (Object 121) contains a system for LRW storage designed by "Soyuzproektverf" that was commissioned in December 1969. It consists of two 20 m³ tanks. The tanks are made of stainless steel, painted by oil paint. There is no biological shielding, but the tanks are in an isolated cellar space. As of April 2000, the two tanks contained 30 m³ of waste with a specific activity of 11 kBq/L and an aggregate activity of 321 MBq comprising ¹³⁷Cs (2.5 kBq/L), ⁹⁰Sr (0.03 kBq/L), and ⁶⁰Co (4.4 kBq/L). In addition, the management and protection section of Object 121 contains another 1.7 m³ tank. The tank is made of stainless steel, painted by oil paint and without biological shielding. As of April 2000, the tank contained 1 m³ of waste with

¹¹ In contrast, *Handler (1994a)* reports that the two PEK-50s contained 80 m³ of waste containing 0.011 TBq as of March 1994.

a specific activity of 7.2 kBq/L for a total activity of 7.2 MBq comprising ^{137}Cs (1.02 kBq/L), ^{90}Sr (0.005 kBq/L), and ^{60}Co (0.03 kBq/L).

A temporary (although the design service life is undefined) storage site for SRW designed by Soyuzproektverf was commissioned in 1980. The site area is 3025 m² and is designated for storage of 600 m³ of SRW. The temporary storage site is located at the pier and is an open asphalt pad. Part of it is covered with shed with a removable roof. Along the perimeter of the site there is fencing made of 3 mm metal sheets. There are two reception appliances for collection and control of groundwater. As of April 2000, 53 m³ of wastes (tanks left after LWR storage, planks, and twelve containers) containing a total of 0.001 TBq were stored at the site. The isotopic composition of the wastes is 60-70% ^{137}Cs , 10-12% ^{90}Sr , 10-15% ^{60}Co , and 3-5% ^{54}Mn . A long-term reinforced concrete storage for SRW (object 130) designed by Soyuzproektverf was commissioned in 1964. The area is 450 m² with a storage capacity of 1530 m³. The walls are 600 to 1000 mm thick. There are no monitoring wells. The object was operated until 1968. As of April 2000, the facility contained 195 m³ of waste with a total radioactivity of 3.5 TBq. The compartment for high activity SRW houses in-bulk spent core rods and automatic control rods which give rise to an exposure rate at 3 m of 9 R/h. There are two compartments for low activity SRW such as rubbish, individual protection means, metal cuts etc. The isotopic composition of the wastes is estimated as the same as for the temporary storage site, namely 60-70% ^{137}Cs , 10-12% ^{90}Sr , 10-15% ^{60}Co , and 3-5% ^{54}Mn . The total shore storage reported in *Lavkovsky (2000)* comprises 3.5 TBq in 248 m³ of SRW and 0.005 TBq in 65 m³ of LRW. In contrast, *Danilyan et al. (2000b)* report only 230 MBq of activity in the zone of controlled radiation safety in the form of reactor internal components.

2.1.3 Chazhma Bay Ship Repair Facility

Chazhma Bay (see Figure 2-1) was the site of the most severe accident in the history of the Russian Pacific Fleet, as discussed above. Chazhma Bay is the site of a ship repair facility that was home of one non-defuelled decommissioned submarine as of January 2000 (*Danilyan et al. (2000b)*). Although there is some information on the contamination resulting from the 1985 accident in *Sivintsev et al. (1994)* and *Chaikovskaya et al. (2001)*, there is very little data on the waste stored there. *Kobzev and Lavkovsky (2001)* reports that the floating radiometric control stations PKDS-5 and PKDS-12, each of which are equipped with two 40 m³ tanks, are located at the Chazhma bay. The LRW storage tanks on the PKDS tanks are allowed to store LRW with specific activity less than 0.37 kBq/L. However, there are no data available from *Lavkovsky (2000)* and *Kobzev and Lavkovsky (2001)* on the inventories stored there. *Danilyan et al. (2000b)* reports that there are SRW containers contain 0.013 TBq in 4 m³, and that tanks 1 and 2 of the Radiation Safety Service (CPБ), with a design volume of 170 m³, contain 80 m³ of LRW with 640 MBq of activity. It is unclear if all the wastes and contaminated soil from the 1985 accident are stored onsite or if they have been transferred to the Cape Sysoeva Waste Facility.

2.1.4 Razboinik Bay Naval Station

Razboinik Bay (see Figure 2-1) is located across the inlet from Chazhma Bay. After submarines are dismantled into three-compartment units at the Zvezda Shipyard, they are towed to Razboinik Bay for storage (*Handler, 1995; cf. Figure 2-3*). This facility was home to nine decommissioned nuclear submarines and thirteen three-compartment units as of January 2000 (*Danilyan et al. (2000b)*). Of these, seventeen had been defuelled, and five were awaiting defuelling. There is also very little data on the wastes at Razboinik Bay. Table 2-15 gives data on the inventory of SRW at this facility taken from *Danilyan et al. (2000b)*.

Table 2-15: Radioactive Waste Inventories at Razboinik Bay
(Danilyan et al. (2000b))

Object	Type of storage	Kind of SRW	Volume, m ³	Aggregate activity, Bq
Division of long-term stored NS	Block-module № 416	Steam-generators, primary circuit components , pumps, reactor compartment internal components, etc.	11.0	3.1x10 ¹¹
	Block-module № 156		12.1	1.7x10 ¹⁰
	Block-module № 141		8.2	7.4x10 ⁰⁸
	Block-module № 908		3.0	7.4x10 ⁰⁸
	Zone of controlled radiation safety		2	2.8x10 ¹⁰

2.1.5 Cape Sysoeva¹² Naval Waste Facility

The Cape Sysoeva Naval Waste Facility, shown in Figure 2-9, is located on the southern tip of the Dunai Peninsula (see Figure 2-1). This site is also referred to by *Handler (1994a)* as the "Shkotovo Waste Site", "Military Unit 40752" or the "joint repair workshop". This facility contains the vast majority of all non-spent fuel waste in the Russian Far East. Contamination at the site is rather extensively discussed in *Danilyan et al. (2000a)*. According to *Lavkovsky (2000)*¹³, the following objects for radioactive storage are located in the Cape Sysoeva Waste Facility. For LRW transfer between the shore base and the technical support vessels there is an enclosure No.1 of the transfer system (pier) located near the service pier. Liquid radioactive wastes containing mainly ¹³⁷Cs, ⁹⁰Sr, ⁶⁰Co, and ¹⁴⁴Ce are stored in a tank farm containing six vertically installed tanks in an open area near Enclosure 1. Solid radioactive wastes are stored both in closed constructions and at open sites.

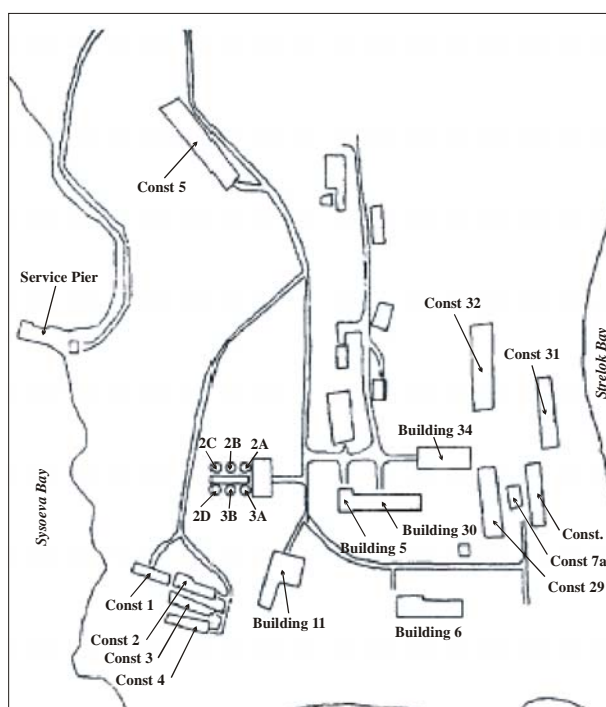


Figure 2-9: Cape Sysoeva Waste Management Facility
(adapted from Danilyan et al, 2000b)

¹² *Handler (1994)* reports this as being located on "Cape Maidelya" on the "Shkotovo Peninsula" rather than Cape Sysoeva on the Dunai Peninsula. The site is the same.

¹³ The location of this is given as "Pavloskogo Bay" in the spreadsheets from *Lavkovsky (2000)*. However, the facility names correspond exactly to those given for the Cape Sysoeva waste facility.

Constructions 1-5 are open concrete pads for storage of SRW. They currently contain 5000 m³ of waste, including soil with traces of radioactive contamination from the accidents in 1985-86, totaling 3,700 TBq (mainly ¹³⁷Cs- and ⁶⁰Co). Construction 29 is a closed storage designed to hold up to 2000 m³ of medium activity SRW. Construction 31 is a closed storage designed to hold up to 2500 m³ of high activity SRW. Construction 32 is a concrete pad for temporary storage of low activity wastes arranged at the stationary technological berth¹⁴. As of January 2000, it contained 1600 m³ of waste, including soil with traces of radioactive contamination from the accidents in 1985-86, with 1,200 TBq of activity. *Handler (1994a)* reports that Construction 31 contains ion exchange resins and contaminated equipment from a number of submarines, including the primary loop of the K-431 that suffered the August 1985 accident in Chazhma Bay. Water is reported to have leaked into this storage unit. He also reported that Construction 32 was built in 1992 and was used for storage of ion exchange resins, and notes that this facility was not reported to be leaking as of 1993.

Construction 7 is a closed (protected) storage of about 750 m² area designed to hold up to 2000 m³ of high activity SRW. *Handler (1994a)* reports that this facility was constructed in 1963, but was out of use by 1990. He reports that "damaged fuel assemblies that could not be packed into TUKs...and shipped to Chelyabinsk and other residue from the Chazhma Bay accident are in this burial...it is rumored that fuel rods that have changed shape or were too damaged to transport after removal from wet storage were put here". Although it is not possible to confirm that damaged spent fuel is buried here, the activity of 3,700 TBq reported by both *Danilyan et al. (2000a)* and *Lavkovsky (2000)* is consistent with this conjecture. It is also stated in the caption of Table 4 in *Danilyan et al. (2000a)* that an unspecified "accident" occurred at storage site 7. However, it is also reported the facility has been remediated, with the 560 tons of LRW being pumped out of the bays (possibly an indication that the storage site had leaked, allowing water to enter the facility), and that the "this source of contamination of the territory and water area has been liquidated". It is not clear if this means that the wastes have been removed or simply that the leaks have been sealed.

Construction 7a is a concrete pad for temporary storage of SRW with a capacity of about 750 m³. *Danilyan et al. (2000a)* refers to the contents of this facility as an "Assembly 26". This may refer to the fresh core that was ejected during the accident at Chazhma Bay, which is also referred to as Assembly 26: "...full active core in form of the special construction (assembly 26) with a freshly loaded nuclear fuel." (*Sivintsev, 2000a*).

Danilyan et al. (2000a) report that Buildings 5, 11, and 30 are used for spent fuel storage. However, the details of the construction are not given. We presume that spent fuel is stored in shipping casks inside these buildings. *Handler (1994a)* reports that the spent fuel assemblies were moved from wet storage in Building 5 to "storage site No. 30" after leaks were found in 1991 from one of the tanks of structure No. 5 for storage of spent fuel assemblies. This building may be similar to Building 5 at Andreeva Bay in the Russian Northern Fleet. He reports that "Buildings 29 and 30 contain the TUKs with spent fuel. No. 29 was built in 1981 and No. 30 in 1986. Both utilize dry storage of the fuel assemblies contained within the TUK shipping containers...These buildings can hold approximately 600 TUKs or some 1,200 containers together." (p. 16). Although the numbering is not the same as that given by *Danilyan et al. (2000a)* (who reports that Construction 29 is a SRW facility, not a SNF facility), it seems reasonable to conclude that facilities 11 and 30 contain spent fuel in dry storage in transport containers, particularly as *Lysenko et al. (2002)* report that "According to the practice of SNF treatment adopted in Russia, after removal from the ship reactors, SFA (*spent fuel assemblies*) are temporarily stored in the transport containers of TUK-18 or MBA type."

¹⁴ It can be noted that in contrast to the report of *Lavkovsky (2000)*, the location of Construction 32 given by *Danilyan et al. (2000a)* and shown in Figure 2-9 above is not near the service pier. Given that there is also an inconsistency in the reported inventories between these two sources, it could be that there are two facilities carrying the number "32".

A summary of the reported information is given below. There are inconsistencies between the inventories reported by *Danilyan et al. (2000a)* and *Lavkovsky (2000)*, most notably in the contents of Constructions 1-5 and 32 and Tank 3B.

Table 2-16: Information on Waste Inventories at Cape Sysoeva as of Jan 2000
(*Lavkovsky (2000)*, *Danilyan et al. (2000a)*)¹⁵

Storage location	Type of Material/Waste	Design capacity* (m ³)	Used Volume* (m ³)	Specific activity* (kBq/L)	Activity* (Bq)	Activity** (Bq)	Amount Entering Env (Bq)**
Building 5	Spent and fresh fuel assemblies						
	LRW, SRW					2.0x10 ¹²	1.5x10 ¹²
Constructions 1-5	SRW	5000	5000		3.7x10 ¹⁵	2.7x10 ¹²	3.7x10 ⁹
Building 6	Fresh fuel assemblies					2.2x10 ¹¹	None
Construction 7	SRW	2000	2000		3.7x10 ¹⁵	3.7x10 ¹⁵	7.4x10 ¹⁰
Construction 7a	SRW* Assembly 26**					-	None
Building 11	Spent fuel assemblies, SRW					8.1x10 ¹⁵	None
Construction 29	SRW	2000	1800		2.1x10 ¹³	2.18x10 ¹³	3.7x10 ⁹
Building 30	Spent fuel assemblies					1.3x10 ¹⁷	None
Construction 31	SRW	2500	895		2.2x10 ¹⁵	2.2x10 ¹⁵	None
Construction 32	SRW	2000	1600		1.2x10 ¹⁵	1.9x10 ¹¹	None
Construction No.2A	LRW	1000	837	130	1.1x10 ¹¹	3.0x10 ¹¹	3.7x10 ⁹
Construction No.2B	LRW	1000	510	120	6.0x10 ¹⁰		
Construction No.2C	LRW	200	188	7.8	1.5x10 ⁹		
Construction No.2D	LRW	100					
Construction No.3A	LRW	1000	550	270	1.5x10 ¹¹		
Construction No.3B	LRW	300	25	48,000	1.2x10 ¹²		

**Lavkovsky, 2000*

** *Danilyan et al., 2000a*

There also appear to be inconsistencies - albeit slight - between the values reported by *Danilyan et al. (2000a)* and *Danilyan et al. (2000b)*. In *Danilyan et al. (2000b)*, the site is reported to have a capacity of 3600 m³, of which 3165 m³ is filled with a total of 0.41 TBq of activity as of January 2000. The total volume of 3600 m³ appears to correspond to the total volume of the six LRW tanks (2A/B/C/D, 3A/B). However, *Danilyan et al. (2000a)* reports that these tanks contain 0.26 TBq of activity. However, the date of measurement is not reported in *Danilyan et al. (2000a)*, and the inconsistency may arise if the tanks are in use and the values refer to different dates. *Danilyan et al. (2000b)* also reports that a total SRW storage capacity of 16,500 m³ is available at the base, of which 14,923 m³ containing 9,900 TBq is present in the form of standard sources of ionizing radiation, cases, steam generators, filters of primary and third circuits of NPP, shells of protective rods, main circulation pumps of primary circuit, circulation pumps of other circuits etc.

2.2 Kamchatka Oblast

The Kamchatka Region (Figure 2-10) is a mountainous peninsula of approximately 171 thousand km² lying between the Sea of Okhotsk on the west and Pacific Ocean and Bering Sea on the east. The central and southern parts of the Kamchatka Peninsula are subject to a frequent seismic activity and have more than 20 active volcanoes.

¹⁵ The location of this is given as "Pavloskogo Bay" in *Lavkovsky (2000)*. However, the facility names, and in some cases the activity levels, correspond exactly to those given for the Cape Sysoeva waste facility.

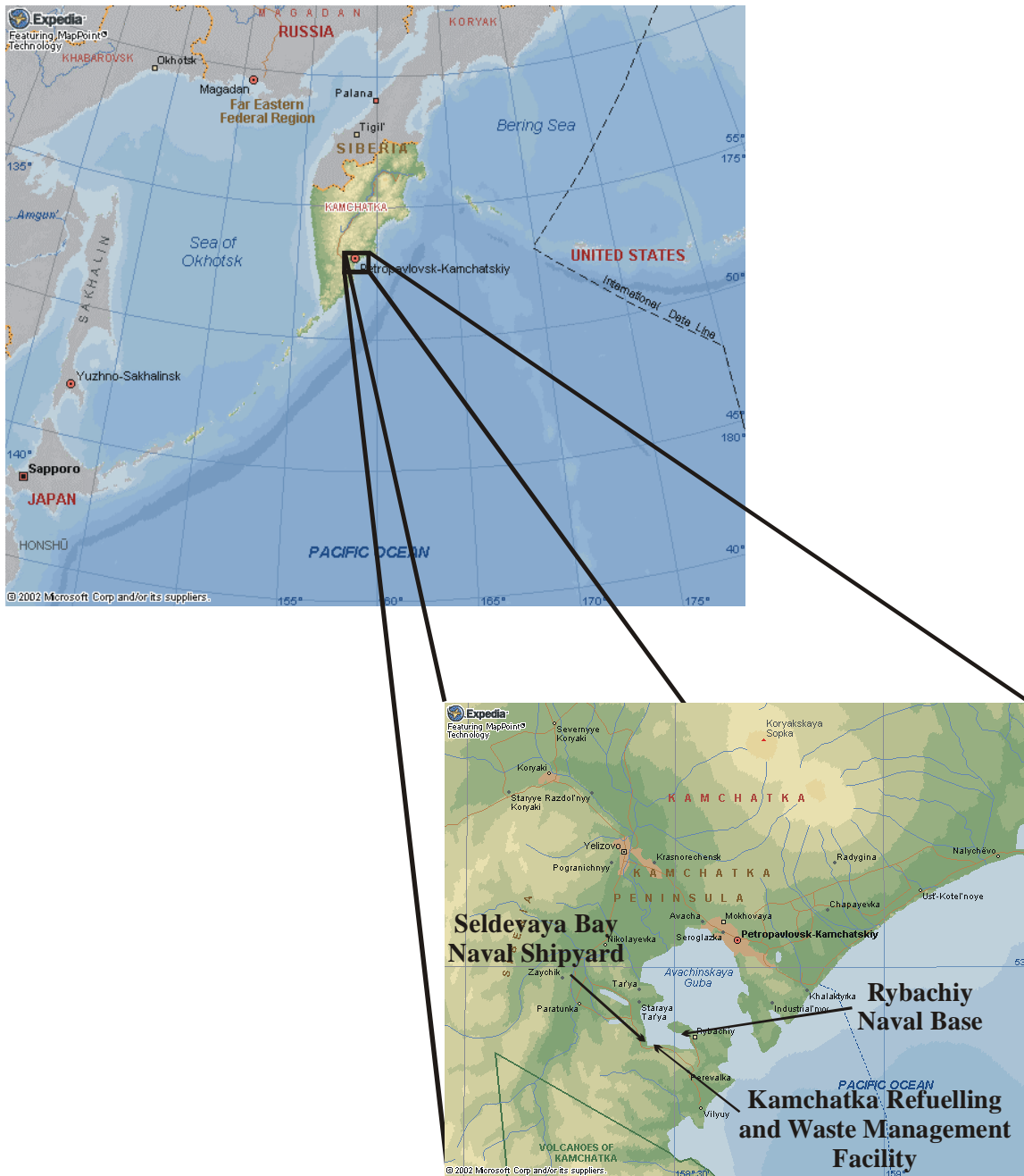


Figure 2-10: Map of Kamchatka Oblast (inset shows naval facilities) (map source: www.expedia.com)

There is considerably less information about the facilities near Petropavlovsk, and the identification of individual facilities given below is provisional. Reports of naval nuclear support facilities in the Kamchatka Oblast mention Seldevaya Bay, Gornyyak Shipyard, Shipyard 30, Primorye, Primorskoe, Petropavlovsk-55, Rybachi, and Vilyuchinsk-3. All of these facilities are located on the shores of Krasheninnikov Bay, as shown below. There appear to be three separate facilities: a shipyard on Seldevaya Bay, a refuelling and waste management facility similar to that located on Cape Sysoeva, and a naval base on the Vilyuchinsk peninsula.

2.2.1 Seldevaya Bay Naval Shipyard

The Seldevaya Bay Naval Shipyard is also referred to by *OTA (1995)* as "Shipyard 30" and the "Gornyak Shipyard" and by *Handler (1994a)* as Gornyak, Primorskoe and Petropavlovsk-55. *Danilyan et al. (2000b)* refers to this site as the "Primorskii ship repair plant" (Table 18) and as the "Town of Primorskii" (Table 19) and reports that it contains a PKDS (floating radiometric control station) with 20.6 m³ of SRW in containers, totalling 0.067 TBq, and 50 m³ of LRW with a total of 0.017 TBq in tanks 1-4 (with a total capacity of capacity of 73.5 m³) of the Radiation Safety Service. This description appears to correspond to the PKDS-60 in Seldevaya Bay reported by *Lavkovsky (2000)* and *Kobzev and Lavkovsky (2001)*, which is reported to contain 25.6 m³ of SRW containing 0.058 TBq and 59.5 m³ of LRW containing 220 MBq. Details are provided in Table 2-17. LRW on PKDS-60 is stored in two 25-m³ tanks and two 10-m³ tanks for high purity water. Low-activity SRW on the PKDS is stored in the storage facility. SRW in containers is allowed to be stored at the open deck. Although the PKDS tanks are officially only allowed to store LRW with specific activity less than 0.37 kBq/L, three of the four tanks exceed the allowable limits.

Table 2-17: Inventory of the LRW on the PKDS-60 as of April 2000 (*Lavkovsky (2000)* and *Kobzev and Lavkovsky (2001)*)

Storage description	Design capacity, m ³	Filled volume, m ³	Activity, Bq	Specific activity, kBq/L
Tank No.1	25	20	1.48x10 ⁰⁸	7.4
Tank No. 2	25	20	2.96x10 ⁰⁷	1.5
High purity water tank	10.5	10	1.85x10 ⁰⁶	0.19
Transportation tank	10	9.5	3.34x10 ⁰⁷	3.5

In addition, *Lavkovsky (2000)* and *Kobzev and Lavkovsky (2001)* report that there are eight 1 m³ SRW containers containing 630 MBq, one 0.6 m³ sorption column containing 0.011 TBq, three 3 m³ solidified processed LRW packages containing 0.016 TBq, two 1 m³ primary circuit circulation pumps containing 740 MBq, and an SRW storage facility containing 6 m³ of SRW with a total of 0.029 TBq.

2.2.2 Kamchatka Refuelling and Waste Management Facility

A refuelling and waste management facility (referred to by *Handler (1994a)* as Military Unit 95051 and also as "Ground 3") is located on the southern shore of Krashenninikova Bay. According to *Handler (1994a)*, the site opened in 1963-1964 and encompasses 50 km² in total. The actively used area comprises about 4-5 km² and contains three burial trenches, two piers, and facilities for refuelling and defuelling. This facility appears to be the Kamchatka equivalent of the Cape Sysoeva facility in Primorskoe Territory.

Danilyan et al. (2000b, Table 2) reports that there are five defuelled nuclear submarines and no three-compartment blocks at "Bukhta Seldevaya", which we presume is the waste management and refuelling facility.

According to *Lavkovsky (2000)*, there were two covered waste storage facilities at this site as of January 2000. Each is designed to contain 1700 m³ of SRW in an area of 600 m². Construction 16 is a high activity waste storage that contained 250 m³ of waste with a total activity of 56 TBq as of January 2000. Construction 19 is a storage site for low activity waste that is reported to contain 100 m³ of waste with an activity of 2,200 TBq. In addition, there is a burial site designed for storage of up to 600 m³ of medium activity SRW beyond the territory of the base. It currently contains 600 m³ of waste with a total activity of 6.9 TBq. This amounts to a total of 4000 m³ of storage capacity with 950 m³ in use containing 2,200 TBq. In contrast, *Danilyan et al. (2000b)* reports that there is a total of 833.5 m³ of SRW at the base out of a total capacity of 3300 m³. The

wastes are reported to consist of standard ionizing radiation sources, cases, steam generators, ion exchange cartridges, shells of protective rods, containers, etc. The total activity is reported as 59 TBq. This is considerably lower than the total of 2,200 TBq reported by *Lavkovsky (2000)*, 97% of which is reported to be in Construction 19. However, it could be that the value reported by *Lavkovsky (2000)* for Construction 19 is a misprint.

These are most likely the three burial sites reported by *Handler (1994a)*; however, it is impossible to determine which facility in his report corresponds to which facility reported by *Lavkovsky (2000)*. *Handler (1994a)* reports that there are two "new" burial sites opened between 1984-1987, both of which are approximately 80 m x 40 m and 4.5 m deep and containing four sections. The site was reported to hold LLW such as contaminated trash and equipment as well as spent ion-exchange resins. Although designed to be watertight, he reports that 80% of the cells have water in them. He also reports on an "old" burial site referred to as the "burial site for high-level waste" which had ceased operations by 1987. He reports that items which may be in this trench include metal containers containing damaged fuel and old neutron sources. This site is the suspected source of leakage of radioactivity. The same reference describes several other facilities, including a temporary dry storage facility, a fresh fuel storage facility, and a spent fuel facility known as Building № 5 intended for wet storage of spent nuclear fuel. However, it has apparently never been used for this purpose and now houses the defuelling machine belonging to the base. These facilities are not mentioned by *Lavkovsky (2000)*, *Kobzev and Lavkovsky (2001)*, or *Danilyan et al. (2000b)*.

Danilyan et al. (2000b) report that there are three service ships docked at nuclear support facilities in Kamchatka, all apparently at the refuelling and waste site. These are the PM-32 floating workshop and the two Project 1783A technological tankers TNT-23 and TNT-42 (also designated as the BNS-204900). According to *Lavkovsky (2000)*, the "Bay of Krashenninikov" (which we presume refers to the Seldevaya Bay Waste Management Facility) is home to the PM-32, the TNT-23, the TNT-27, and the TNT-43. As previously noted, the TNT-27 is elsewhere reported as being berthed at Pavlovsk Bay Naval Base, and we presume that it is currently located at Pavlovsk Bay.

The PM-32 is a Project 326 non-self propelled floating workshop designed by the "Iceberg" CDB and built in 1966 by the 61 Communars Shipyard Production Association Nikolaev. Forward storage and aft storage compartments for spent fuel were installed in the fourth compartment in 1966. Each compartment has 410 holders for spent fuel assemblies. The spent fuel assemblies stored onboard the PM-32 are wedged, damaged, and in an emergency condition. There is some inconsistency in the reported amount of fuel onboard the PM-32. According to *Zakharkin (1995)*, there were 126 fuel assemblies as of 1995. This is also the figure used by *Kobzev and Lavkovsky (2001)* in which it is reported that the operation of the spent fuel assemblies onboard the PM-32 was completed not later than in 1969 and that the total activity is 2,300 TBq. The activity given in Table 2-18 is based upon the assumption that they have reached the design generation. However, *Lavkovsky (2000)* reports that the spent fuel assembly storage houses 126 damaged spent fuel assemblies in the bow storage plus an additional 101 spent fuel assemblies in the aft storage, totalling 1,800 TBq. The results of both assessments are given below. The point may however be moot, as it was planned to unload the PM-32, and *Sivintsev (2000a)* reports that a considerable portion had already been extracted. The level of activity of the LRW is not consistent between the two available sources. *Danilyan et al. (2000b)* reports that out of a capacity of 388.6 m³, 47 m³ of LRW containing 210 TBq of activity is present in Tanks No 1-4 and montejesus. However, *Lavkovsky (2000)* reports only roughly a third of that amount (60 TBq total) is present in 49 m³. In any event, it is clear that the PM-32 is a major source of LRW. According to the data of *Danilyan et al. (2000b)*, the water in the spent fuel storage tanks of the PM-32 contained 95% of the LRW (by activity) in the Russian Far East - including the shore-based LRW facilities. With respect to solid waste, *Lavkovsky (2000)* reports that there was one 5-m³ SRW container containing 0.033 TBq of activity stored onboard the PM-32 as of April 2000. This is the same as that reported by *Danilyan et al. (2000b)*. The PM-32 is in critical condition, having probably the most severe

contamination problems of all the Russian Pacific Fleet floating workshops. The degree of damage to the spent fuel assemblies is indicated by the fact that the specific activity of the water in the forward spent fuel storage tank increased by a factor of fifty over a period of two months. The last routine repair was conducted in 1979, and a partial repair docking was conducted in 1994. Hull corrosion is severe, reaching up to 30% at the waterline. Corrosion has also destroyed most of the equipment inside the hull. The gamma-background in the spent fuel assembly storage compartment is 40 mR/h and beta-contamination is 1500 dpm/cm². The exposure rate is 400 mR/h in the refrigeration plants spaces and fourth compartment hold, 30 mR/h in the sewage tank room, 20 mR/h in the water flushing room, 18 mR/h on the aft bulkhead of the third compartment, 15 mR/h on the forward bulkhead of the 5th compartment, and 10 mR/h on the upper deck of the fourth compartment in the strict control zone. The level of radioactivity in the cooling water is 890 MBq/L in the forward spent fuel assembly storage tank and 2900 MBq/L in the aft spent fuel assembly storage tank. The state of special systems in the spent fuel assembly storage units is unsatisfactory, as all of the systems to ensure nuclear and radiation safety and monitoring systems are defective due to long-term operation and absence of repair.

Table 2-18: Assessment of activity in spent fuel on the PM-32

	²³⁹ Pu	²⁴⁰ Pu	²⁴¹ Pu	²⁴¹ Am	⁹⁰ Sr	¹³⁴ Cs	¹³⁷ Cs	Total
<i>Lavkovsky (2000)</i>	2.2x10 ¹²	3.6x10 ¹¹	5.0x10 ¹²	6.7x10 ¹¹	7.6x10 ¹⁴	2.6x10 ¹⁴	8.0x10 ¹⁴	1.8x10 ¹⁵
<i>Kobzev and Lavkovsky (2001)**</i>	8.6x10 ¹¹	9.7x10 ¹¹	3.7x10 ¹³	3.5x10 ¹²	1.1x10 ¹⁵	5.7x10 ¹⁰	1.2x10 ¹⁵	2.3x10 ¹⁵

* Conservative assessment based on 227 spent fuel assemblies (126 forward, 101 aft).

** Based upon data from *OKBM (1998)* and 126 spent fuel assemblies

Table 2-19: LRW on the PM-32 (*Kobzev and Lavkovsky, 2001*)

Storage description	Designed capacity, m ³	Filled in volume, m ³	Activity, Bq	Specific activity, kBq/L
Bow spent fuel assembly storage tank	12.3	12	2.2x10 ¹²	1.8x10 ⁵
Aft spent fuel assembly storage tank	12.3	12	5.8x10 ¹³	4.8x10 ⁶
Sewage water tank No.1	23.5	13.5	5.0x10 ⁹	370
Sewage water tank No.2	23.5	11.8	1.0x10 ¹⁰	850

According to *Danilyan et al. (2000b)*, the Project 1783A technological tankers TNT-23 and TNT-42 are berthed at Seldevaya Bay ("Bukhta Sel'devaya"). According to data from *Kuzin and Nikolsky (1996)* and *Lavkovsky (2000)*, each of these vessels is 74.4 m long and 12 m wide, and displaces 2300 tons at a draft of 3.95 m. The vessels require a crew of 33, and can cruise for 1000 km at a speed of 9 knots. Top speed is 11 knots. The tanks of special-purpose tankers are allowed to store LRW with specific activity up to 0.37 kBq/L.

The TNT-23, built in 1968, has a design LRW capacity of 877.2 m³ consisting of eight tanks. The inventory onboard the TNT-23 is reported in *Lavkovsky (2000)* and *Kobzev and Lavkovsky (2001)* and is fairly consistent with the value reported by *Danilyan et al. (2000b)*, who reports a filled LRW volume of 678.66 m³ with a total radioactive inventory of 1.4 TBq contained in Tanks 1-9. However, it can be noted that the activity levels in the LRW on the ship exceed the allowable levels considerably, by over four orders of magnitude in some cases. *Danilyan et al. (2000b)* also reports that there is 1.3 m³ of SRW containers in the "Zone of controlled radiation safety" containing 0.026 TBq.

Table 2-20: LRW onboard the TNT-23 (*Kobzev and Lavkovsky (2001)*)

Storage description	Designed capacity, m ³	Filled in volume, m ³	Activity, Bq	Specific activity, kBq/L
Tank No.1	105	55.8	3.3x10 ¹⁰	590
Tank No.2	105	46.9	4.0x10 ¹⁰	850

Tank No.3	124.3	104	8.9×10^{09}	85
Tank No.4	124.3	112	5.0×10^{11}	4,400
Tank No.5	114.8	101	6.7×10^{11}	6,700
Tank No.6	114.8	100	7.8×10^{10}	780
Tank No.7	94.5	88.9	4.6×10^{10}	520
Tank No.8	94.5	69.8	1.3×10^{11}	1,900
Total	877.20	679	1.5×10^{12}	

The TNT-42, built in 1968, has a design LRW capacity of 966 m³ in nine tanks. The inventory onboard the TNT-42 is reported in *Lavkovsky (2000)* and *Kobzev and Lavkovsky (2001)*. It appears that the vessel has been essentially emptied, as can be seen from the "filled volume" column. The vessel holds a total of 0.8 m³ of LRW with 130 MBq of activity, which in comparison with the other tankers is essentially empty. This would appear consistent with *Danilyan et al. (2000b)*, who appears to report that the TNT-42 is empty. However, because there is no data for Tanks 1,4 or 9 given in *Lavkovsky (2000)* and *Kobzev and Lavkovsky (2001)*, this cannot be confirmed.

Table 2-21: LRW onboard the TNT-42 (*Kobzev and Lavkovsky (2001)*)

Storage description	Designed capacity, m ³	Filled in volume, m ³	Activity, Bq	Specific activity, kBq/L
Tank No.1	120			
Tank No.2	120	0.2	4.8×10^7	240
Tank No.3	120	0.2	9.6×10^6	48
Tank No.4	120			
Tank No.5	120	0.1	2.6×10^7	260
Tank No.6	120	0.1	2.7×10^7	274
Tank No.7	118	0.1	1.7×10^7	170
Tank No.8	118	0.1	4.4×10^6	44
Tank No.9	10			

2.2.3 Rybachy Naval Base

There is relatively little information on the Rybachy Naval Base (Vilyuchinsk-3). *Danilyan et al. (2000b)*, Table 2) reports that there are seventeen nuclear submarines and no three-compartment blocks at the "Bukhta Krasheninnikov", which we presume is the naval base. Three of these are defuelled and fourteen still contain fuel. The estimated inventory of a single reactor core was previously given in Table 2-1. The following information is given for the "Town of Rybachiy" in *Danilyan et al. (2000b)*

Table 2-22: RW at the Rybachy Naval Base (adapted from *Danilyan et al, 2000b*)

Object	Type and No of storage or capacity.	Volume, m ³ (total/currently filled)	Aggregate activity, Bq
Dosimetric control service	Zone of controlled radiation safety, SRW Containers	1	1.5x10 ⁰⁹
Radiation safety service	Tanks No 1,2	1000 / 52.3	1.0x10 ⁰⁸
Blocks*		- / 76.7	1.6x10 ¹⁰
Withdrawn NS	Apparatus enclosure, Driving gears and directors of reactivity control system	- / 3.1	6.7x10 ¹⁰

*may refer to components from decommissioned submarines; cf. Table 2-15 for information at Razboinik Bay

2.3 Spent Fuel Storage Characteristics¹⁶

Spent fuel in the Russian Pacific Fleet is stored both afloat and ashore. There are two classes of ships in the Russian Pacific Fleet that contain spent fuel. These ships are known as "floating workshops" ("plavuchaya masterskaya"). The Project 326 class ships are non-self propelled barges converted for use in refuelling nuclear submarines. The Project 326M class ships are Project 326 barges with upgraded spent fuel handling and containerized storage facilities. The later class of ships (Project 2020) was designed for submarine support. Ships of this class are self-propelled. These are discussed in more detail below. In addition, the transport casks presumed to be used for shore-based storage are discussed below.

2.3.1 Shore Based Storage in Transport Casks

In *Lysenko et al. (2002)*, it is reported that the land-based storages rely on interim dry storage in transport casks. Four types of special casks for holding and shipping spent nuclear fuel from naval reactors have been identified: TUK-11s, TUK-12s, TUK-12/3s, and TUK-18s. The first three types are old spent fuel shipping containers. TUK-11s are thick-walled hermetic cylinders made of corrosion-resistant steel, 2.8 m long and 0.9 m in diameter. TUK-12s are of similar construction, although longer and thinner: 3.5 m long and 0.7 m in diameter. Each TUK consists of two parts: a protective cover (the outward container) and a closed cylinder (internal casing). TUK-18s consist of a large thick-walled hermetic cylinder made of corrosion-resistant steel and an extricable part holding seven smaller cylindrical ChT-4 cases. The large cylinder is 4.7 m long and 1.4 m in diameter with 300 mm thick sidewalls. The extricable part holding the ChT-4 cases is 780 mm in diameter. Each ChT-4 case holds seven fuel assemblies and weights 265 kg when empty. The entire TUK-18 cask with the ChT-4 case then holds 49 spent fuel assemblies and weighs 40 MT when fully loaded. Using the data given in Table 2-1 on the inventory of a typical submarine core three years after shutdown, and assuming that each core contains 287 spent fuel assemblies, the typical inventory of TUK-18 loaded with spent fuel is provided in Table 2-23.

Table 2-23: Estimated isotopic inventory (Bq) of a TUK-18 fully loaded with spent fuel

Radionuclide	²³⁸ Pu	²³⁹ Pu	²⁴⁰ Pu	²⁴¹ Pu	²⁴¹ Am	⁹⁰ Sr	¹³⁴ Cs	¹³⁷ Cs	¹⁴⁴ Ce	¹⁰⁶ Ru
T _{1/2} years	87.7	24100	6540	14.4	432	29.1	2.06	30	0.78	1.01
Inventory (Bq)	7.0x10 ¹²	1.1x10 ¹²	7.0x10 ¹¹	1.9x10 ¹⁴	1.9x10 ¹²	7.2x10 ¹⁴	3.2x10 ¹⁴	8.4x10 ¹⁴	3.9x10 ¹⁴	5.5x10 ¹³

¹⁶ Data on characteristics of support ships is summarized from *Kobzev and Lavkovsky (2001)* unless otherwise noted.

2.3.2 Project 326 Class Floating Workshops

This class of ship comprises barges converted for nuclear service. The modifications necessary for nuclear service were designed by the CDB "Iceberg" and carried out by the 61 Communars Shipyard Production Association Nikolaev. Each vessel is 92 m long and 13.4 m wide, with a full displacement (4000 ton) draft of 4.5 m, and requires a crew of 59.

On Project 326 class barges, spent fuel is stored in two compartments, arranged fore-and-aft (Drawing 326-490.2-2-1, CDB "Iceberg", St. Petersburg). Each compartment contains a tank that can contain up to 287 spent fuel assemblies in stationary holders. The total spent fuel capacity of the floating workshop is therefore approximately 574 spent fuel assemblies, which represents approximately two cores of a first- or second-generation nuclear submarine. Each floating workshop can therefore manage the fuel from one first or second-generation submarine.

The storage is arranged in a specially shielded compartment in the forward part of the workshop between frames Nos. 36 and 49. The forward compartment is 7.8 m long and about 6 m wide. The storage compartment is fitted with a double hull to reduce the likelihood of the loss of the storage tightness in the event of the workshop grounding or in case of collision with another vessel. The space between the primary and secondary hull is about 1 m. There are also 3 m wide side cofferdams. A biological shield is fitted to the tank and is made of steel with a thickness of 400 mm on the bottom and 500 mm on the sides and top.

The tanks have a diameter of about 2.5 m and a height of about 2 m. The stationary holders are arranged along six circumferences. The tops of the stationary holders are affixed to the tank cover. The bottom of the holders are held in place by a space grating that keeps them in place, preserving the assigned distance between them. The system allowing loading of spent fuel assemblies into the holders comprises a system of guiding gears above the tank roof that are remotely rotated with the help of an electric drive. The biological shielding is fitted with 6 removable plugs for loading of spent fuel assemblies to the holders. The holders are arranged in six circles with radii corresponding to the removable plugs. A 600 mm diameter cylindrical coolant water-distributing device is installed in the central part of the tanks. High-purity distilled water is used as cooling water. Water is supplied to the distributing device from the bottom. In its top part there are outlets for release of cooling water for spent fuel assemblies. The cooling water is removed from the tanks through the conic bottom part of the tanks near the distributing device. Arrangement of cooling water supply and removal through the tank bottom allows their drainage without installation of additional systems or devices. The cooling water system includes both primary and backup heat exchangers cooled by seawater from the general ship cooling system, primary and backup VTsN-80 circulation pumps, and pipelines with shut-off fixtures. The VTsN-80 circulation pumps can supply 50 m³/h of water at a head of 80 m. The storage compartments are equipped with a ventilation system that is connected to the ventilation system of the strict control zone. The ventilation system is fitted with fine filters and exhausts through the top of the foremast.

Project 326 and 326M class barges have essentially the same systems for LRW and SRW storage. The LRW and SRW storage facilities have no special-purpose cooling systems. Air-conditioning systems are installed in the spaces where tanks with LRW or containers with SRW are located if operating conditions require long-term presence of personnel in them. All tanks with LRW and spaces for SRW storage are serviced by a uniform ventilation system of the strict control zone with air release in the top of the foremast after its passage through fine filters. LRW specific activity should not exceed the following values:

Table 2-24: Permissible levels for liquid radioactive waste storage on PM-326 floating workshops

System	Allowable Level, kBq/L
Circuit water tanks	3.7×10^5
Spent fuel assembly tanks, equipment post-decontamination water tanks, over-flow spent fuel assembly and control ones	3,700
Waste and treated water tanks	37
Special laundry and special shower water tanks	0.37

SRW storage facilities comprise a special storage with five containers for storage of 2 sets of spent containers for the control and shielding system, thermometers and suspensions with ionisation chambers. Storage of SRW in containers is allowed on the upper deck of the workshop, if required.

2.3.3 Project 326M Class Floating Workshops

The Project 326M class barges are modified Project 326 class barges (hence the "Project 326M" designation) that were refitted between 1970 and 1975. The retrofit primarily affected the spent fuel storage tanks, as shown in "Storage facility for spent technological channels, drawing 326M-283-06, CDB "Iceberg", St. Petersburg). Instead of 287 stationary holders, 41 ChT-4 removable containers were installed in the storage tanks. Each container contains seven spent fuel assemblies of first- or second-generation nuclear submarines. The total spent fuel capacity of the floating workshop is therefore approximately 574 spent fuel assemblies, which represents approximately two cores of a first- or second-generation nuclear submarine. Each floating workshop can therefore manage the fuel from one first- or second-generation submarine.

The spent fuel storage tanks are larger, with a diameter of about 2.8 m and a height of about 3 m. The removable containers are arranged along 3 circumferences and are held in position by top and bottom space gratings. The upper biological shielding is penetrated by openings for loading containers to the tank. These openings are coaxial to the openings in the space gratings and are closed by protective plugs, which also allow fixing of the containers in the tank with sealing of the holder - upper space grating assembly. The tanks are filled with high purity distilled water. A cylinder with openings in the top and bottom is welded into the center of the tank and contains a heat exchanger for cooling the tank water. Forced circulation of tank water is not provided. Cooling water is supplied and removed from the heat exchanger through the top above the biological shielding. A fresh water circuit cools the heat exchangers in the tank with both primary and backup NTsV-63/30 electric pumps. The freshwater cooling loop contains a primary and a backup heat exchanger that are cooled by seawater from the general ship cooling system. A water level signalling device and a thermal gauge are installed to allow monitoring the water temperature and the level of water in the spent fuel storage tank. The removable containers are also filled with high purity distilled water and are sealed hermetically by a cover. A pipeline running from the center of the tank bottom to its sidewall is used for filling and draining the tanks. As in the Project 326 class barges, the storage compartments are equipped with a ventilation system that is connected to the ventilation system of the strict control zone. The ventilation system is fitted with fine filters and exhausts through the top of the foremast.

The systems for LRW and SRW storage are essentially the same as those on the unmodified PM-326 class ships, as discussed in the previous section.

2.3.4 Project 2020 ("Malina") Class Floating Workshops

The Project 2020 class floating workshops represent a newer generation of support ships which were designed for servicing (including defueling and refueling) of nuclear submarines. A Project

2020 Class ship was shown in Figure 2-6. The vessels are 137.8 m long and 21 m wide with a full displacement draft of 7 m at the full displacement of 13,900 tons. The vessel requires a crew of 218 and can cruise for 45 days or 13,000 miles at a speed of 10 knots. The top vessel speed is given as 11.5 knots.

The spent fuel assembly storage facility (Drawing 2020-283-088SB, CDB "Iceberg", St-Petersburg) on the workshop consists of 4 compartments (tanks), each of which can house 51 ChT-4 removable containers similar to those on the project 326M vessels. Although *Kobzev and Lavkovsky (2001)* states that these ships are designed to hold 582.1 m³ of LRW and cores from one nuclear submarine or one surface vessel, the reported inventories and the description above indicate that they are capable of storing considerably more. It would appear that the capacity is approximately 1428 spent fuel assemblies, or approximately five first/second generation cores (at least two nuclear submarines).

Each compartment is rectangular with a length of about 2.8 m, a width of about 3.5 m, and a height of about 4.8 m. The total cooling water volume is approximately 32 m³. The biological shielding is constructed of 400-500 mm thick steel. A 650 mm diameter cylindrical cooling water distribution device is welded at the centre of the compartment. It has up to 4 oval orifices of 400 x 200mm size each in the top and bottom parts, in which a heat exchanger for cooling the water in the compartment is installed. The cooling system is chilled by seawater from the ship general cooling system with the aid of two NTsV-160/20A-P pumps and two TK600/90-1 heat exchangers. The water level and temperature in the compartment are monitored. A pipe line for filling and draining of the compartment is also installed. The cooling and ventilation systems are similar to those of the project 326M workshops.

The liquid radioactive waste storage capacity of the Project 2020 class workshops comprises four 40 m³ compartments (tanks) for spent fuel assemblies, a 3.8 m³ overflow tank for the spent fuel assembly storage tanks, a 33.5 m³ decontamination water tank, two tanks (57 m³ and 20.5 m³) of acid (post-decontamination) waste waters from spaces, two tanks (24.5 m³ and 29 m³) of alkaline (post-decontamination) waters, a 29 m³ special laundry water tank, an 18.2 m³ sanitary control station water tank, three treated water tanks (two 82.6 m³ tanks and a 29 m³ tank), and two 6.2 m³ control (inspection) tanks.

For solid radioactive waste storage, there are four shielded special cells for storage of containers from the control and shielding system, thermometers, and suspensions of ionisation chamber and thermocouples; a container in a space for preparation of the dismantled equipment; and special cells for SRW storage.

2.4 Conclusions

There are significant variations between reported descriptions of the radiological situation in the Russian Far East. The task of developing a reliable source term is hampered by the variety of names used to refer to different facilities, the inconsistencies between reported inventories from different sources, and the omissions in reports of important facilities. For example, any discussion of the spent fuel situation at the Russian Pacific Fleet bases that did not include Building 30 would miss the largest single source in the Russian Far East¹⁷. There are no data on spent fuel storage on shore in Kamchatka. It is unclear if this is because there is no spent fuel in storage at Kamchatka

¹⁷ Consideration of SNF aboard all non-defuelled submarines at a facility could yield higher total inventories. However, it is difficult to imagine a common mode failure that would affect all submarines, or even more than one core on a single submarine. In contrast, depending upon the conditions of storage, all stored fuel elements in a single building could be affected by a common mode failure, such as an airplane crash or a major fire. There is also presumably considerably less provision for containment in the spent fuel storage buildings. When submarines are laid up, the spent fuel is isolated from the environment by at least two major barriers: the reactor pressure vessel and the pressure hull of the submarine, which is designed to be made air- and watertight.

or because it is not reported. It would be very useful to clarify the status of the PM-32 and the PM-80, as these are major sources both of damaged spent fuel and of LRW. If the damaged fuel has been removed, it would be useful to know how the damaged fuel is being managed.

Despite these problems, it has been possible to draw a general picture of the sources of radioactive contamination in the Russian Far East. Spent fuel contributes the vast majority of the radioactive inventory. Much of this appears to be in land-based dry storage – probably in transport casks – although considerable amounts are stored in the holds of floating workshops or remains in non-defuelled submarines. Although details of the source term at the Cape Sysoeva waste facility are not given, it is clear that this is a major source of radioactivity.

In almost all cases, there are a few large sources that dominate all others. For spent fuel and solid radioactive waste, the inventories are dominated by the Cape Sysoeva facility. The largest single source of radioactivity in spent fuel is Building 30. For solid radioactive waste, the dominant sources are constructions 1-5, 7, 31, and 32, all of which contain more than 1,000 TBq and which together constitute 99% by activity (11,000 TBq) of the solid radioactive waste in the Russian Far East¹⁸. The vast majority (97.5%) of the reported radioactive inventory in liquid radioactive waste is onboard the two floating workshops containing damaged spent fuel, with most of this being onboard the PM-32 (210 TBq out of a total of 220 TBq, or 95%) (*Danilyan et al. 2000b*, Table 18).

Most of the ships are in extremely poor condition and are storing wastes for which they were not designed. The PM-80 and PM-32 had contained wedged and damaged fuel. It is worth noting that the major problems with wedged damaged fuel are associated with the unmodified PM-326 class ships that store fuel assemblies separately. It is not clear if this implies that the upgrades to containerized fuel in removable cases solved the problem of wedged fuel or if the fuel on the PM-125, PM-133, and PM-74 is simply wedged in the removable containers rather than in the tank itself. The technological tankers store wastes dramatically in excess of their allowable limits, by up to four orders of magnitude. Basic systems for vessel safety to prevent fires or flooding or to monitor wastes are out of order. Fires have broken out on ships on several occasions, including onboard the PM-80 in 1999 (*Kudrik, 1999*) and onboard a decommissioned submarine as recently as November 2002 (*Interfax, 2002*).

¹⁸ Or 83% of a total inventory of 13,000 TBq, depending upon the true inventory of Construction 19 in Kamchatka. The inventory of Construction 19 in Kamchatka needs to be clarified, as the discrepancy has a significant impact on the results.

3 Transboundary Atmospheric Transport

Main Contributors: Alexander Mahura, V. Mordashev, A. Pechkurov, Vanya Romanova, and Makoto Takano

Edited by Keith Compton

The previous chapter provided a discussion of the potential sources of radioactive contamination. Work has also been carried out in the framework of the Far Eastern Study to evaluate the likelihood of transboundary transport and to scope the potential impacts to neighboring countries. An evaluation of the environmental conditions in the Russian Far East, including the regional climatology, was prepared by V. Mordashev and A. Pechkurov based on publications of the Far East Geological Institute (*Mordashev and Pechkurov 2000*). This work has been supplemented by evaluations provided by *Romanova and Takano (2002)* and *Mahura (2002)*. In this chapter, the probability that contamination released into the atmosphere will reach surrounding countries is assessed based upon the work reported in *Mahura (2002)* and a scoping analysis of the potential deposition and doses in the case of atmospheric transport from a site in the region of Vladivostok to the Japanese Islands is provided based upon the work of *Takano et al. (2001)* and *Romanova and Takano (2002)*.

3.1 Climactic Settings

The Primorye region lies in the monsoon belt of the temperate climate zone. The typical winter and summer surface pressure patterns are shown in Figures 3-1a and 3-1b, respectively. The annual average atmospheric humidity is 71%. The annual average precipitation is 770 mm. Precipitation greater than 0.1 mm occurs, on average, 115 days per year. Light breezes (2 - 3 m/sec) are the most common winds in the region, although winds can reach almost hurricane force. The maximum sustained wind velocity observed at Vladivostok has been registered as 34 m/sec and gusts of up to 38 m/sec have been recorded. Based on statistical analysis of historical data, there is a 5% probability in any given year of wind velocity exceeding 41 m/sec. The weather in the region is dominated by the movement of several large atmospheric systems, resulting in two seasons (a cold, dry winter and a warm, wet summer) with relatively consistent wind patterns, with transitional periods in the spring and fall. These are discussed in more detail below.

Winters are relatively short, cold, and dry, with both the lowest average temperature (-20°C) and the lowest monthly average precipitation (15.4 mm) observed in January. Figure 3-1a shows the mean January sea surface pressure system. A large high-pressure system (anticyclone) known as the Asian High covers most of northeastern Asia during the winter. It is a shallow low-level phenomenon (up to 500 hPa) and is the strongest one in the Northern Hemisphere during the winter season. A low-pressure zone known as the Aleutian Low dominates the northern part of the Pacific Ocean. The location of these pressure fields results in a flow of cold, dry continental air from the mainland to the ocean (winter monsoon) from the Asian High to the Aleutian Low. Another low-pressure system (the Equatorial Low) is situated near Australia and New Guinea. The southward streaming from the Asian High to the Equatorial Low can influence the wind system, causing the air masses to move south and influence Korea.

As a result of this circulation, the typical winter weather in the region is characterized by relatively clear skies and limited precipitation with strong, recurrent (70%) northern and northwestern winds. The average cloud cover ranges from 20% - 40%, with upper and mid-level clouds predominating. The maximum wind velocities are observed in winter. The monthly average wind velocity in

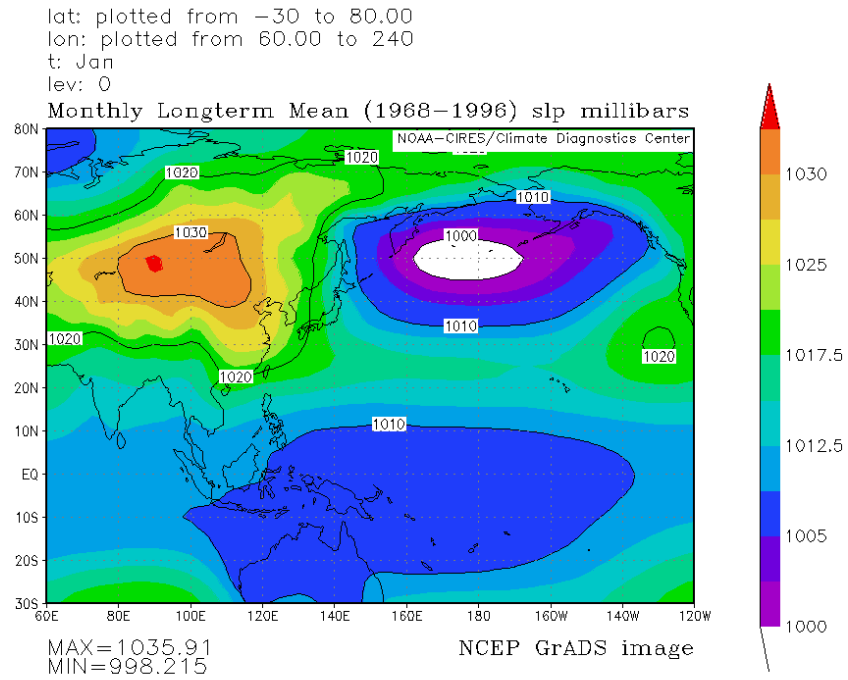


Figure 3-1a: January Sea Surface Pressure (image source: <http://www.cdc.noaa.gov/cgi-bin/DataMenus.pl?stat=mon.ltm&dataset=NCEP>)

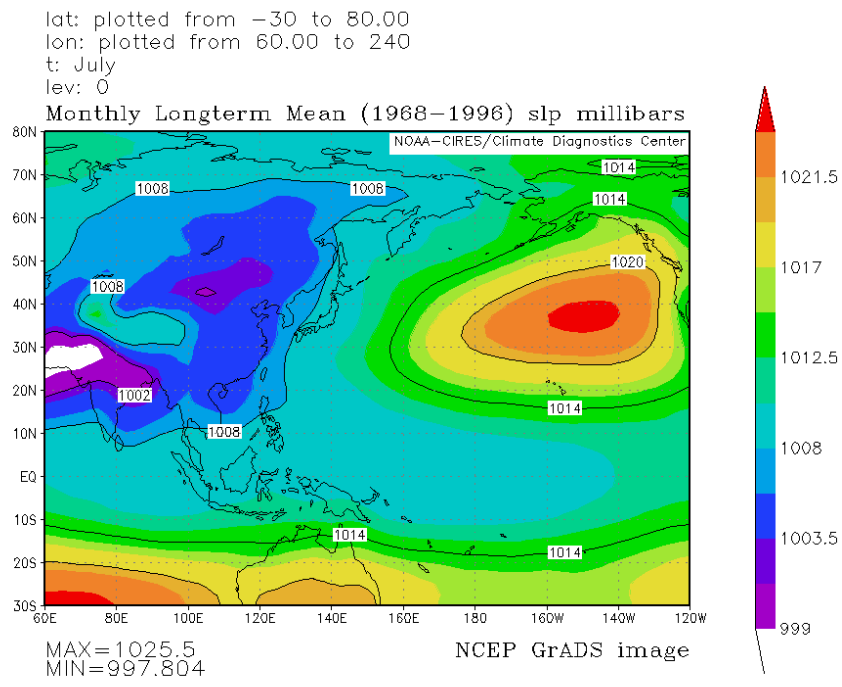


Figure 3-1b: July Sea Surface Pressure (image source: <http://www.cdc.noaa.gov/cgi-bin/DataMenus.pl?stat=mon.ltm&dataset=NCEP>)

January ranges from 5 to 8 m/sec. Strong winds (exceeding 14 m/sec) are observed with a recurrence of 14% on the coast and 5% in enclosed bays. Winters are colder than in the regions of the European Russia located at the same latitude. The average monthly temperature on the southern coast in January ranges from -10° to -13°C . The absolute minimum temperatures are -31°C in Vladivostok and -46°C in Ussuriysk. However, thaws may occur on the coast even in the most severe winters and last for three or four days, with temperatures rising up to $+8^{\circ}\text{C}$. The lowest relative humidity is observed in December and January, with an average value in January of only 61%. During October through March the total average precipitation on the coast is over 129 mm, only 17% of the annual total. The driest months are January and February, when the monthly average precipitation is less than 20 mm. In winter precipitation occurs mainly as snow. The snow cover lasts on average 77 days, with an average depth of about 68 cm. Snowstorms are infrequent. On average, 4 to 14 snowstorms are observed per year (two to four per month) and occur mainly between November and January. The snowstorms are often accompanied by winds exceeding 14 m/sec and air temperatures below -10°C , and last for four to nine hours. In the spring, a change in atmospheric circulation occurs as the atmospheric pressure centers begin to shift position. This causes a rather unstable wind regime with low air temperatures and infrequent precipitation. Southerly winds begin to recur more frequently, accompanied by a rise in relative humidity. Average temperatures rise above freezing across most of the territory by late March. In April the average temperature ranges from 2° to 6°C , and in May from 6° to 12°C . Daily high temperatures in May can rise to 30°C .

An extensive low-pressure system dominates much of Asia in the region of Northern India, Pakistan and Southwest China (Figure 3-1b) during the summer. A subtropical high-pressure system is situated in the northern Pacific east of Japan. Summers are relatively cloudy with frequent rain. The warmest month is July, with an average temperature of 25°C . In the city of Vladivostok, the average precipitation from July to September exceeds 100 mm per month, with the highest monthly precipitation (148.7 mm) observed in August.

In contrast to the winter, warm and wet masses of air flow from the ocean onto the mainland during the summer monsoon. Summers are therefore characterized by higher rainfall, more overcast weather, and weaker, more variable southerly and southeasterly winds. In summers the average cloud cover increases up to 70% - 90%, with low-level clouds predominating. In July the winds are mild and generally do not exceed 2 - 6 m/sec. Strong winds (>14 m/sec) are observed with a recurrence of between 2-9% on the coast and less than once per year in enclosed bays. The greatest amount of precipitation (641 mm, or $\sim 83\%$) occurs during the warm period. The relative humidity is highest between June and August, with the July monthly average reaching 89%. August is the warmest summer month on the coast of the territory, with an average daily temperature of 24°C and a maximum of 35°C .

In the first half of the summer monsoon (June and July) air flowing from the Sea of Okhotsk (*cf.* Figure 1-1) results in cool, overcast, and drizzly weather with southerly and southeasterly winds prevailing. A cold ocean current flows along the coast resulting in relatively frequent (10-22% recurrence) and long (up to ten hours) periods of mist and fog, predominately during nights and in the morning. In the protected bays the recurrence of mists is much less. The relative humidity increases rapidly between May and June, with steady rain predominating in the first half of summer. The temperature in July averages 14°C to 21°C . In the second half of the summer, from the middle of July till September, air masses originating from the east and south result in warm (temperatures often above 25°C), wet (80-90% humidity) weather with periods of intense precipitation caused by typhoons and southeast cyclones. The typhoon season is from June till November, with approximately 75% of the typhoons occurring in August and September. The passing of a tropical cyclone is accompanied by a thick cloud cover with very heavy and continuous showers, and by very rough seas. The sharp changes of atmospheric pressure can cause sea level fluctuations with a period lasting from several minutes to one hour. In gulfs and bays, the value of such fluctuations range from 0.2 to 0.5 m, and in rare cases can reach 0.7 to 1.0 m. In

the Sea of Japan tropical cyclones come from the southwest. About 16% of all observed cyclones enter the northern Sea of Japan and the Primorye Territory. However, even tropical cyclones in the southern part of the Sea of Japan can influence weather in this region, resulting in strong rains and storm force winds. On average, from three to eleven thunderstorms are expected per year, and these occur mainly during the summer. Thunderstorms typically last from 1 to 1.8 hours, but storms lasting 10-12 hours have been recorded.

The air temperature begins to decrease starting from the middle of August, although autumn is much warmer than spring. Daily high temperatures in September averages 12° - 16°C. In October the daily high temperature ranges from 8°C to 10°C. The relative humidity begins to decrease in September. In the autumn (sometimes up to the end of November) the weather is warm, dry, and sunny. Average air temperatures drop below freezing in November, leading back into the winter weather pattern.

The Kamchatka region shares some general characteristics with the weather of the southern Primorye Territory due to the impact of the major synoptic systems discussed above. However, the climate of Kamchatka is much more more diverse and unstable. Surrounded by seas, the Kamchatka Peninsula has a relatively mild climate in relation to its latitude. The coastal areas of Kamchatka exhibit a maritime climate. However, there are very few warm days in Kamchatka. In the coastal areas, the temperature exceeds 20°C on average only one to six times per summer. The highest temperature in the coast and on islands is observed in August. Thaws are frequently observed in January and February, during which the temperature can rise up to +5°C. Cyclones coming from the southeastern coast exert a considerable impact on the climate of Kamchatka. They bring warm and moist air from the Sea of Japan and Yellow Sea, resulting in snowfalls, continuous snowstorms and strong gales. Precipitation on Kamchatka is higher than in any other region of Russia, but with enormous spatial variability. In contrast to Primorye Territory, more precipitation occurs in the winter than during the summer. The greatest amount of precipitation - up to 2500 mm per year - falls on the mountain slopes in the south of the peninsula. In the central Kamchatka lowland, protected from the effect of cyclones by the Middle and Eastern Ridges, precipitation is less, reaching only 400 mm per year. In the northeastern coastal area this index makes 500-600 mm per one year. In winter, weather conditions are very much unsteady that may be expressed, for example, by sudden snowfalls and strong winds. The monthly snowfall or more can be accumulated within a single day. The summer on Kamchatka may turn out rainy.

3.2 Probability of Transport: Trajectory Analyses

The likelihood that contamination released into the atmosphere in the region of either Vladivostok or the Kamchatka Region could reach neighboring countries was evaluated by *Mahura (2002)*. An atmospheric trajectory model was used to calculate trajectories originating over the main locations in Primorye Territory and Kamchatka Oblast. A statistical analysis consisting of exploratory, cluster, and probability field analyses was then used to explore the structure of the set of modeled trajectories. The purpose of the analysis was to evaluate the general atmospheric airflow patterns and the characteristics of the atmospheric transport (e.g., the number of trajectories and/or days throughout the year when released air parcels might reach specified regions, predominant atmospheric layers for transport, average and minimum transport times, etc) from the naval nuclear facilities in the Russian Far East. We also investigated the variations in seasonal, monthly, and annual flow patterns to better characterize the uncertainty in these trajectories.

As discussed in Chapter 1, each of the two regions contain a number of facilities. Because these facilities are close to each other in relation to the model grid (one degree grid spacing, which is approximately 100 km) used for evaluating atmospheric trajectories, the facilities were grouped into two Nuclear Risk Sites (NRS) for modeling purposes. The Vladivostok NRS (VNRS) comprises the Far Eastern Plant Zvezda, the Pavlovsk Bay naval base, the ship repair facilities in

Chazhma and Razboinik Bays, and the waste management facility at Cape Sysoeva. The Kamchatka NRS (KNRS) comprises the Gornyyak Shipyard, the Seldevaya Bay Waste Management Facility, and the Rybachiyy submarine base. For atmospheric transport modeling, the geographical coordinates of the VNRS are taken as 42°55'N and 132°25'E (see Figure 3-2), and those of the KNRS are taken as 52°55'N and 158°30'E. The geographical region of interest for modeling impacts on potential receptor countries covers the North Pacific region from 2.5° to 77°N latitude and 90°E to 82.5°W longitude. This region includes Japan, Korea, eastern Russia, northeastern China, and parts of the USA (primarily the state of Alaska and the Pacific coast).

3.2.1 Methodology

3.2.1.1 Specification of regions of potential impact

Due to the large amount of radioactive material present in the Russian Far East, a major accident at one of these facilities followed by a release of radioactive material could result in adverse impacts in neighboring countries. A complete evaluation of such an accident requires an evaluation of both the probability of such an event, the probability of impacts to the individual neighboring regions, and the evaluation of potential consequences in the neighboring regions. This study comprises an evaluation of the probability and characteristics of long-range atmospheric transport from the nuclear risk sites near Vladivostok and Petropavlovsk-Kamchatskiy counties to the different receptor regions.

For this study, we defined (as shown in Figure 3-2) five regions (Japan, Korea, China, Aleutian Chain Islands, and the state of Alaska) as the regions of the NRS potential impact. The regions of interest were defined by setting bounding boxes (an eastern and western boundary and a northern and southern boundary) to enclose the specified regions. A more precise delineation of the geographical regions could be achieved by the use of a GIS. This would allow a more precise evaluation of trajectory passages through the selected country's borders. However, in light of the uncertainties in trajectory modeling and for purposes of a scoping evaluation, the definition of impact regions by the use of latitude vs. longitude parallelograms was considered adequate.

Japan was divided into three major sub-regions comprising the northern (140-145°E vs. 38-45°N), central (136-142°E vs. 33-38°N), and southern (130-136°E vs. 30-36°N) territories of Japan. These include the islands and adjacent seashores. In a similar manner, the Korean peninsula was divided into two areas, comprising North (124-130°E vs. 38-43°N) and South (125-130°E vs. 34-38°N) Korea. Due to more complex configuration of the Chinese border, we defined two areas. The first is the region of China bordering Primorye Territory close to Vladivostok, which we defined as the Northern Chinese Territories (120-132°E vs. 43-48°N). The second, more distant region was defined as Central Shoreline China (112-124°E vs. 31-43°N). For the USA, we considered only two northern regions – the Aleutian Chain Islands (170E-160°W vs. 50-55°N) and the western territories of the State of Alaska (166-150°W vs. 55-72°N). The west coast of the continental US¹⁹ was not considered because the trajectory travel times averaged more than five days to reach this region. Because of the questionable accuracy of trajectory calculations after five days, and because of constraints on computer resources used for statistical analysis of the longer series, trajectories reaching the west coast were not analyzed.

3.2.1.2 Isentropic trajectory modeling

Each computed atmospheric trajectory represents the movement of an air parcel in time and space, which we take as an estimate of the motion of the center of a diffusing cloud. Modeling of fully

¹⁹ California, Oregon, and Washington.

three-dimensional trajectories is complex and requires incorporation of a large number of variables and parameters into the simulation. There are a few simplified approaches to model atmospheric

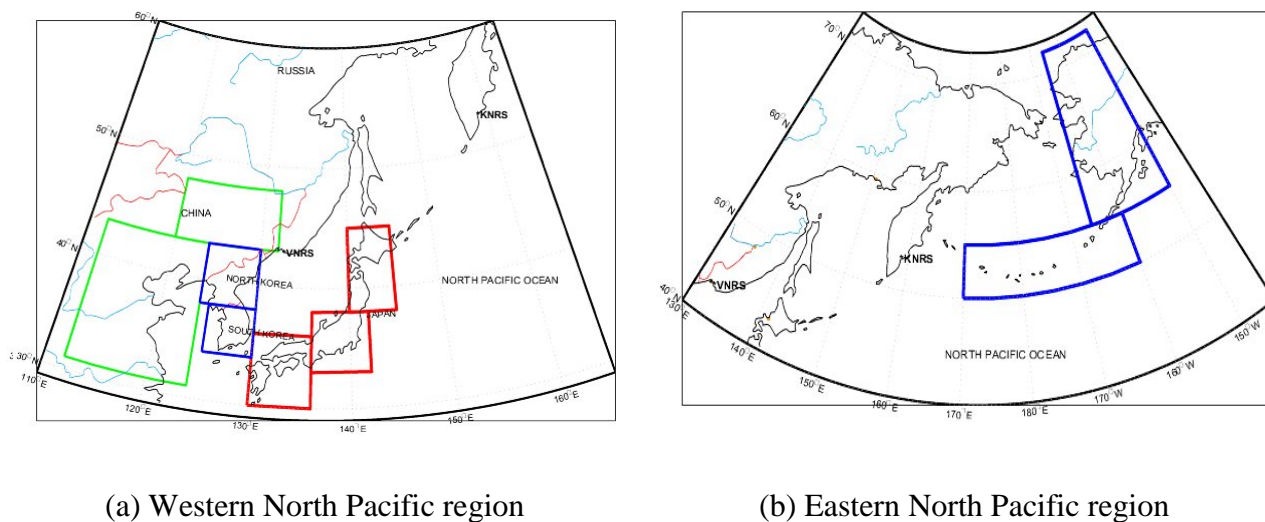


Figure 3-2: Geographical impact regions

trajectories. Two commonly used approaches are isobaric trajectory modeling and isentropic trajectory modeling (*Danielsen, 1961*). For isobaric trajectories, it is assumed that air parcels move along constant pressure surfaces. For isentropic trajectories, it is assumed that air parcels move along constant potential temperature surfaces. Our study used an isentropic approach. Although this type of trajectory model requires the assumption of adiabatically moving air parcels and neglects various physical effects, it is still a useful research tool for evaluating airflow patterns within meteorological systems on various scales (*Merrill et al., 1985; Harris & Kahl, 1990; Harris & Kahl, 1994; Jaffe et al., 1997a; Mahura et al., 1997a; Jaffe et al., 1997b; Mahura et al., 1999 and others*). Some uncertainties in these models are related to the interpolation of meteorological data from sparse measurements, the applicability of the horizontal and vertical scales, and assumptions on vertical transport (*Merrill et al., 1986; Draxler, 1987; Kahl, 1996*). More detail about the methods of computation, accuracy, and applications of trajectory models is given in an excellent review prepared by *Stohl (1998)*.

The model grid domain selected for this study, covering the North Pacific territories with adjacent countries and seas, is located between 2.5°-77°N and 90°E-82.5°W. We extracted data covering a period of 10 years (1987-1996) from the National Center for Environmental Prediction (NCEP) Global Tropospheric Analyses dataset DS082.0 for use as input meteorological data. More information about the DS082.0 dataset can be found at <http://dss.ucar.edu/datasets/ds082.0/> and in publications by *Baker, 1992; Trenberth & Olson, 1988; and Randel, 1992*. We interpolated the original gridded wind fields to potential temperature (isentropic) surfaces by applying a technique described by *Merrill et al., 1986*. All forward isentropic trajectories from the nuclear risk sites regions were computed twice per day (at 00 and 12 UTC²⁰) at sixteen different potential temperature levels. These levels ranged from 255°K to 330°K with a 5°K interval. We calculated four trajectories per site per temperature level per time step. The use of four trajectories permitted an evaluation of the consistency of the wind field in the direction of the atmospheric transport. The initial points of trajectories are located at each corner of a 1°x 1° of latitude vs. longitude box, where the NRS is in the center of the box. Overall, a total of 467,200 trajectories (10x365x2x16x4) were computed for each NRS. All trajectories chosen for further statistical analysis have duration of five days. We decided to limit trajectories to five days because 1) the

²⁰ Universal Coordinated Time

quality and accuracy of trajectory calculations drops significantly after five days, 2) observing development frames of the synoptic scales systems in the North Pacific region, and 3) the relative proximity of the analyzed NRS impact geographical regions from the sites of interest.

We should note that quality of trajectory calculation is highly dependent on the quality of the original NCEP fields, which have a resolution of 2.5° latitude by 2.5° longitude. In particular, the computed trajectories may not reflect the contribution of the frontal passages and local terrain phenomena. In addition, although we used all calculated trajectories for the further analysis, we should note that here are differences in the representation of the general flow along trajectories. The flow is considered to be reasonably consistent along the transport pathway if all four trajectories show a similar direction of transport for one time period (as shown in Figure 3-3a). Trajectories showing a strong divergence of flow are defined as “complex trajectories” (as shown in Figure 3-3b). These trajectories reflect more uncertainties in the air parcel motion.

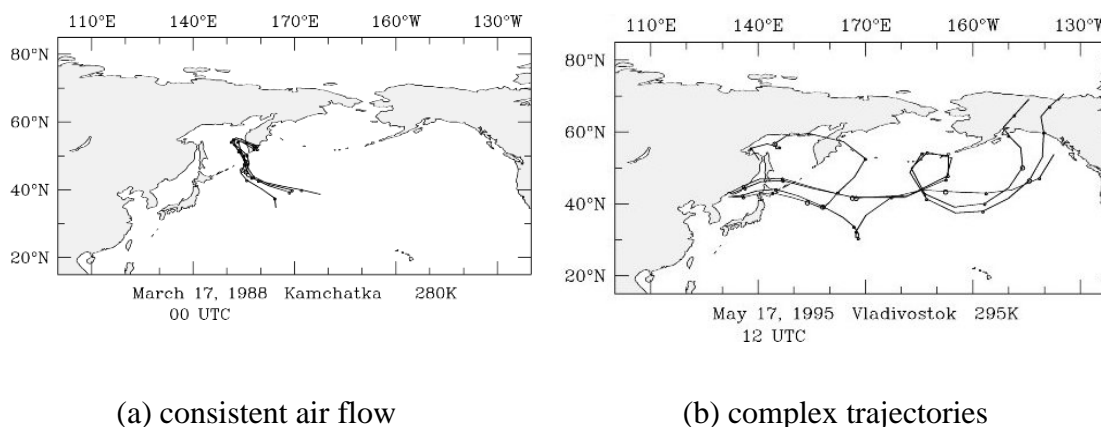


Figure 3-3: Examples of trajectories

For both NRS the most probable release heights in a case of an accidental release would be within the surface layer of atmosphere (*i.e.*, within the first hundred meters above the ground) provided that there would be no intense thermal forces or meteorological conditions driving the release to higher altitudes. Therefore, at the next step, from all isentropic trajectories we selected only those trajectories originating within this layer. This results in approximately 29,000 trajectories per site. Trajectories originating at the top of the boundary layer (~1.5 km above sea level) were selected to study altitudinal variations in the flow patterns.

3.2.1.3 Data analysis

Two main analyses were performed on the computed trajectories in order to evaluate the atmospheric transport patterns. Cluster analysis was used to divide calculated trajectories into groups that represent major airflow patterns. A probabilistic analysis was then carried out to evaluate the likelihood of phenomena of interest such as fast transport.

Cluster analysis comprises a variety of multivariate statistical analysis techniques that can be used to explore the structure within data sets (*Romesburg, 1984*). In this study, we used the technique that was applied in *Jaffe et al. (1997a)*, *Jaffe et al. (1998)*, *Mahura et al. (1999a)*, and *Baklanov et al. (2002)* to summarize the airflow patterns for the Vladivostok and Kamchatka regions. The analyses were carried out on a monthly, seasonal, and annual basis, as well as for the entire ten-year period of 1987-1996. The results of the cluster analysis are presented in Section 3.2.2.2.

The second type of analysis was the construction of probabilistic fields in order to estimate the likelihood of phenomena of interest. Two types of probabilistic fields were constructed. Airflow fields were constructed to provide a general overview of the likely direction of the radioactive cloud's transport as well as the probability that it would reach or pass any particular geographical

area. The second field represents the typical transport time to different regions. The final field represents the relative likelihood of the fast movement of air parcels during the first day of transport. To construct these fields we used latitude, longitude, altitude, and time step values for each five-day and single day trajectory. The results of the probabilistic analysis are presented in sections 3.2.2.3 (airflow), 3.2.2.4 (transport time), and 3.2.2.5 (fast transport). In our study, analysis for each site was performed for the period of 1987-1996 and by seasons. A complete description of the method used to construct the different fields can be found in *Mahura (2002)* and *Mahura et al. (2002)*

3.2.2 Results And Discussion

3.2.2.1 Nuclear risk sites possible impact

The analysis of the probability of the NRSs impact comprises five elements:

1. the number and percentage of *trajectories* reaching the boundaries of the chosen geographical regions
2. the number and percentage of *days* that at least one trajectory originating from the release site had reached the region²¹.
3. the average transport time of air parcels to reach these regions.
4. the probability of transport within different atmospheric layers.
5. the likelihood of very rapid (fast) transport of air parcels, i.e. transport in one day or less.

A summary of the transport from the Kamchatka and Vladivostok NRSs to the chosen geographical regions is shown in Tables 3-1 and 3-2

²¹ Note that this is different than 1), in that there are 128 trajectories originating in any given day.

Table 3-1: Summary of atmospheric transport from the Kamchatka NRS to geographical regions during 1987-1996

Parameter vs. Region	North Japan	Central Japan	South Japan	North Korea	South Korea	North China	Seashore China	Aleutian Chain	Alaska State
Trajectories reached regions <i># (%) of trajectories</i>	612 (2.3)	67 (0.3)	39 (0.2)	111 (0.4)	48 (0.2)	287 (1.1)	105 (0.4)	7813 (29.9)	3511 (13.4)
Days when trajectories reach regions <i># (%) of days</i>	291 (8.0)	40 (1.1)	22 (0.6)	60 (1.6)	28 (0.8)	133 (3.6)	52 (1.4)	1964 (53.8)	1172 (32.1)
Transport time <i>Average ± std.dev. (in days)</i>	4.3±2.2	5.4±2.3	5.3±2.0	5.0±2.1	5.3±1.7	4.8±2.4	6.3±2.1	3.0±2.2	5.1±2.3
Higher occurrence of transport (<i>months</i>)	Dec-Apr	Jan-Mar	Nov-Feb	Nov-Feb	Nov-Feb	Nov-Mar	Nov-Mar	Apr-Nov	Jul-Aug
Higher occurrence of boundary transport (<i>months</i>)	Dec-Mar	Jan-Mar	Nov-Feb	Jan-Feb	Nov	Mar	Mar	Apr-Nov	May-Aug
Fast Transport events (<i># (%) of trajectories reaching the region within one day</i>)	15 (2.5)	0	0	0	0	0	0	1886 (24.1)	3 (0.1)
Transport within boundary layer (<i>% of trajectories reaching the boundary layer of the specified region</i>)	42.5	47.8	69.2	7.2	43.8	9.8	6.7	53.1	26.9

Table 3-2: Summary of atmospheric transport from the Vladivostok NRS to geographical regions during 1987-1996

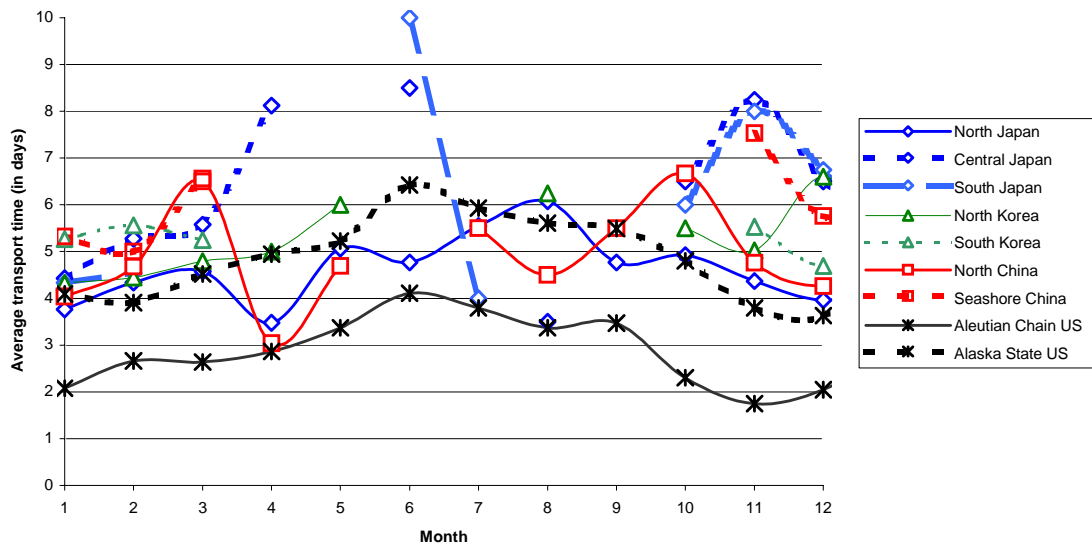
Parameter vs. Region	North Japan	Central Japan	South Japan	North Korea	South Korea	North China	Seashore China	Aleutian Chain	Alaska State
Trajectories reached regions <i># (%) of trajectories</i>	7249 (31.9)	1674 (7.4)	754 (3.3)	1435 (6.3)	777 (3.4)	7891 (34.7)	512 (2.3)	2234 (9.8)	1232 (5.4)
Days when trajectories reach regions <i># (%) of days</i>	1919 (53.5)	669 (18.3)	338 (9.3)	458 (12.5)	283 (7.8)	3174 (86.9)	189 (5.2)	822 (22.5)	525 (14.4)
Transport time <i>Average ± std.dev. (in days)</i>	1.6±1.5	1.8±1.8	2.5±2.0	2.0±1.9	2.8±2.1	0.5±1.4	3.9±2.3	5.7±2.2	7.0±1.8
Higher occurrence of transport (<i>months</i>)	Dec-Mar, May	Dec-Mar, May	Mar-June, Aug-Oct	May-Sep	May-June, Aug-Oct	May-Sep	June-Sep	May, Aug-Oct	May, Aug-Oct
Higher occurrence of boundary transport (<i>months</i>)	Win-Spr	Dec-Mar, May	Mar-June, Aug-Oct	June-Sep	June, Aug-Oct	May-Sep	June-Sep	Oct-Mar	Nov-Mar
Fast Transport events (<i># (%) of trajectories reaching the region within one day</i>)	4555 (62.8)	1030 (61.5)	240 (31.8)	774 (53.9)	152 (19.6)	1077 (13.7)	19 (3.7)	0	0
Transport within boundary layer (<i>% of trajectories reaching the boundary layer of the specified region</i>)	45.6	62.5	87.1	51.5	72.6	49.2	52.3	12.1	4.5

Monthly variations in the average transport time (in days) and number of trajectories reaching the specified regions over the entire 1987-1996 period are shown in Figures 3-5 (KNRS) and 3-6 (VNRS). To estimate the probability of impact, the number of trajectories reaching the region and the number of days this took were calculated. If one or more trajectories crossed a region during a day, that day was counted as a day of impact in that region. This approach yields two values to estimate the probability of impact that air in the VNRS region will be transported to geographical region. For example, as shown in Table 3-2, 31.9% of all forward trajectories starting at the Vladivostok NRS reach the North Japan region. However, an annual average value of 53.5% is obtained if instead one considers the percentage of days when one or more trajectories from the VNRS reach the northern Japan. To some extent, the choice of which value to consider is related to the duration of the release. For example, for an accident characterized by an "instantaneous" release (a release that occurs over a period short in relation to a day, e.g., less than one hour, such as a criticality accident), the number of trajectories would provide a better metric because the percentage of all trajectories represents the probability that an air parcel released at any given *moment* from the Vladivostok NRS region is transported to the North Japan region. However, if a release were to occur over an extended period (e.g., a fire lasting several hours), then the 53.5% value is probably more appropriate to consider because this represents the probability that an air parcel released on any given *day* from the Vladivostok NRS region is transported to the North Japan region. Therefore, the 53.5 and 31.9% values represent upper and lower bounds to the probability of impact.

The results can be summarized as follows. For the Vladivostok NRS, the North China and North Japan regions are at a higher risk of possible impact than any other regions due to their proximity to NRS and their position with respect to prevailing winds. Although the Korean peninsula is geographically closer to the VNRS than much of Japan, the probability of impact is lower due to peculiarities in the general airflow patterns of westerly origin. The probability of impact is 32-54% and 35-87% for the North Japan and North China regions, respectively. On average, atmospheric transport to these regions could occur in less than one day to North China and slightly over one day to northern Japan. Fast transport events are not common for the US territories, but these events could represent major concerns for the Japanese and North Korean regions. Boundary layer transport is common for all regions except the US, occurring over half of the time.

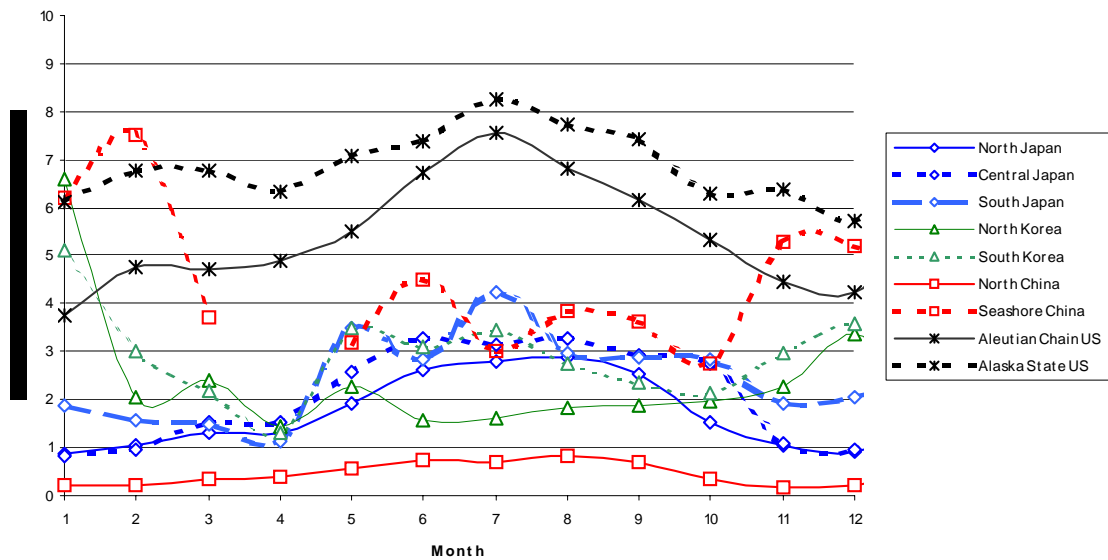
For the Kamchatka NRS, the US territories are at the highest risk compared to the other regions. The probability of impact is 30-54% and 13-32% for the Aleutian Chain Islands and Alaska State, respectively. On average, atmospheric transport to these regions could occur in three days to the Aleutians and five days to the Alaskan mainland. The likelihood of impact within five days from an accident at the Kamchatka NRS is much less for the other regions, reaching only eight percent for northern Japan and less than two percent for all other regions. Similarly, fast (one day) transport events from an accident at the Kamchatka NRS are also observed only in the north Japan, Aleutian Chain Islands, and Alaska State geographical regions. Boundary layer transport dominates in most of the studied regions, but the free troposphere transport dominates transport to the Chinese and North Korean regions.

Monthly average transport time from the Kamchatka NRS to the geographical regions



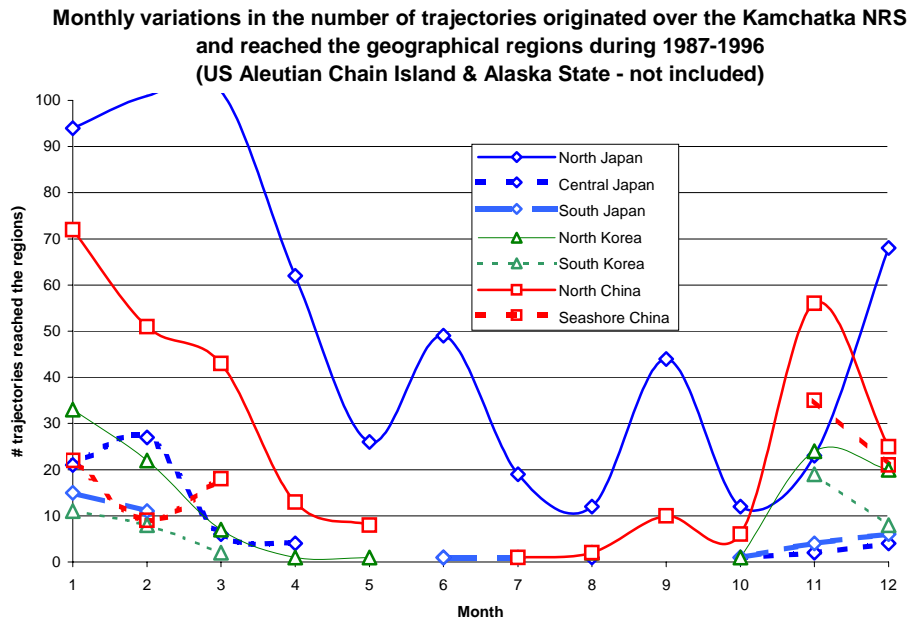
(a) Originating in Kamchatka Oblast

Monthly average transport time from the Vladivostok NRS to the geographical regions

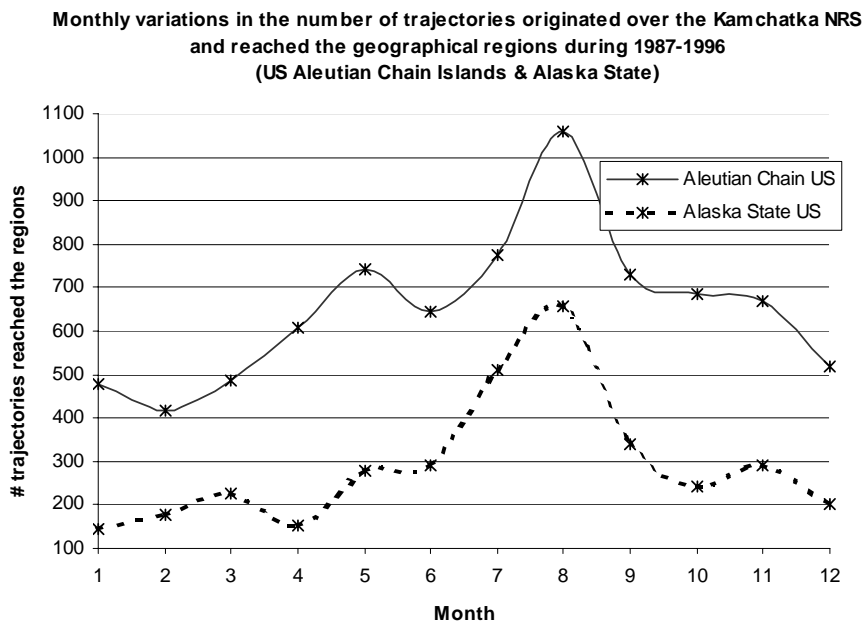


(b) originating from Southern Primorye Territory

Figure 3-4: Monthly variations in the average atmospheric transport time (in days) to specified regions based on the forward trajectories during 1987-1996



(a) *Originating from Kamchatka and reaching regions in the Western Pacific*



(b) *Originating from Kamchatka and reaching regions in the Eastern Pacific*

Figure 3-5: *Monthly variations in the number of trajectories originating at lower altitudes within the boundary layer in Kamchatka Oblast and reaching the specified regions during 1987-1996*

Monthly variations in the number of trajectories originated over the Vladivostok NRS and reached the geographical regions during 1987-1996

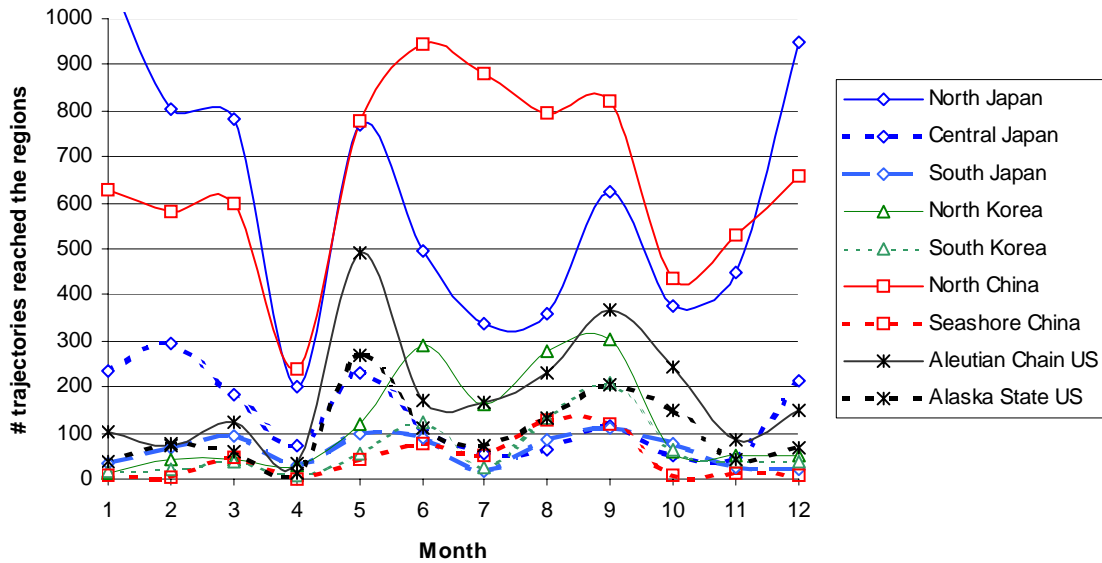


Figure 3-6: Monthly variations in the number of trajectories originating at lower altitudes within the boundary layer in southern Primorye Territory and reaching the specified regions during 1987-1996

3.2.2.2 Cluster analysis results

Because of uncertainties in the trajectory calculations after five days, we decided to use only five-day trajectories in the cluster analysis. Figures 3-7 and 3-8 show the atmospheric transport pathways from the KNRS and VNRS regions using trajectories during 1987-1996 originating within the atmospheric boundary layer. The mean trajectory for each cluster is given with points indicating 12-hour intervals. Two numbers were used for each cluster. The first number identifies the cluster and the second is the percentage of trajectories within the cluster. The seasonal summary for atmospheric transport pathways from both NRSs is shown in Tables 3-1 and 3-2. For both NRSs westerly flow is dominant throughout the year, occurring more than 60% of the time. Relatively rapid westerly flow toward the North American continent is most common during fall-winter (8-11% of the time) for the Kamchatka NRS and during winter-spring (12-13% of the time) for the Vladivostok NRS. The probability of transport from the west increases up to 85% of the time at higher altitudes (1.5 and 3 km above sea level, i.e., within the free troposphere).

Westerly flow is predominant for the Kamchatka NRS (see Table 3-1) throughout the year. Transport from the west varies from 63% (in winter) to 87% (in spring) of the time. Transport from the east occurs from 15% (in fall) to 37% (in winter) of the cases. Transport to the north occurs only during fall and it is equal to 17% of the cases. Six clusters were identified for trajectories originating within the boundary layer over the Kamchatka NRS region (Figure 3-7). Four of them (#1, 2, 3 and 4 with 2, 31, 8 and 22% of occurrence, respectively) illustrates that westerly flow is most common in the

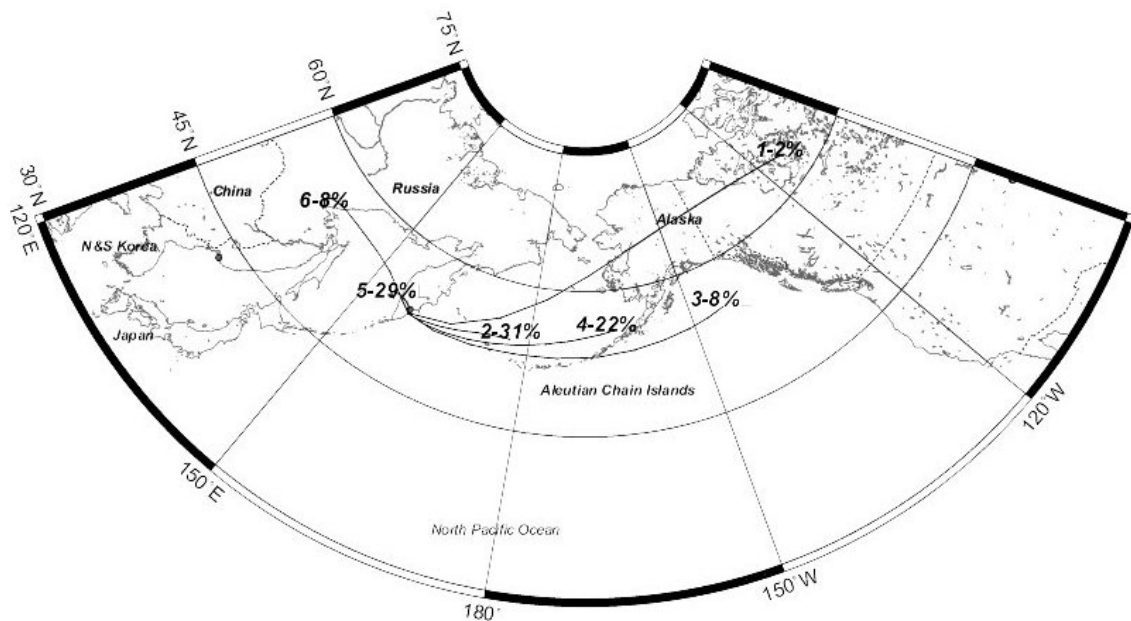


Figure 3-7: Atmospheric transport pathways (cluster mean trajectories) from the Kamchatka NRS region based on the forward trajectories during 1987-1996

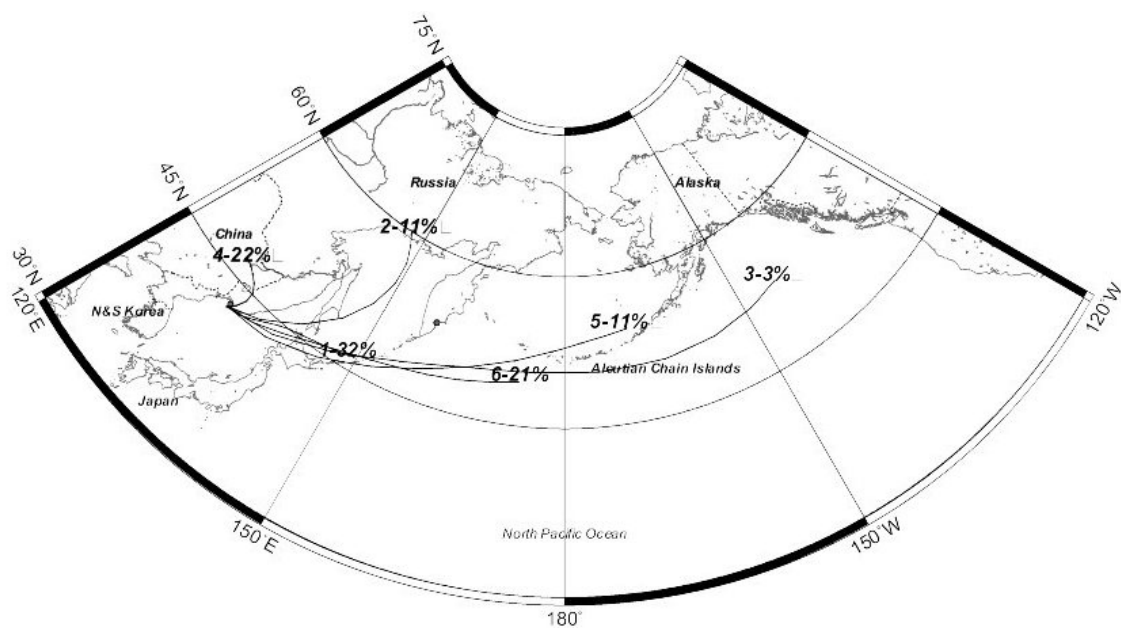


Figure 3-8: Atmospheric transport pathways (cluster mean trajectories) from the Vladivostok NRS region based on the forward trajectories during 1987-1996

Kamchatka Region, occurring about 63% of the time. Cluster #1 illustrates a rather infrequent (2%) but relatively rapid westerly flow toward the State of Alaska and Canadian territories. Cluster #6 (8%) illustrates a somewhat infrequent (8%) easterly flow toward the continent within both the boundary layer and free troposphere. Cluster #5, which occurs 29% of the time, also represents easterly flow but is significantly slower in comparison with cluster #6.

Throughout the year, westerly flow is also dominant for the Vladivostok NRS (see Table 3-2). Transport from the west varies from 68% (in fall) to 82% (in summer) of the time. Transport from the east occurs only during winter-spring and varies from 7% (in spring) to 10% (in winter) of the cases. Transport to the north is a peculiarity of the Vladivostok NRS. It can occur in any season of the year and varies from 14% (in winter) to 32% (in fall) of the time. Six clusters were identified for trajectories originating within the boundary layer over the Vladivostok NRS region (Figure 3-8). Four of them (#1, 3, 5 and 6 with 32, 3, 11 and 21% of occurrence, respectively) show westerly flow. These were observed about 67% of the time. Among these clusters, cluster #3 represents the possibility of the relatively rapid westerly flow toward the North America territories. Cluster #4 (22%) shows easterly flow. Cluster #2, which occur 11% of the time, is transport with the northward component of the flow through the Okhotsk Sea.

3.2.2.3 Probabilistic airflow fields

To test and compare the results of cluster analysis we calculated the airflow probability field using all forward trajectories that originated over the Kamchatka and Vladivostok NRSs regions during 1987-1996. Such probability fields show geographical variations in the airflow patterns from the chosen sites. In a climatological sense, the path of airflow from the chosen site could be represented by a superposition of the probability of air parcels reaching each grid region on a geographical map. The regions with higher occurrence of trajectory passages are areas where the probability of the possible NRSs impact will be higher.

In order to construct the airflow probability field, a new rectangular grid domain centered on the NRS was created with a resolution of 2.5° latitude by 2.5° longitude. The total number of five-day trajectories intersecting each grid cell was counted. The grid cell that was crossed by the most trajectories was identified as an “absolute maximum cell” (AMC). This represents the area that is traversed most often by parcels originating at the NRS. This area is assigned a value of 100 and the other areas are scaled with respect to the number of intersections at the AMC. In other words, the fields show the likelihood - **relative to the maximum** - that a trajectory will pass through a given area. The analysis was done for the period of 1987-1996, by year, season, and month.

Because all trajectories start near the site, the cumulative probability is 100% there. In order to account for contribution at the greater distances from the site, we compared the number of intersections in cells adjacent to AMC and assigned the adjacent cells to the AMC if they had at least 90% of intersections as the AMC. Thus, the field was altered using a correction factor similar to that described by *Poirot & Wishinski, 1984* and *Merrill, 1994*. This factor takes into account the contribution of flow at greater distances. The airflow probability fields (Figure 3-9) also show that westerly flows are

predominant for the Kamchatka and Vladivostok NRSs and is therefore in agreement with the results of the cluster analysis.

Figure 3-9 shows the airflow probability fields for the Kamchatka and Vladivostok NRSs constructed using all the 1987-1996 trajectories. Each probabilistic field is presented using isolines at 5% intervals on the background of the geographical maps. The areas of the higher probability, which are located close to the NRSs regions, indicate that trajectories have spent more time in this geographical area. For the Kamchatka NRS, the airflow is concentrated along the major tracks of the high and lower pressure systems. These systems are under the influence of the Aleutian Low and Asian High. During the fall, the airflow reaches the North America continent. During May-November the possibility for the air masses to pass over the North Japan region is the lowest. November is a time when air masses have ability to reach the Arctic shore territories, and it is a time for the Arctic front to move northward at the Russian Far East. During August, the airflow could pass over the parts of the state of Alaska. For the Vladivostok NRS, westerly flow was also dominant. During summer, the northward component of the airflow became evident. At the end of the spring, it passes over the northern parts of the continental areas of the Russian Far East. During August-November, the airflow could reach the northern areas of the Okhotsk Sea and seashore of the Magadan Region. In September, the airflow pattern could be observed in the Seashore China region reaching the lower 30°N latitudes. Detailed seasonal airflow probability fields within the boundary layer for both sites are shown in *Mahura (2002)*.

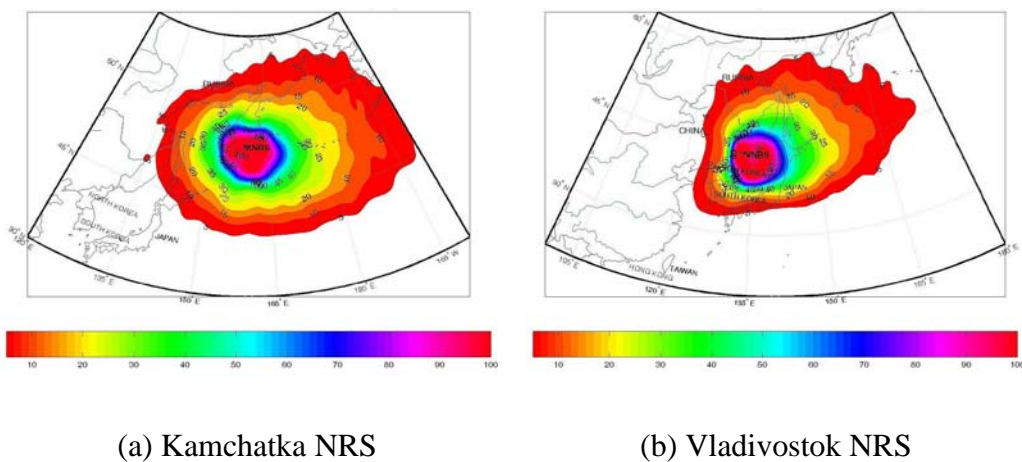


Figure 3-9: Airflow probability field within the boundary layer for the trajectories during 1987-1996 (isolines are shown every 5 units)

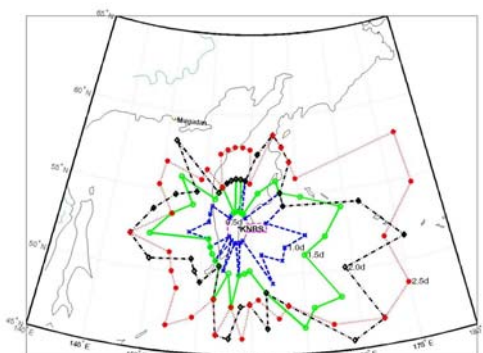
3.2.2.4 Probabilistic transport time fields

Transport time fields were constructed to show 1) how long it will take to reach a particular region from the nuclear risk site location, and 2) which areas could be impacted within one day of release. The construction of the transport time field is similar to the construction of the airflow fields. A new polar grid domain was constructed with the risk site in the center. The entire region was divided into 36 ten-degree sectors extending 70 degrees (approximately 7.1 thousand km) at two-degree intervals along each sector line. The number of trajectories intersecting each grid cell of

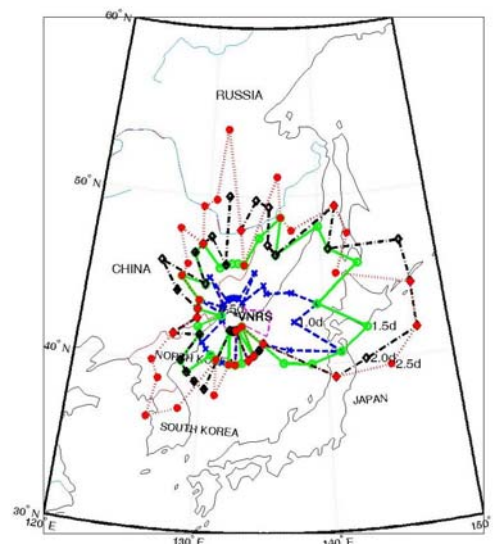
domain and ending at a specified time (for example two days) was counted. The locations of local maxima were identified along each of the 36 sectors. Because our concern is a possibility of the fastest transport, we selected the maximum that was closest to the release site. After maxima had been identified for all 36 sectors, the locations of the nearest maxima were converted back into latitude vs. longitude coordinates. Finally, an isoline for the typical transport time was drawn through the nearest maxima. Applying a similar procedure, we are able to construct isolines for other transport times (e.g., 0.5, 1, 1.5 and etc days of transport)²².

The typical transport time fields can be used for emergency preparedness and response because these fields show 1) how far the air parcels might travel from the NRS during a given number of days of transport, and 2) how long it could take for an air parcel to reach a particular region. Typical transport time fields are shown in Figure 3-10.

Isolines of 0.5, 1, 1.5, 2, and 2.5 days of transport were constructed using 36 points (i.e. for each 10° sector there is one point). Only the fields for the entire 1987-1996 period are shown here. A more complete breakdown of the results can be found in *Mahura (2002)*.



(a) Kamchatka NRS



(b) Vladivostok NRS

Figure 3-10: Typical atmospheric transport time fields for the trajectories during 1987-1996

²² A pitfall in the interpretation of such analytic results is the fact that the airflow pattern is not usually symmetrically distributed around the site of interest. Therefore, the constructed typical transport time fields in the direction of the lower probability of atmospheric transport will not reflect a realistic figure. For construction of the typical transport time isolines, we use only those AMCs which are above 1.4% in the total contribution from individual sectors. To resolve differences in contribution issue the AMC data represented in table with higher (threshold is higher than 1.4%) and lower (threshold is lower than 1.4%) percentage of occurrence were marked differently (“OK” - 100% and more of the AMC contribution into the 360 degrees belt; “>75” - 75-100%; “>50” - 50-75%, “*” - 25-50%, “-“ - <25%).

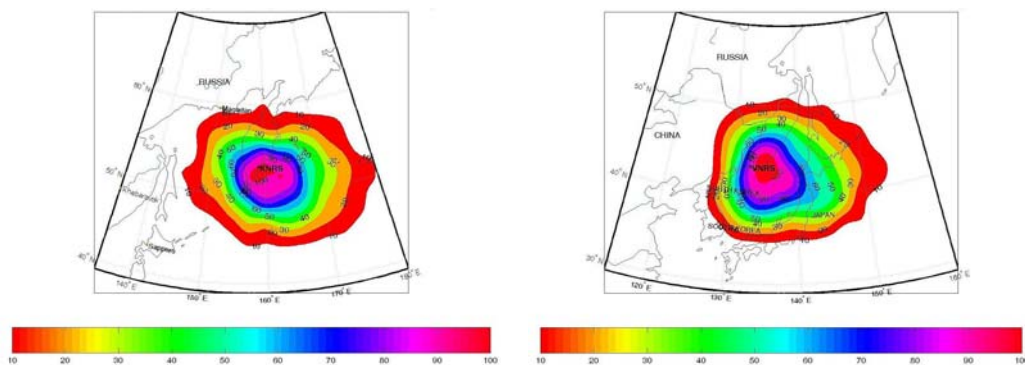
For the Kamchatka NRS (Figure 3-10a), only the territories of the Kamchatka Region and islands in the adjacent seas (the Komandor Islands of Russia and the far western islands of the Aleutian chain in the USA) are likely to be impacted within the first 2.5 days after a release. In contrast, as shown in Figure 3-10b, the typical transport time from the Vladivostok NRS to northern areas of Japan is only one to two days. Typical transport time to reach the Koreas is about two days. We should note that the pattern of these fields depends strongly on the dominance of the westerly flows. Therefore, it is stretched toward the main tracks of the cyclones traveling to the Bering Sea and Gulf of Alaska.

3.2.2.5 Probabilistic fast transport fields

Although atmospheric transport from the radiation risk site or region to another geographical area might occur at any time, fast transport is of particular concern due to the potential for exposure to short-lived radionuclides and due to the time necessary to implement any preventative emergency countermeasures such as public warnings. The fast transport field is a special case of the transport time, being constructed for the one-day trajectories. In this case, a procedure applied for computation of the airflow field was used with one-day trajectories rather than five-day trajectories. All these fields show the probability of air transport from the NRSs during the first day with respect to the area of the maximum possible impact from the NRSs marked as 100 (Figure 3-11). The analysis has been done for the entire period and each year, as well as by season and month. We analyzed the lowest altitude of trajectories, i.e. trajectories starting within the lower 500 m of the atmosphere. Our analysis of the fast transport probability fields showed that the westerly flow is dominant for both NRSs. It is also in agreement with the results of the cluster analysis of trajectories.

For the Kamchatka NRS, the area of the highest probability of fast transport from the NRS is located to the southeast from the site during all seasons except the summer. During winter, there is a possibility of the fast transport toward Sakhalin Island, and during the fall and spring transitional periods, it could reach the territories of the Magadan Region. Because of generally lower wind speeds in summer, the fast transport area is concentrated around the release point in the summer.

The area of the highest probability of fast transport is also to the east and south of the site for releases from the Vladivostok NRS. As for the Kamchatka site, fast transport to relatively distant regions is most likely during the winter, fall and spring; the most likely region to be impacted within the first day after a release occurring in the early summer is near the site. In the late summer and fall (June-August and October-November), the area most likely to be affected within one day after a release lies over the Sea of Japan. During September-November, northerly winds prevail and there is a possibility to reach rapidly the Korean peninsula. During December-April, it lies over the northern and central regions of Japan. In May, which might be considered as a transition period, there are two areas likely to be impacted by fast transport, one over the Sea of Japan and one to the north of Vladivostok in the Russian Far East.



(a) Kamchatka NRS

(b) Vladivostok NRS

Figure 3-11: Fast boundary layer transport (one day) probability field for trajectories during 1987-1996 (isolines are shown every 10 units)

3.2.3 Conclusions

The main findings of the atmospheric trajectory analysis are as follows. For both sites, westerly flow is dominant throughout the year, occurring more than 60% of the time within the boundary layer and 85% of the time at higher altitudes (1.5 and 3 km above sea level, i.e., within the free troposphere). Relatively rapid westerly flow toward North America is most likely during fall-winter (8-11% of the time) for the Kamchatka NRS and during winter-spring (12-13% of the time) for the Vladivostok NRS.

For the Vladivostok NRS, the north China and north Japan regions are at the highest risk of possible impact in comparison with other regions, because of their proximity to the release site and the prevailing wind patterns. The probability of impact is lower for the Korean peninsula due to the fact that the airflow patterns are generally of westerly origin. On an annual basis, the lower and upper bounds of the probability of impact from the Vladivostok NRS are 35-87% for North China and 32-54% for the North Japan regions. On average, atmospheric transport to northern China is likely to require less than one day and slightly over one day to northern Japan. Fast transport events are not common for the US territories, but they could represent major concerns for the Japanese and North Korean regions. Except for the US territories, material transported within the boundary layer is expected to reach all regions more than half of time.

For releases from the Kamchatka NRS, US territories are at the highest risk compared to the other regions. The lower and upper bounds of the probability of impact from the KNRS are 30-54% for the Aleutian Islands and 13-32% for Alaskan mainland. On average, atmospheric transport to these regions could occur in three and five days, respectively. For all other regions, the bounds of possible impact are only a few percent with the exception of the North Japan region (8%). Similarly, fast transport events are observed only in these three regions (Aleutian Chain Islands, State of Alaska, and Northern Japan). Boundary layer transport dominates in most of the considered regions, but free troposphere transport dominates in the Chinese and North Korean regions.

The typical transport time from the Vladivostok NRS to reach the northern seashore areas of Japan is one day. Within 1-2 days the air parcels will pass over the Northern Japan. Typical transport time to reach the Korean Peninsula is about two days. For

releases from the Kamchatka NRS, only the territories of the Kamchatka Region and islands in the adjacent seas (the Komandor Islands of Russia and the far western islands of the Aleutian Chain islands of the USA) are likely to be reached during the first 2.5 days

3.3 Case Study: Atmospheric Transport and Deposition to Japan from an Accident in Southern Primorye Territory

The discussion in the previous section had indicated a significant probability of atmospheric transport of radioactive material to the Japanese islands or the Korean Peninsula from an accident occurring at one of the facilities in southern Primorye Territory. Because of this, combined with proximity to the sites near Vladivostok (the distance between Vladivostok and Japanese Islands varied from 700 to 1000 km and to Korea is about 400 km), the high population density of the Japanese islands and the Korean Peninsula, and the large inventories of radioactivity present in southern Primorye Territory, a case study was carried out to evaluate the possible impacts, including the doses that could be received as a result of exposure in the first few days after an accident and the level of deposition that could occur and give rise to long-term exposure. Because winter is the time that winds are most likely to carry material from the Vladivostok region toward Japan, wind field measurement data for January 1997 were made available for the study. These results are described in more detail in *Takano et al. (2001)* and *Romanova and Takano (2002)*. The discussion that follows is a summary of the work carried out by those authors.

3.3.1 Brief Description of WSPEEDI

The computer code WSPEEDI (Worldwide System for Prediction of Environmental Emergency Dose Information) was developed in JAERI (Japan Atomic Energy Research Institute) (*Chino et al. (1995)*; *Ishakawa (1994)*; *Ishikawa (1995)*; *Yamazawa et al. (1998)*). WSPEEDI is a system for prediction of radiological impacts due to a nuclear accident. WSPEEDI consists of a wind model (WSYNOP) to generate large-scale mass-consistent gridded wind fields from observations and a particle random walk model (GEARN) to simulate atmospheric dispersion and dry and wet deposition of radioactivity. The simulations can be made for regions extending to hemispheric scales and vertically up to the top of the troposphere (10 km). The accumulated external gamma dose during cloud passage is calculated from the time-integrated air dose rate. Finally, the cumulative committed (70 years) internal dose due to inhalation during the period of contaminated air passage can be computed. The model accounts for complex source, terrain conditions, and the heterogeneous non-steady state conditions in the atmosphere.

Inputs for the WSYNOP and GEARN models used in the current study included the following:

- grid point value (GPV) meteorological data for WSYNOP for January 1997, provided by JAERI;
- geographical data, covering 2500 km x 2500 km, centered at Vladivostok with latitude of 43.1°N and longitude 131.9°E (This was taken as the release point);

- table of yields of iodine and xenon isotopes with reactor type (BWR or PWR), fuel burn-up and cooling time;
- physical data of 60 fission products, fertile material and activated nuclides (nuclide names, decay constants, conversion factors of dose from nuclide concentration);
- starting date and time of calculation and duration of calculation for wind field system; and
- starting date and time of release, duration of analysis, step of calculation, duration of the particle release, release height, reactor type, fuel burn-up, and the time of reactor shut down.

The output of the model is as follows:

- wind field data in vertical mesh boundary and date and time to which it corresponds, serving as input for GEARN;
- concentration of radioactivity in the atmosphere and total deposition of radioactivity to the ground surface; and
- internal and external dose due to inhalation and external cloud irradiation during cloud passage.

The WSPEEDI code estimates internal and external radiological doses from obtained radiation concentrations in the air and on the ground. The radiological dose by an inhaled radionuclide is evaluated as an integrated dose over lifetime (70 y) considering the biological half-life of the radionuclide. However, the WSPEEDI code does not evaluate the long-term dose from prolonged exposure to radionuclides deposited on the ground.

3.3.2 Wind Field Analysis for January 1997

As discussed in Section 3.1, meteorological conditions over the Sea of Japan, East Russian coasts and Japanese Islands in the winter are characterized by northerly or northwesterly winds. During winter the temperature falls below -20°C and the wind speed can vary from less than 5 m/s to about 20 m/s. The atmospheric transport has two typical directions: one toward the Japanese Islands and the other toward North Korea.

A visual examination of the surface wind patterns occurring in January 1997 allowed the identification of three typical wind patterns of interest for modeling. The WSPEEDI calculations for the horizontal components of the wind field for different dates in January 1997 are shown in Figure 3-12. Figure 3-12a illustrates a condition that we term Strong North Winds (SNW), with horizontal velocities of about 20 m/s toward Japan Islands. We consider this case to examine the impact of fast transport to Japan. Figure 3-12b illustrates the effect of slow northerly winds, with wind velocities of less than 5 m/s, and we term this case as the Weak North Wind condition (WNW). Figure 3-12c illustrates a more complicated situation in which the wind rotates over Korea and the Japanese Island under the influence of a cyclonic system located over the Sea of Japan. We term this condition as the Cyclonic Wind (CW). These three wind conditions serve as a basis for the analyses of the radionuclide air concentrations, ground depositions, and radiation doses.

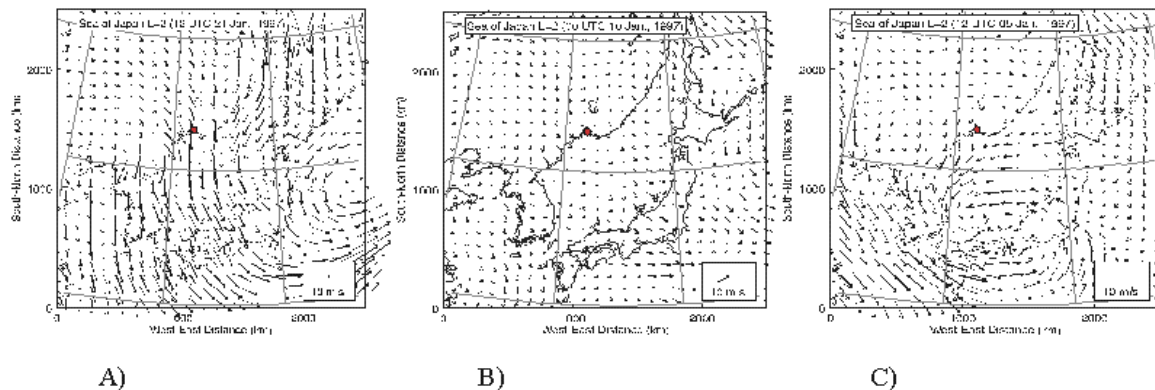


Figure 3-12: Typical Wind Patterns in January 1997

3.3.3 Analysis of the Results

In order to illustrate the results of atmospheric transport under these conditions, the atmospheric concentrations resulting from a unit (1 Bq) release were computed for a short duration (sixteen minute) low altitude (75 m) release of six different nuclides. The code calculates the concentration every 6 hours after the release at Vladivostok (Figures 3-13 through 3-15 illustrate the concentration of ^{137}Cs). The maximum air concentration and resulting internal and external committed dose for a unit release are shown in Tables 3-3 and 3-4.

Table 3-3: Maximum Radionuclide Concentration in Air 25 m over the ground (Bq/m³ per Bq released)

Isotope	25 m over Japan Islands		25 m over Korea
	Strong North Winds 24 h after release	Weak North Winds 72 h after release	Cyclonic North Winds 30 h after release
^{137}Cs	9.3×10^{-15}	2.8×10^{-15}	7.5×10^{-15}
^{134}Cs	9.3×10^{-15}	2.8×10^{-15}	7.5×10^{-15}
^{90}Sr	9.3×10^{-15}	2.8×10^{-15}	7.5×10^{-15}
^{131}I	7.2×10^{-15}	1.2×10^{-15}	5.1×10^{-15}
^{133}I	4.3×10^{-15}	1.8×10^{-16}	2.6×10^{-15}
^{135}I	1.2×10^{-15}	1.6×10^{-18}	4.8×10^{-16}

Table 3-4: Maximum External and Internal Dose (mSv per Bq released)

Wind Condition	Strong North Winds 5 days after release		Weak North Winds 7 days after release		Cyclonic Winds 7 days after release			
	Japan		Japan		Korea		Japan	
Country	External	Internal	External	Internal	External	Internal	External	Internal
I-131	$>10^{-20}$	$>10^{-18}$	$>10^{-20}$	$>10^{-18}$	$>10^{-20}$	$>10^{-19}$	$>10^{-20}$	$>10^{-19}$
I-133	$>10^{-20}$	$>10^{-19}$	$>10^{-20}$	$>10^{-20}$	$>10^{-20}$	$>10^{-20}$	$>10^{-21}$	$>10^{-20}$
I-135	$>10^{-20}$	$>10^{-20}$	$>10^{-22}$	$>10^{-22}$	$>10^{-21}$	$>10^{-21}$	$>10^{-21}$	$>10^{-21}$
^{137}Cs	$>10^{-20}$	$>10^{-18}$	$>10^{-20}$	$>10^{-18}$	$>10^{-20}$	$>10^{-18}$	$>10^{-20}$	$>10^{-18}$
^{134}Cs	$>10^{-20}$	$>10^{-18}$	$>10^{-19}$	$>10^{-18}$	$>10^{-19}$	$>10^{-18}$	$>10^{-20}$	$>10^{-19}$
^{90}Sr	-	$>10^{-17}$	-	$>10^{-17}$	-	$>10^{-18}$	-	$>10^{-18}$

Under strong north wind conditions, (Figure 3-12a) the contaminated air masses reach Japan in 12 hours and the maximum concentrations over central Japan occur 24 hours after the release. The maximum concentration for ^{137}Cs is $9.3 \times 10^{-15} \text{ Bq/m}^3$. The contaminated air masses cover the central part of Japan and quickly leave the populated territory. The residence time over Japan is about 12 hours. Under a weak north wind condition (Figure 3-12b), the contaminated cloud requires considerably more time (36 hours) to reach Japan. However, because of the longer travel time, the contaminated cloud is much larger and it expands to cover almost the whole territory of the Japanese main island. Although the maximum value for ^{137}Cs is about three times less than under strong north wind conditions, ($2.8 \times 10^{-15} \text{ Bq/m}^3$), the residence time is more than three days. Under cyclonic wind conditions (Figure 3-12c), the air masses are transported towards the Korean peninsula and subsequently rotate over the southern Japanese islands. Korea is affected mainly in the coastal regions. The maximum concentration 30 hours after the release is over the sea, and the maximum values are comparable to those under strong north wind conditions (table 3-3). The residence time is longer due to the closed rotation system, which does not permit outflow of the air masses. The lower results for radioiodines are due to the shorter half-lives (^{133}I : 20.8 h and ^{135}I : 6.61 h).

The total dry deposition to the ground for the three wind conditions is shown in Figure 3-16. Because precipitation data during this month was not available, wet deposition was not modeled. The deposition velocity was set at 0.001 m/s for ^{137}Cs and at 0.003 m/s for ^{131}I (aerosol). The largest affected territory is in the case of weak north winds, in which case nuclide deposition can be expected over the whole Japan territory. In the other two cases, deposition occurs in central Japan (SNW) and in Korea and South Japan (CW). The maximum value of deposition in Japan is in the interval of 10^{-12} to 10^{-13} Bq/m^2 per Bq released.

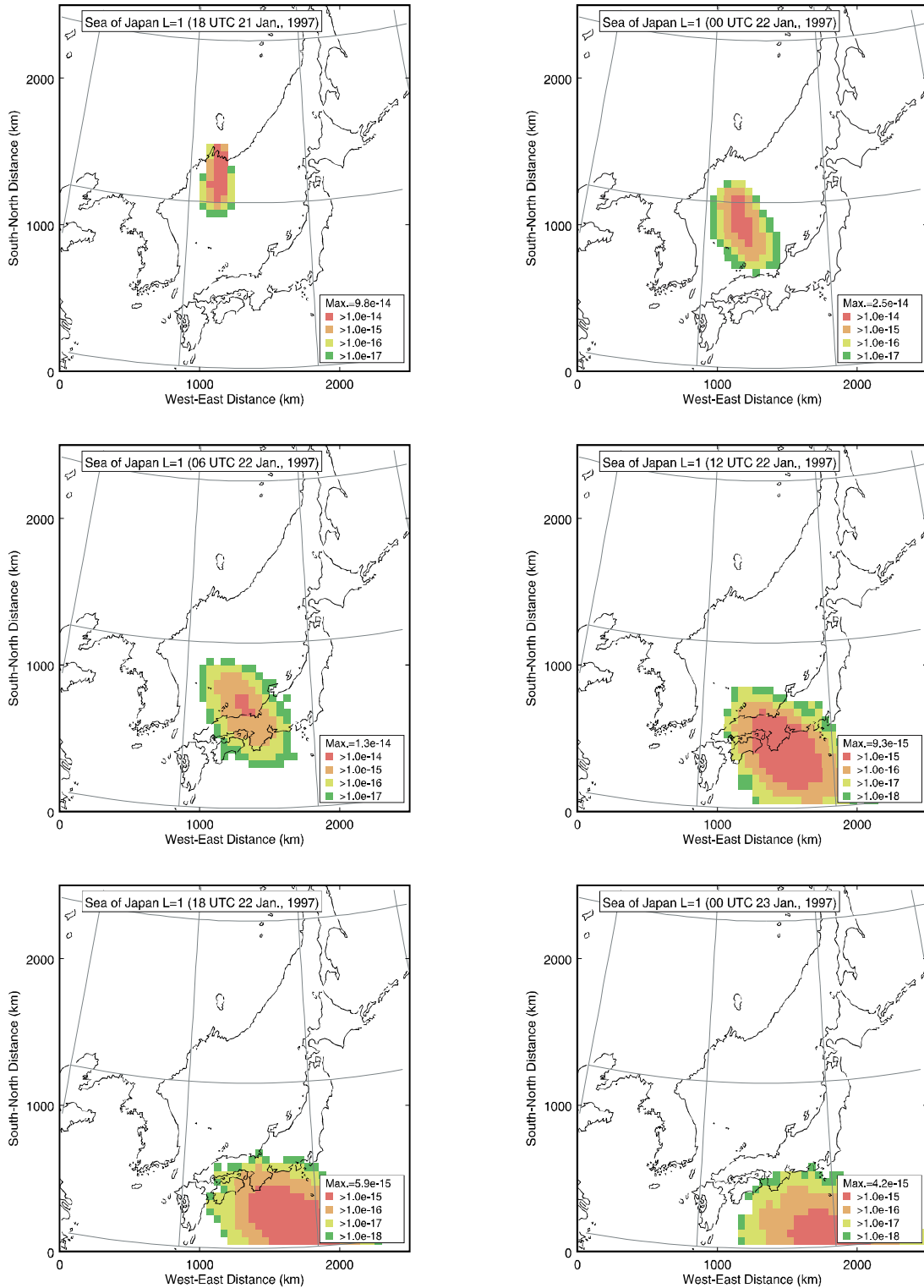


Figure 3-13: Atmospheric Concentrations under Strong North Wind Conditions

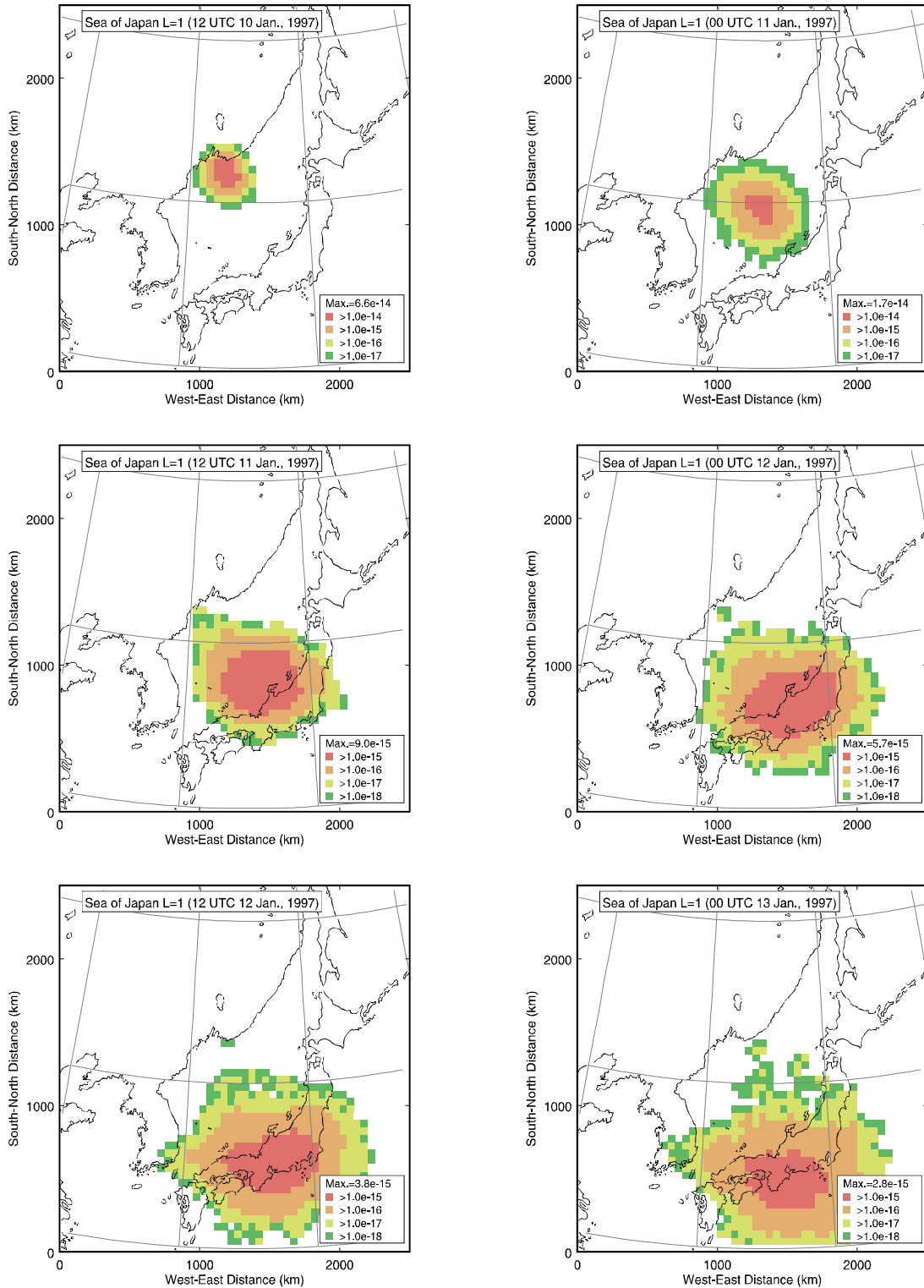


Figure 3-14: Atmospheric Concentrations under Weak North Wind Conditions

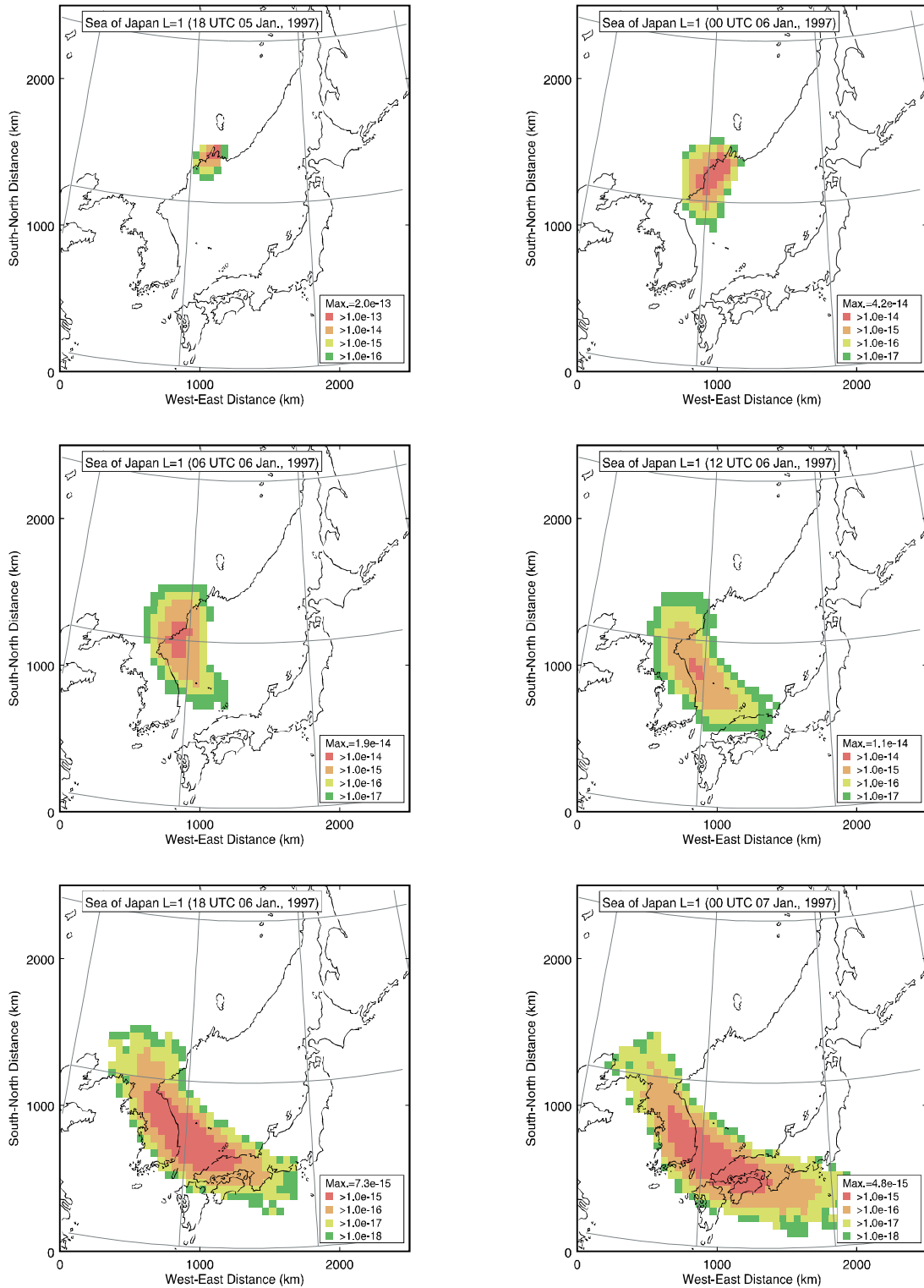


Figure 3-15: Atmospheric Concentrations under Cyclonic Wind Conditions

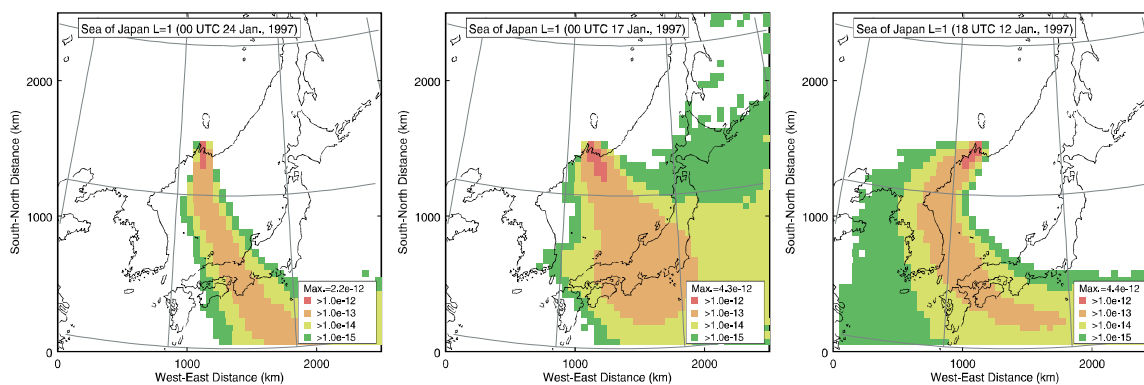


Figure 3-16: Total Ground Deposition for a Unit Release (Bq/m^2 per Bq released)

3.3.4 Parametric Study

Although the main radionuclide release in the 1985 Chahzma Bay accident occurred in less than one minute, combustion products were released to the atmosphere for an the subsequent four hours as a result of the fire that broke out onboard. This demonstrates the need for a parametric evaluation to cover the large number of possibilities in accident release scenarios. Such an evaluation was carried out, with parameter variations including the duration of the release and the height of the release. The structure of the parametric study is summarized in Table 3-5. In all cases, the output of the calculation of the atmospheric concentration at the surface (25 m), external and internal doses, and total ground deposition. In addition, calculations were carried out to estimate atmospheric concentration at different levels (Levels 1-10, corresponding to 50, 171.05, 334.21, 539.47, 786.84, 1076.32, 1407.89, 1781.58, 2197.37, and 2655.26 m) from a 75 meter, 16 minute unit release of one Bq of ^{137}Cs .

Table 3-5: Structure of the simulations modeled using WSPEEDI

Wind condition	Strong Northwest Wind	Weak Northwest Wind	Cyclonic North Wind
Wind velocity	15-20 m/s	> 5 m/s	10 m/s
Fixed duration of the release 16 min and fixed unit release 1 Bq	$^{131}I, ^{133}I, ^{135}I, ^{134}Cs, ^{137}Cs, ^{90}Sr$		
<i>Release height sensitivity</i> Variation of the release height for a fixed release duration (16 min) and unit release (1 Bq of ^{137}Cs)	75 m	-	
	950 m		
	2500 m		
<i>Release duration sensitivity</i> Variation of the release duration for a fixed release height (75m) and unit release (1 Bq of ^{137}Cs)	16 min		
	1 hour		
	24 hours		

Simulations including different release durations at Vladivostok were carried out to estimate the effect of short and long release times. The code resolution permits 120 second release duration. Calculations were carried out to evaluate ^{137}Cs concentrations

for the three meteorological conditions for release durations of 16 min, 1 hour and 24 hours. The simulations for 16 min and 1 hour release do not show a significant difference in the shape of the contaminated air masses or of the max values of the concentration. This is because the wind field is interpolated for every 6 hours and almost the same meteorological circumstances affects nuclide dispersion. The simulations for a 24-hour continuous release of one becquerel showed that the concentrations are smaller but the time of residence over the islands is longer. Under weak north wind conditions the contaminated air masses stay over Japan more than four days, resulting in higher values for external and internal doses and ground deposition.

Variations of the release height (such as might occur due to thermal rise during a major fire) were carried out for a point release. Calculations were made for release heights of 75 m, 950 m, and for 2500 m corresponding to a release in a slightly unstable layer, a release in a neutral layer, and a release in a stable layer, respectively. The maximum concentration at level 25 m over the ground for the both SNW and WNW can be observed in a case of a low (75 m) release height (Table 3-6).

Table 3-6: Maximum concentration of ^{137}Cs (Bq/m^3) at different heights of the point release.

Height of the release	Strong North Winds (24 hours after the release)	Weak North Winds (36 hours after the release)
75 m	9.3×10^{-15}	9.0×10^{-15}
950 m	7.6×10^{-15}	8.0×10^{-15}
2500 m	1.6×10^{-15}	2.0×10^{-15}

3.3.5 Dose Assessment

In order to place these figures in context and to evaluate the doses that could result due to the exposure immediately after an accident, two accident release scenarios were constructed. The first accident scenario is similar to the Chazhma Bay accident, in which a freshly loaded core undergoes a prompt criticality accident. The nuclide of concern for long-range transport in this case is radioactive iodine, due to a rather high fission yield and sufficiently long half-life. The second scenario differs from the first in that a spent core is assumed to undergo a criticality accident during defueling. The accumulated fission products are the main radionuclides for the atmospheric transport analysis.

A hypothetical reactivity accident onboard a submarine was analyzed by the North Atlantic Treaty Organization (NATO) (*NATO, 1998*). The NATO study includes an atmospheric transport analysis around the city of Murmansk, where navy bases of the Russian Northern Fleet are located. However, the submarines of the Northern Fleet and of the Pacific Fleet are very similar, with the same submarine and reactor types and similar fuel burn-ups. Therefore, the source term data used for the atmospheric transport analysis in NATO study can be used for the present analysis.

The source term for the first accident (Reactivity Accident: Fresh Fuel) can be computed by assuming a total number of fissions (5.0×10^{18}) equal to that of the Chazhma Bay accident (*cf. Chapter Two*). The total inventory of iodine radioactivity generated in a criticality accident can be estimated as 0.15 TBq ^{131}I , 3.1 TBq ^{133}I and 9.2 TBq ^{135}I . Adopting the iodine release factor of 0.2 taken from *NATO (1998)*, the estimated released inventories of radioiodine used in the atmospheric analysis are

shown in Table 3-7. For the second scenario - a reactivity accident involving spent fuel - the release term used by the NATO study (*NATO, 1998*) are adopted. In the NATO study, the fission product inventory was calculated by assuming reactor operation at 67.5 MW for 1.25 y followed by five years of cooling after the final reactor shutdown. Further, the estimated excursion power was assumed to be 2500 MWs (8×10^{19} fissions), which is considered to be sufficient to result in melting of the fuel cladding with a consequent steam explosion. The atmospheric release was based upon the adjustment of the computed core inventory by a release factor for cesium and strontium. The resulting source terms are given in Table 3-7.

Table 3-7: Source Terms used for estimation of accident scenarios (after *NATO, 1998*)

Scenario	Nuclide	Half-Life	Activity (TBq)
Reactivity Accident: Fresh Fuel	^{131}I	8.04 days	0.029
	^{133}I	20.8 hours	0.620
	^{135}I	6.61 hours	1.840
Reactivity Accident: Spent Fuel	^{137}Cs	30.0 years	350
	^{134}Cs	2.06 years	35
	^{90}Sr	28.8 years	70

As previously discussed, the WSPEEDI code estimates the seventy-year committed dose due to inhalation of contaminated air during cloud passage and the dose from the acute exposure due to external irradiation from the passing cloud and from the ground. However, the WSPEEDI code does not evaluate either the long-term external dose from prolonged exposure to radionuclides deposited on the ground or the internal dose resulting from contamination of the food chain. The doses are presented in Table 3-8.

Table 3-8: Total Dose in Areas of Maximum Impact in Japan and Korea (mSv)

Wind Pattern	Affected Country	Dose (mSv)	Reactivity Accident: Fresh Fuel			Reactivity Accident: Spent Fuel		
			^{131}I	^{133}I	^{135}I	^{137}Cs	^{134}Cs	^{90}Sr
Strong North Wind	Japan	External	3×10^{-10}	6×10^{-9}	2×10^{-8}	4×10^{-6}	4×10^{-7}	-
		Internal	3×10^{-8}	6×10^{-8}	2×10^{-8}	4×10^{-4}	4×10^{-5}	7×10^{-4}
Weak North Wind	Japan	External	3×10^{-10}	6×10^{-9}	2×10^{-10}	4×10^{-6}	4×10^{-6}	-
		Internal	3×10^{-8}	6×10^{-9}	2×10^{-10}	4×10^{-4}	4×10^{-5}	7×10^{-4}
Cyclonic Wind	Korea	External	3×10^{-10}	6×10^{-9}	2×10^{-9}	4×10^{-6}	4×10^{-6}	-
		Internal	3×10^{-9}	6×10^{-9}	2×10^{-9}	4×10^{-4}	4×10^{-5}	7×10^{-5}
	Japan	External	3×10^{-10}	6×10^{-10}	2×10^{-9}	4×10^{-6}	4×10^{-7}	-
		Internal	3×10^{-9}	6×10^{-9}	2×10^{-9}	4×10^{-4}	4×10^{-6}	7×10^{-5}

It can be seen that the doses received as a result of exposures immediately following the accident can be expected to be relatively low. The highest dose resulting from a reactivity accident involving fresh fuel is expected to occur in Japan under strong north wind conditions, but would only reach 1.4×10^{-7} mSv. Doses from a reactivity accident involving spent fuel could be higher - reaching up to 1.2×10^{-3} mSv in Japan and 5.2×10^{-4} in Korea - but would still be well below one mSv.

3.3.6 Conclusions and Discussions

The WSPEEDI code developed in JAERI was used for assessment of the consequences for Japan and Korea after a hypothetical nuclear accident in southern Primorye Territory. Meteorological conditions during the winter are characterized by strong northwesterly winds, leading to a high likelihood of atmospheric transport of released material to Japan in the event of an atmospheric release. The nuclide concentrations, radiological doses and surface deposition were calculated for the three most common wind conditions in this region (Strong North Winds, Weak North Winds and Cyclonic Winds). The calculations showed that although maximum concentrations over Japan varied according to the wind condition because of the difference in the wind velocities, the accumulated radiation doses have similar values for the three meteorological conditions due to the increased residence time under slow wind conditions.

An evaluation of different accident scenarios indicates that the doses received in Japan due to the acute exposure during passage of the contaminated cloud are not expected to exceed allowable limits for exposure to members of the public. However, it should be noted that China and the Korean Peninsula are much closer to Vladivostok than Japan and the dose could become larger in these areas under certain wind conditions. The dose to members of the public in Russia could be considerably higher. Furthermore, the doses due to chronic exposure to external irradiation or ingestion of contaminated foods as a result of radioactivity deposited during the passage of the cloud could be considerably higher. These effects are being examined in our ongoing studies.

4 Consequence Assessment

Main Contributors: Tsunetaka Banba and Keith Compton

Edited by Keith Compton

This chapter describes a screening approach for identifying the facilities in the Russian Far East that may pose the greatest risk to neighboring countries. The approach is based on the identification of a minimum critical emission in the source region that is necessary to cause unacceptable levels of contamination in a neighboring country (*i.e.*, receptor region), based upon the meteorological characteristics of the region. This minimum critical emission is then compared to the inventory of radioactive materials at each facility to whether there is sufficient radioactive material present in the facility in the source region to pose a threat to the specified receptor region. If sufficient material is present, the necessary airborne release factor is determined by dividing the critical emission by the inventory to determine the necessary airborne release factor of atmospherically transportable material. This release factor is then compared to the release factor for a variety of accidents (*e.g.*, reactor accidents, high-temperature fires, low-temperature fires, *etc.*) to determine whether a feasible pathway requiring further study exists.

The approach is illustrated by the evaluation of the radiological risk to Japan from nuclear naval facilities in southern Primorye Territory. These sites were chosen because of the high likelihood of atmospheric transport from southern Primorye Territory (*cf.* Chapter Three), the proximity of the Japanese Islands to the sites near Vladivostok (the distance between Vladivostok and Japanese Islands varies from 700 to 1000 km), the high population density of the Japanese islands, and the large inventories of radioactivity present in southern Primorye Territory (*cf.* Chapter Two). It should be noted that the approach is applicable to other regions and other pollutants where atmospheric pathways may transport contaminants across political or administrative boundaries. It may thus be used as a tool in negotiations on transboundary risk mitigation.

The utility of this approach is the ability to rapidly identify facilities with the potential for transboundary impacts. It was seen in Chapter Two that there are a wide variety of facilities containing radioactive materials in the Russian Far East, ranging from buried liquid waste tanks and solid waste burial ground to spent fuel storage facilities and decommissioned submarines. It is clear that not all of these facilities pose a transboundary threat. However, obtaining the detailed information necessary to establish a reliable source term for modeling transboundary atmospheric transport and carrying out a detailed simulation of all possible scenarios would be a prohibitive task. Information on the design details of naval facilities that is necessary to construct an accurate source term may be classified or otherwise difficult to obtain. Detailed modeling of long-range atmospheric transport and deposition is computationally expensive and is still subject to considerable uncertainty even when the meteorological

conditions at the time of release and the exact details of the source term are known²³. For these and other reasons, a simplified screening model is useful for either providing policy-relevant information (e.g., that there are no facilities that are capable of causing doses above the permissible level in the receptor region) or for designing further studies to adequately inform the policy process. Facilities that cannot be screened out by such an analysis may, for example, be subject to more detailed analysis or may be candidates for mitigation assistance provided by neighboring countries.

It should also be noted that such an analysis requires an adequate definition of the policy goal to be attained²⁴. The use of the approach presented here requires a quantifiable endpoint that has been accepted as a decisionmaking standard, such as dose to members of the public or intervention levels in foodstuffs. In some cases, a screening analysis may be a sufficient quantitative policy analysis, e.g., when clear and relatively non-controversial quantitative standards exist and it can be demonstrated that these standards will not be exceeded even under the worst cases. A more complex model may be necessary if the simple model proves too conservative or cannot adequately capture the relevant physical processes - recognizing, however, that more complex models are not necessarily more accurate nor are they necessarily characterized by less uncertainty (*cf.* the fourth point of the conclusions of *Davis et al. (1998)* and others). In other cases, the policy goals may be either subject to controversy (*e.g.*, radiation standards) or may be primarily non-quantitative (*e.g.*, national security issues). We therefore emphasize that a screening analysis of this type is therefore not a prescriptive analysis. It is only an aid to decisionmaking.

4.1 Methodology

The method is based on the assumption that the maximum areal concentration of the i^{th} nuclide in a target country j ($\chi_{i,j}$) arising as a result of deposition after an accident and atmospheric transport is a linear function of the total emission - namely, that can be expressed as

$$4.1 \quad \chi_{i,j} = Q_i \cdot \text{ATF}_{i,j},$$

where $\chi_{i,j}$ is the maximum total (wet and dry) areal deposition after passage of the contaminated cloud (Bq/m^2), Q_i is the emission (Bq) from the source facility in an atmospherically transportable form (*e.g.*, vapor or aerosol release to the atmosphere), and $\text{ATF}_{i,j}$ is the atmospheric transfer factor (defined as the maximum level of total deposition in a target country j resulting from a unit release of nuclide i in the source country).

²³ Examples of the uncertainties in long-range atmospheric modeling can be seen in the results of the ETEX experiment (summarized by *Van Dop et al., 1998*). It should be noted that the ETEX experiment, which used an inert non-depositing perfluorocarbon tracer, does not yield information necessary to validate the deposition component. For an evaluation of the ranges in model uncertainty and the pitfalls in modeling deposition and foodchain uptake, see *Kirchner et al. (1998)*.

²⁴ See, *e.g.*, *Quade (1980)* for a discussion of the importance of problem formulation in analysis. A clear understanding of the goal of the analysis, and particularly the decision which the analysis is intended to inform, is a *condicio sine qua non* for a sound policy-relevant analysis.

The minimum critical emission is defined as the emission that gives rise to the critical deposition level χ_{crit} (discussed below), and can be computed by rearranging the deposition equation 4.1 to yield

$$4.2 \quad Q_{\text{crit},i,j} = \frac{\text{dry ATF}_{i,j} + \text{wet ATF}_{i,j}}{\chi_{\text{crit},i}}.$$

If the emission exceeds the minimum critical deposition, the level of deposition in the target country would (given the same atmospheric conditions) exceed the critical deposition level.

The fundamental problem is the selection of the critical deposition level χ_{crit} and the identification of the atmospheric transfer factor for a given source-receptor pair. The issues surrounding the selection of appropriate values for these parameters will be discussed in the following sections 4.1.1 and 4.1.2.

4.1.1 Selection of Critical Deposition Level

The critical deposition level χ_{crit} (kBq/m²) for the specified region is a policy-based constraint that represents a quantitative expression of a particular policy goal. It therefore requires consideration of both scientific and policy factors. For example, the policy goal could be to restrict doses to individual members of the public to below some level generally regarded as safe; alternatively, the policy goal could be to ensure that exposure to artificial sources of radiation not exceed some specified percentage of the total radiation exposure. For dose-based standards, the case of prolonged exposures (such as might arise due to the deposited radioactivity) has been discussed in some detail in ICRP Publication 82 (*ICRP, 2000*). In that report, it was considered that post-accident interventions to reduce existing annual doses below 10 mSv could be considered optional but would not generally be justifiable. Standards for practices are more restrictive, ranging from annual doses of 0.01 mSv (as an exemption level) to 1 mSv (as a constraint)²⁵.

If a dose-based constraint is selected, the dose must be converted into a specified level of deposition. In other words, the analyst must derive the level of deposition that could lead to the specified dose under a particular set of exposure conditions. The scientific (as opposed to policy) considerations arise when trying to estimate the dose arising from the deposition. Such an approach has been used by *UNSCEAR (1993)* to estimate the committed effective dose resulting from a lifetime of exposure to fallout from weapons testing. It can also be computed, given exposure patterns in the country, by computer codes such as RESRAD (*Yu et al., 1993, 2000*). However, as *Kirchner et al. (1998)* suggest, deposition-dose transfer factors can be difficult to compute and subject to considerable uncertainty. Furthermore, because of variations in exposure patterns within a country, estimations of exposure involve implicit policy judgements regarding the proper characterization of the population at risk.

²⁵ The question arises as to whether ex-ante planning to prevent an accident that could occur (as opposed to ex-post responses to an accident that has already occurred) should be treated as a "practice" or an "intervention".

We note that the difficulties associated with a dose-based standard could be avoided to some extent by resorting to the use of regulatory default values in exposure assessments or by selecting a non-dose based level. For example, a critical deposition level could be defined as that which would double the existing contamination due to fallout. However, background levels of contamination are often quite variable. Selecting an appropriate value for "background" may be technically difficult. Furthermore, issues of equity may arise as individuals residing in areas of higher natural background would be afforded a different level of protection than those residing in areas of low background. Resorting to such decision criteria is also likely to be a source of controversy and raises a different set of policy issues. It is not our purpose to advocate any particular approach. The analysis that follows will use a dose-based approach because this has been widely accepted as a relatively impartial and equitable approach and because it illustrates the application of this method.

4.1.2 Selection of Atmospheric Transfer Factor

The next step is the estimation of an appropriate atmospheric transfer factor. The atmospheric transfer factor is the total deposition of a given radionuclide i in the specified region j resulting from a unit emission of radionuclide i at the source (*cf.* Equation 4.1). It is a measure of the ground deposition per unit radioactivity released, and has units of Bq/m² per Bq released, or 1/m².

Dry deposition is expected to occur whenever there is atmospheric contamination present at ground level, whereas wet deposition requires the occurrence of rainfall coinciding with the passage of the contaminated cloud. Wet deposition can result in considerably higher levels of deposition than dry deposition but generally over much smaller areas and with a lower probability of occurrence for any given location. Because of these differences, it is appropriate to define a separate expression for the minimum critical emission under either wet or dry deposition conditions:

$$4.3a \quad \text{dry } Q_{\text{crit},i} = \frac{\text{dry ATF}_i}{\chi_{\text{crit},i}}, \text{ and}$$

$$4.3b \quad \text{wet } Q_{\text{crit},i} = \frac{\text{wet ATF}_i}{\chi_{\text{crit},i}}.$$

It should be noted that the transfer factor for a short-term release is likely to be quite different from that for a long-term release. Long-term releases average over the full spectrum of atmospheric conditions and therefore tend to result in lower levels of contamination spread over larger areas. Short-term releases, in contrast, tend to affect smaller areas, but result in higher levels of contamination in the areas where contamination does occur. Because of the uncertainty and variability inherent in modelling atmospheric transport, the transfer factor for a particular source-receptor-nuclide combination is a random variable. The transfer factor is better represented by a probability distribution rather than a single expected value. The statistics used to characterize this distribution can be based on simple analytical expressions (e.g. for a maximum value). A more complete characterization can be developed by the use of more complex models such as WSPEEDI (*Chino et al., 1995*), DERMA (*Sørensen, 1998*), or others.

Analytical models that treat the emission as an instantaneous puff, neglect both synoptic-scale dispersion (thereby assuming that long-range dispersion can be characterized by a constant horizontal dispersivity coefficient in the range of 10^4 - 10^5 m^2/s ; cf. *Desiato et al. 1998*) and depletion due to deposition, and assume a relatively low boundary layer height (~ 200 m) are likely to be reasonably conservative and can be used to develop a maximum value for the atmospheric transfer factor. At long distances from the site, a dry deposition velocity for aerosols on the order of 10^{-3} m/s may be appropriate. Wet deposition is considerably more difficult to model. It can be handled by applying a simplification for scoping model purposes and define a wet deposition velocity analogous to a dry deposition velocity as $v_{wet} = W \cdot J$, (*Hanna, Briggs, and Hosker, 1982*), where the deposition flux is proportional to the vertically integrated average atmospheric concentration. If we assume that the plume is completely vertically mixed within the boundary layer, then the atmospheric concentration averaged over the mixing layer and the ground level atmospheric concentration are the same. The wet and dry deposition velocities can then be directly compared. The volumetric washout coefficient W_v for small ($\sim 1 \mu m$) aerosols (such as radiocesium) is between 10^5 - 10^6 (*Till and Meyer, 1983*). Defining a daily rainfall of 100 mm as a heavy rainfall event, we can define an "average" wet deposition velocity over a period of one day as 12-120 cm/s. We can see that this value is approximately two to three orders of magnitude higher than the removal rate from dry deposition. However, dry deposition occurs over a longer period and the removal rate of contaminants may exhibit a saturation effect during heavy rainfall. This can occur if the scavenging rate exceeds the rate of replenishment from advection into the area affected by rainfall. As pointed out by *Hanna, Briggs, and Hosker (1982)*, "the washout ratio has been observed to decrease with precipitation amount during any given experiment, presumably because the pollutant cloud becomes more dilute. On average, W_r decreases by a factor of 2 for every order of magnitude increase in rainfall." The authors go on to note that "Washout ratios are probably best suited to long-term estimates, in which the variability induced by single storm events is integrated out." Application of a ratio of 100 for the dry/wet deposition transfer factor is therefore taken as a reasonably conservative estimate of the potential effect of wet deposition. However, this estimate is subject to considerable uncertainty.

More complex models such as WSPEEDI (*Chino et al., 1995*), DERMA (*Sørensen, 1998*), or others are an alternative to simple analytical models. If more detailed modeling results are available, the distribution of computed values of depositions can be used (see *Mahura et al., 2002* and *Brown et al., 2003* for a more detailed evaluation of such results) as a surrogate for the probability distribution of the atmospheric transfer factor. This is likely to be a reasonable approach for evaluating dry deposition patterns. However, the use of more complex models in deriving estimates of the distribution for wet deposition may not yield either increased accuracy. The uncertainty in estimates of distributions describing wet deposition arise from a number of factors, including the inherent uncertainty in the state of the art in wet deposition modeling and because operating the model with sufficient historical data to characterize the statistical distribution of deposition during rainfall events may require simulating daily releases

over a period of decades.²⁶ When attempting to estimate the conditional distribution (e.g., the deposition at a specific point given that rainfall has occurred), a large number of samples would be required to generate a reliable distribution at all points, and particularly when trying to estimate the tail of a conditional distribution. The results obtained from a more limited sample (e.g., one year of meteorological observations) are likely to significantly underestimate the potential for maximum wet deposition peaks. Furthermore, against a backdrop of potential changes in rainfall patterns due to global climate change, we note the intrinsic uncertainty entailed by the use of historical measurements to forecast future events. The computational expense of deposition modeling is quite high, and coupled with the potential lack of data over a sufficient period of time and the potential changes in rainfall patterns as a result of global climate change, render accurate statistical estimates of potential for wet deposition difficult.

4.1.3 Critical Release and Critical Release Factor

Provided that the critical deposition and the atmospheric transfer factor can be obtained, they can be combined to identify a "critical" emission ($Q_{crit,i,j}$) by equation 4.3. This is the amount of a radionuclide nuclide that must be released at the source location necessary to yield the specified critical deposition level ($\chi_{crit,i,j}$) of nuclide i at the receptor location j . This critical emission can then be compared to inventories of material at individual facilities. If the inventory of radioactive material in a facility is less than the critical emission, then it is clear that there is no possibility (to within the specified level of confidence used to derive the critical emission) of any accident causing transboundary contamination greater than the critical level.

For facilities that contain inventories greater than the critical emission, the ratio of the critical emission to the inventory yields a critical release fraction.

$$4.4 \quad CRF_{i,j} = \frac{Q_{crit,i,j}}{I_i}$$

It is clear that facilities containing less radioactive material than the critical emission ($CRF > 1$) are, by definition, incapable of causing deposition levels above the defined critical deposition level.

Screening a facility containing multiple nuclides can be carried out with the use of a "sum of fractions" rule, namely,

$$4.5a \quad \sum_i \frac{I_i}{Q_{crit,i,j}} \leq 1$$

where I_i is the inventory of the i^{th} nuclide at the facility. A physical interpretation of a sum of fractions rule is available when the assessment endpoints are additive (e.g., under dose standards) and when all radionuclides are characterized by a release fraction of 100%. If the sum of fractions is less than unity, then it follows that no combination of nuclides can result in deposition yielding doses exceeding the dose standard. If the

²⁶ When run for purposes of reconstructing a release - such as Chernobyl - the meteorological conditions are known and it is not necessary to estimate a distribution of possible events. However, when run in a predictive mode, numerical models require a considerable amount of historical data in order to generate adequate statistical distributions.

sum exceeds unity, then either a single nuclide or a combination of nuclides may be capable of deposition exceeding the dose standard, and an examination of individual nuclide-specific release factors is necessary.

Under non-additive endpoints (e.g., ratio to background), more caution is needed. A maximum of fractions may be more appropriate in such a case, *i.e.*

$$4.5b \quad \text{MAX}_i \left(\frac{I_i}{Q_{crit,i,j}} \right) \leq 1,$$

in order to satisfy the condition that no isotope will exceed a given critical value.

The advantage of this approach is that it requires essentially no data on the construction of the facility or the characteristics of the accident in order to perform the screening assessment. This is because the approach assumes that all of the material is released in a transportable form into a fully mixed atmosphere, *i.e.*, a release fraction of 100% for all radionuclides. The approach only requires a reasonable estimate of the total inventory.

In the case that the critical release fraction is less than 100%, the computed critical release fraction assists in identifying the type of accident that may give rise to a sufficient emission. For example, a facility that with an inventory of 125% of the critical emission for ¹³⁷Cs would require an accident releasing 80% of the ¹³⁷Cs. Depending upon the physical form of the material, such a release fraction may be infeasible (e.g., for refractory nuclides such as plutonium) or may be possible under only the most severe accident conditions (e.g., complete spent fuel melting). Conversely, if the facility contains one thousand times more material than the critical emission, then an accident releasing only 0.1% of the material present could result in deposition above the defined critical deposition level. This level of release may be possible even under a less severe accident scenario (e.g., a "normal" low-temperature industrial fire affecting only a part of the more volatile materials present). A discussion of radionuclide specific release fractions under different accident scenarios will be discussed in section 4.2.

4.2 Release Fractions from Severe Accidents

Computation of the critical release fraction allows an identification of the types of accidents that may require more detailed evaluation. Comparison of the critical release fraction with the respirable airborne release fraction (RARF) provides an indication of the atmospherically transportable material released as the result of an accident. The RARF is the product of the airborne release fraction²⁷ and the respirable fraction²⁸ (DOE, 1994). The respirable fraction is important in this case because of size limitation, not because of the inhalation pathway. Particles greater than 10 μm, which

²⁷ defined as the "the coefficient used to estimate the amount of a radioactive material that can be suspended in air and made available for airborne transport under a specific set of induced physical stresses"

²⁸ defined as "the fraction of airborne radionuclides as particles that can be transported through air and inhaled into the human respiratory system and is commonly assumed to include particles 10-μm Aerodynamic Equivalent Diameter (AED) and less"

are not considered as part of the respirable fraction, are also likely to be depleted by gravitational setting before significant long-range transport can occur (*cf. Hanna, Briggs, and Hosker, 1982*). References such as *DOE (1994)* provide tabulations of respirable airborne release fractions (RARF) for different chemical and physical forms under different types of accidents (*e.g.*, drops, spills, fires, etc).

For the case of a severe criticality accident on a nuclear submarine, *NATO (1998)* estimated an excursion power of 2500 MWs (8×10^{19} fissions), which was considered to be sufficient to result in melting of the fuel cladding with a consequent steam explosion. For fire accidents in spent fuel facilities, release fractions were evaluated by *Banba (2001)* for two cases. The first case is a high-temperature fire in which the clad combustion is assumed to propagate throughout the stored spent fuel, and other case is a low-temperature fire in which fuel is exposed to air but does not reach temperatures at which a Zircaloy fire ignites. The latter case also includes a normal industrial-type fire condition.

During a criticality accident, releases to containment are expected to be typical of severe reactor accidents such as Chernobyl. According to *Travis et al. (1997)*, the estimated Chernobyl release during the accident occurring at the Chernobyl Unit-4 power plant in the Ukraine, as a percentage of core inventory, was 100% of the noble gases, 20% of the iodine, ~13% of the cesium and tellurium, 4% for strontium, 5.6% for barium, and approximately 3% for ruthenium and the lanthanides.

The release fractions during high and low temperature fires were discussed by *Banba (2001)* based upon a review of *Alexander et al. (1984)*, *DOE (1994)*, and *Lorenz and Osborne (1995)*. If self-sustaining cladding oxidation (a "clad fire") occurs, fuel rods are predicted to reach 1,500 to 2,100°C over a substantial portion of their length. At these temperatures, the release fraction is predicted to be substantial. Table 4-1 summarizes the results for the high-temperature cladding fire discussed in *Banba (2001)*.

Table 4-1: Estimated Release Fractions of Main Elements During a High-Temperature Fire in Spent Nuclear Fuel Storage Facilities (after *Banba, 2001*).

Chemical Family	Element or Isotope	Release Fraction
Noble gases	Kr, Xe	1.0
Alkali Metals	Cs, Rb	0.9
Halogens	I	0.8
Chalcogens	Te, Se	0.02
Alkali Earths	Sr, Ba, Y	2×10^{-3}
Transition Elements	Zr	$2 \times 10^{-4} - 2 \times 10^{-3}$
Miscellaneous	Mo	10^{-6}
	Ru	2×10^{-5}
	Eu, Ce	$2 \times 10^{-4} - 2 \times 10^{-3}$
	U	$10^{-6} - 6 \times 10^{-5}$
	Pu	$10^{-6} - 10^{-2}$

Additional information on potential release fractions from heated spent fuel is provided by *Restrepo (1991)*, as reported in *DOE (1994)*. The values are given in Table 4-2. It can be seen that the values are somewhat lower for the noble gases, alkali metals, and halogens, but higher for chalcogens, alkali earths, and most other elements.

Table 4-2: Estimated Release Fractions of Main Elements From Heated Spent Fuel (after *Restrepo, 1991*).

Chemical Family	Element or Isotope	Release Fraction
Noble gases	Kr, Xe	0.5
Alkali Metals	Cs, Rb	0.2
Halogens	I	0.05
Chalcogens	Te, Se	0.07
Alkali Earths	Sr, Ba, Y	0.03
Miscellaneous	Mo	0.03
	Ru	2×10^{-3}
	Ce, U, Pu	4×10^{-4}
	Eu, Am	6×10^{-4}

For a less severe accident in which fuel is exposed to air but does not reach temperatures at which a cladding fire ignites, and for a usual industrial type fire, it is assumed that a maximum temperature of fire is less than 900°C. Estimated release fractions of main elements during a low-temperature fire are given in Table 4-3. For noble gases the value of 0.4 estimated by *Travis et al. (1997)* on the basis of the high burnup/high linear power calculation was used. This value is therefore believed to be conservative. The fractions for the alkali metals, halogens, chalcogens, alkali earth, molybdenum, ruthenium, and lanthanides were based on experimental observation (*Lorenz, 1995; DOE, 1994*).

Table 4-3: Estimated Release Fractions of Main Elements During a Low-Temperature Fire in Spent Nuclear Fuel Storage Facilities (after *Banba, 2001*).

Chemical Family	Element or Isotope	Release Fraction
Noble gases	Kr, Xe	0.4
Alkali Metals	Cs, Rb	$10^{-6} - 10^{-8}$
Halogens	I	3×10^{-3}
Chalcogens	Te, Se	$10^{-5} - 10^{-7}$
Alkali Earths	Sr, Ba, Y	10^{-8}
Miscellaneous	Mo, Ru,	$10^{-7} - 10^{-8}$
	Eu, Ce	$10^{-7} - 10^{-8}$
	U, Pu	$10^{-7} - 10^{-8}$

For mechanical destruction of the fuel, a complete failure of the cladding is assumed. This leads to a release of the volatile material present in the gap between the fuel matrix and the cladding. A suggested release fraction in this case is reported by *DOE (1994)* to be 5% for noble gases, halogens (specifically, iodine), and alkali metals (specifically, cesium), and zero for all other elements.

4.2.1 Identification of Potential Accidents

4.2.1.1 Reactivity accident during refueling

A risk estimation for a reactivity accident during defueling was carried out by *Takano et al. (2001)*. It is known that there have been two reactivity accidents during refueling by

the year of 1985. It is possible to roughly estimate that about 270 submarine refuelings had taken place by the year 1985²⁹. Each submarine is presumed to contain two identical reactor cores. On this basis, it can be estimated that the frequency of reactivity accidents during refueling is approximately 0.37 % per refueling (two reactivity accidents among 540 reactor refuelings). There are about 40 nuclear submarines in service and about 60 retired submarines at Russian Far East. If we assume that all of these submarines will experience defueling within the next ten years, there will be 200 reactor defueling processes. Assuming the frequencies of reactivity accidents during defueling and refueling are the same³⁰, the expected number of reactivity accidents over the next ten years is approximately 0.74. The above estimation is very simple and the value might include large uncertainties. After experiencing such accidents, some countermeasures were taken to prevent the occurrence of the similar sequences and, in this case, the frequency might be reduced. However, such information is not available. In any case, it is clear that the likelihood of a criticality accident is non-negligible.

It is difficult to estimate the amount of material that would be released in the event of a criticality accident. However, the estimated excursion power used in the *NATO (1998)* study was estimated to be 2500 MWs (8×10^{19} fissions), which was considered to be sufficient to result in melting of the fuel cladding with a consequent steam explosion. We note that the Chazhma Bay accident was estimated to have had a power excursion of 5×10^{18} fissions, approximately one order of magnitude less (*Sivintsev et al., 1994*). We expect that the release fractions from a severe criticality accident on the order of that assumed in *NATO (1998)* would lie somewhere between the Chernobyl-type accident and those estimated in Table 4-1. For less severe criticality accidents resulting in mechanical fuel destruction, a gap release of 5% for noble gases, iodine, and cesium may be more appropriate as the primary release would arise from the mechanical destruction of the fuel.

4.2.1.2 Fire in dry storage facility or during defuelling

Lysenko et al. (2002) have evaluated the short-range (<20 km) impacts of a fire accident involving spent nuclear fuel. An estimation of the likelihood of such an accident was not provided. A hypothetical aircraft accident can be assumed for the dry storage facilities, as the consequences of this accident are expected to bound all other dry storage accident scenarios involving an impact that results in fire. Depending upon the method of construction of the facility and the exact location of the impact, much of the aircraft structure may be stopped by the dry storage building structure. However, the heavy dense jet engine rotor shaft is expected to be capable of penetrating the building and damaging the containers within. Due to the severity of the impact, it can be conservatively assumed that the cask is breached and the fuel elements in the cask are damaged. The release of fission products occurs due to the impact and resultant fire. The fire is probably a normal industrial-type fire below 900 - 1000°C (that is, a low temperature fire), because this fire occurs from aviation fuel. Therefore, fire

²⁹ If the refueling cycle was longer than that assumed, the estimated frequency would increase since the number of refuelings would have been less. By the same reasoning, the existence of retired submarines will also make the frequency slightly higher.

³⁰ Which is likely to be conservative. Defueling procedures call for the maintenance of the core in a dry condition. This significantly lowers the risk of a criticality accident by removing the moderator.

propagation is unlikely after an aircraft accident. The likely release fractions for a low temperature fire were presented in Table 4-3. The values given in Table 4-2 by *Restrepo (1991)* provide an upper bound on the release fraction for an intense fire that did not result in clad combustion. For the fuel that is directly impacted and mechanically destroyed, the release fractions given by *DOE (1994)* are expected to be reasonable.

4.2.1.3 Clad fires

It is difficult to evaluate the potential for fuel fires, because the composition of the fuel and clad are not known. Although it is believed that the fuel is stainless-steel clad (*Lysenko et al, 2002*), zirconium cladding cannot be ruled out. If the fuel is clad with stainless steel, the maximum potential release fraction is likely to be less than that given in Table 4.1 because of the lack of a significant potential for a clad fire. Stainless steel clad fuel may be subject to the formation of uranium hydride (UH₃). Uranium hydride is an ignitable and combustible compound for which a mass of 1 g is required for ignition. Low-temperature ignition and combustion of UH₃ may become an issue if water has been allowed to enter the transport casks. As mentioned above, the formation of UH₃ is of concern because of its low temperature of ignition and combustion. The moisture level in dry storage facilities will be important to the spent fuel condition. It was estimated that approximately 10 g of moisture could remain after drying spent fuel in a 7 m³ internal free volume storage system. If the potential quantity of reactive residual gas were approximately 0.6 moles of H₂ and it all were to react with metallic U as a single location, the approximately 70 g of UH₃ that could be formed. This is considerably more than the quantity that may be required for ignition during subsequent fuel handling, packaging, or drying operations. However, even if the burning of the fuel occurs, the temperature of fire is not expected to exceed the melting temperature of clad because of unfavorable self-sustaining rapid oxidation of clads.

In the event that the fuel is zirconium clad, hydride formation is not likely. Thermodynamic calculations for the reaction of zirconium-clad UO₂ commercial spent fuel with water indicate that UH₃ formation is thermodynamically unfavorable (*Guenther et al. 1996*), and UH₃ has not been a problem during pool storage of commercial UO₂ spent fuel clad with zirconium alloys. However, zirconium presents other potential problems. *Sailor et al. (1987)* evaluated the likelihood of zirconium fires in drained spent fuel pools. Although their results are primarily applicable to relatively fresh spent fuel in which the loss of decay heat removal is the initiating event, some aspects of the study are relevant if there are other heat sources (such as fuel oil fires or other chemical fires) present. They found that temperatures as low as 650°C can be expected to cause clad failure and release of some fission products if the temperatures are sustained over a long period (several hours). However, below 800°C the energy from oxidation is insufficient to significantly increase the fuel rod temperature. If the external heat load is sufficient to heat zircalloy-clad fuel elements to about 900°C, a self-sustaining oxidation of zirconium (cladding fire) can occur. That is, the exothermic oxidation reaction provides sufficient energy to match the external heat contribution and the temperature rises rapidly. If self-sustaining oxidation occurs, the fuel rods are predicted to reach 1,500 to 2,100°C over a substantial portion of their length. For the case of decay heat initiated clad fires, the most sensitive parameters for clad fire initiation are the decay heat level and the fuel element geometry (related to natural

circulation flow resistance). This problem has been studied by *Kupca and Natalizio (1999)* for the case of spent fuel onboard decommissioned non-defueled submarines, who concluded that decay heat removal was unlikely to be a problem after two years of storage, even if there is a loss of coolant. In summary, a zirconium cladding fire could result in a high-temperature fire, and thus the release fractions given in Table 4-1 are feasible. Depending upon the storage configuration, the fire may or may not propagate. However, in the event of cask storage, it is not expected that the fire would propagate beyond a single casks. For stainless-steel clad fuels, the limits given in Table 4-2 are expected to be reasonable upper bounds.

4.3 Data

4.3.1 Selection of Target Region

The analysis is carried out for Japan as the target region. The selection of Japan is due to the following reasons:

- As indicated in Chapter 2, Japan has a high probability (34-87%) of being affected by a major release from one of the facilities in southern Primorye Territory. Furthermore, the probability is highest in the winter, when precipitation in western Japan could result in washout or rainout of the transported material.
- Japan is a densely populated region. Widespread deposition over large areas could yield large collective doses.
- Japan has expressed concern over the impact of the radiological impact of the Russian Pacific Fleet, as indicated by the financial assistance provided to the Russian Federation in construction of the LRW processing facility at Bolshoi Kamen.

The selection of Japan as the target region does not imply that other regions, such as Korea, China, or Alaskan territories of the United States are not of interest. However, with the possible exception of Northern China or the Korean peninsula, it is expected that the impacts on Japan would bound the impacts on the other neighboring countries. However, with the development of an appropriate atmospheric transfer factor, a similar analysis could be carried out for the different regions of these countries.

4.3.2 Critical Deposition Level

In this study, the critical deposition level χ_{crit} was defined on the basis of a total effective equivalent dose standard. Because the 10 mSv annual dose discussed in ICRP 82 (*ICRP, 2000*) refers to all sources of exposure (i.e., not only exposure due to the accident), and because this refers to post-accident intervention rather than pre-accident planning, a level below this was taken. In this case, the intervention level is defined as the level of deposition necessary to yield an individual lifetime effective dose of 1 mSv. Given that the accident occurs, this gives rise to a lifetime risk of death from exposure to the deposited nuclides at the level of 5×10^{-5} , which we consider to be consistent with standards for both practices (exposures which are lower but more likely to occur) and interventions (in which the benefit of the intervention must be weighed against the cost

and disruption entailing from the intervention). It should be emphasized again that the purpose of this analysis is simply to screen the facilities giving rise to the risk. A lifetime dose of 1 mSv from an exposure that has a relatively low probability of occurrence is, in our view, a reasonably conservative figure for use in screening assessments.

The scientific challenge arises in the identification of the appropriate deposition-dose conversion factor. There are a number of methods for determining this conversion factor, two of which were examined in this study. The first approach involved the computation of nation-specific dose factors for Russia, Japan, South Korea, and the United States for the nuclides identified above. The computer code RESRAD (Yu *et al.*, 1993, 2000) was used to develop dose factors for soil contamination. This computed dose factor was based on the dose received in the first year after deposition and is thus suitable for comparison with annual dose limits. The second approach was simply the use of the deposition-dose parameter P_{25} calculated by UNSCEAR for estimating the effect of fallout from atmospheric testing of nuclear weapons (UNSCEAR, 1993). This value is more suitable for estimating the total dose received. The values in this report are based on the UNSCEAR (1993) values and a basic lifetime dose limit of 1 mSv from all pathways (ingestion, inhalation, and external ground-plane irradiation) because these resulted in more limiting (lower) critical deposition values, in keeping with the conservative nature of the assessment.

4.3.3 Determination of Atmospheric Transfer Coefficient

The goal of the atmospheric transport analysis is to determine the feasible range of the atmospheric transfer coefficients for different radionuclides. At a given location, one can define a transfer coefficient for dry and wet deposition. As discussed in Section 4.1.2, the transfer coefficient can be estimated by a variety of methods. An example of a computational approach was previously discussed in Section 3.2. Romanova and Takano (2002) used the computer code WSPEEDI (Chino *et al.*, 1995) to determine the ground level deposition of ^{137}Cs under three wind conditions, assuming a unit release. The results of dry deposition modeling in that report were shown in Figure 3-16. In each wind condition, the maximum value (observed at or near the release point) was computed to be between $2\text{-}4 \times 10^{-12} \text{ m}^{-2}$, and maximum centerline deposition over much of Japan ranges between $10^{-13} - 10^{-12} \text{ m}^{-2}$.

Based upon the results of Romanova and Takano (2002), the dry deposition transfer coefficient is set at $5 \times 10^{-13} \text{ m}^{-2}$. We set this transfer coefficient equal for all radionuclides, which is functionally equivalent to assuming that all nuclides are characterized by the same deposition velocity. In reality, this transfer coefficient is likely to be different for each radionuclide. It will vary according to both the chemical form of the radionuclide and with the aerosol size fraction. Both of these will be strongly affected by the release event. It will also vary considerably according to the region of the atmosphere where the radioactivity is transported (i.e., boundary layer transport, stratospheric transport, etc). However, for the sake of simplifying the example, we assume that the dry deposition velocity for all radionuclides is equal to 0.1 cm/s, as assumed by Romanova and Takano (2002). As previously discussed, the ratio of the atmospheric transfer factors for wet deposition to that of dry deposition is set at 100.

4.4 Results

The limited set of radionuclides for which both inventory and dose information is available is used. This subset includes cesium, strontium, americium, and isotopes of plutonium. Table 4-4 shows the critical deposition values and the minimum critical emission under wet and dry conditions for the selected radionuclides

Table 4-4: Nuclide-Specific Parameters for Facility Screening Analysis

Nuclide	Deposition-Dose Value (mSv per kBq/m ² , <i>UNSCEAR 1993</i>)	Critical Deposition Value (kBq/m ²) (based on 1 mSv)	Minimum Critical Emission $Q_{crit,I,Japan}$ (Bq)	
			(based on dry deposition)	(based on wet deposition)
²³⁹ Pu	0.85	1.2	2.4×10^{15}	2.4×10^{13}
²⁴⁰ Pu	0.85	1.2	2.4×10^{15}	2.4×10^{13}
²⁴¹ Pu	0.012	83.3	1.7×10^{17}	1.7×10^{15}
²⁴¹ Am	0.98	1.0	2.0×10^{15}	2.0×10^{13}
⁹⁰ Sr	0.057	17.7	3.5×10^{16}	3.5×10^{14}
¹³⁷ Cs	0.15	6.6	1.3×10^{16}	1.3×10^{14}

It should be noted that the computed critical deposition values for ¹³⁷Cs are of the same order of magnitude as that existing across much of the Northern Hemisphere as a result of atmospheric weapons testing (3.4 kBq/m²), about ten times background for ⁹⁰Sr (2.1 kBq/m²), and roughly two orders of magnitude greater than background for the plutonium isotopes.

We then use data on radionuclide inventory provided by *Lavkovsky (2000)*³¹ for spent fuel storage on floating workshops and shore-based facilities in the Primorye Region. Because we have no isotope-specific data on the material in storage at the facilities at Cape Sysoeva, we assume that the isotopes are present in the same ratio as in the spent fuel stored onboard the PM-74. This results in the computed inventory provided in Table 4-5. This is probably reasonable for Buildings 11 and 30, which are stated to contain spent nuclear fuel (*Danilyan et al., 2000a*). However, because the contents of Construction 7 and 31 are only given as solid waste - with no indication of the type or form - this is less accurate.

The net inventory in the major ($I_{total} > 1000$ TBq) facilities in Southern Primorye Territory is given in Table 4-6. The ratio of the minimum critical emission to the activity in each source yields the critical release fraction for an accident involving the spent fuel in each facility. Dividing the critical emission values in Table 4-4 by the inventories given in Table 4-6 yields the critical airborne release fraction under either wet or dry conditions, shown in Table 4-7 and 4-8 respectively. A designation of ">>100%" indicates a ratio greater than 10. A designation of ">100%" indicates a ratio

³¹ Updated information on inventories has been prepared by *Kobzev and Lavkovsky (2001)* and is being summarized by *Brown et al. (2003)*. The updated inventories will be used in subsequent analyses.

Table 4-5: Estimated Radionuclide Inventories (Bq) in Spent Fuel Storage Facilities and Waste Management Facilities Based upon Analogy with Spent Fuel Stored on the PM-74 (based on Table 3 of *Lavkovsky, 2000*)

	Building 11	Building 30	Construction 7	Construction 31
²³⁹ Pu	9.08x10 ¹²	1.47x10 ¹⁴	4.13x10 ¹²	2.41x10 ¹²
²⁴⁰ Pu	2.14x10 ¹²	3.46x10 ¹³	9.71x10 ¹¹	5.67x10 ¹¹
²⁴¹ Pu	1.61x10 ¹⁴	2.62x10 ¹⁵	7.34x10 ¹³	4.28x10 ¹³
²⁴¹ Am	5.0x10 ¹¹	8.0x10 ¹²	2.3x10 ¹¹	1.3x10 ¹¹
⁹⁰ Sr	3.48x10 ¹⁵	5.64x10 ¹⁶	1.58x10 ¹⁵	9.22x10 ¹⁴
¹³⁷ Cs	3.74x10 ¹⁵	6.07x10 ¹⁶	1.70x10 ¹⁵	9.93x10 ¹⁴
Total	8.14x10 ¹⁵	1.32x10 ¹⁷	3.70x10 ¹⁵	2.16x10 ¹⁵

Table 4-6: Isotopic Inventories (Bq) in Major Facilities in Southern Primorye Territory (Based On Table 3 of *Lavkovsky, 2000*, and Table 1 of *Lysenko Et Al., 2002*)

Nuclide	Bolshoi Kamen	Pavlovsk Bay				Cape Sysoeva				Reference Submarine (<i>Lysenko et al., 2002</i>)	
	PM-74	PM-80	PM-125	PM-133	K-610	Bldg 11	Bldg 30	Bldg 7	Bldg 31	One core	Both cores
²³⁹ Pu	2.7x10 ¹³	3.2x10 ¹²	1.1x10 ¹³	1.1x10 ¹³	3.4x10 ¹²	9.1x10 ¹²	1.5x10 ¹⁴	4.1x10 ¹²	2.4x10 ¹²	6.5x10 ¹²	1.3 x10 ¹³
²⁴⁰ Pu	6.4x10 ¹²	5.1x10 ¹¹	2.7x10 ¹²	2.7x10 ¹²	8.0x10 ¹¹	2.1x10 ¹²	3.5x10 ¹³	9.7x10 ¹¹	5.7x10 ¹¹	4.1x10 ¹²	8.2 x10 ¹²
²⁴¹ Pu	4.8x10 ¹⁴	7.2x10 ¹²	2.2x10 ¹⁴	2.2x10 ¹⁴	3.2x10 ¹³	1.6x10 ¹⁴	2.6x10 ¹⁵	7.3x10 ¹³	4.3x10 ¹³	1.1x10 ¹⁵	2.2 x10 ¹⁵
²⁴¹ Am	1.5x10 ¹²	9.6x10 ¹¹	8.3x10 ¹⁰	8.3x10 ¹⁰	1.2x10 ¹²	5.0x10 ¹¹	8.0x10 ¹²	2.3x10 ¹¹	1.3x10 ¹¹	1.1x10 ¹³	2.2 x10 ¹³
⁹⁰ Sr	1.0x10 ¹⁶	1.1x10 ¹⁵	4.5x10 ¹⁵	4.5x10 ¹⁵	9.5x10 ¹⁴	3.5x10 ¹⁵	5.6x10 ¹⁶	1.6x10 ¹⁵	9.2x10 ¹⁴	4.2x10 ¹⁵	8.4 x10 ¹⁵
¹³⁷ Cs	1.1x10 ¹⁶	1.1x10 ¹⁵	4.8x10 ¹⁵	4.8x10 ¹⁵	1.0x10 ¹⁵	3.7x10 ¹⁵	6.1x10 ¹⁶	1.7x10 ¹⁵	9.9x10 ¹⁴	4.9x10 ¹⁵	9.8 x10 ¹⁵

Table 4-7: Critical release fractions under dry deposition conditions

	Bolshoi Kamen	Pavlovsk Bay				Cape Sysoeva				Reference Submarine	
Nuclide	PM-74	PM-80	PM-125	PM-133	K-610	Bldg 11	Bldg 30	Bldg 7	Bldg 31	One core	Both cores
<i>Sum of Fractions</i>	<i>1.1</i>	<i>0.12</i>	<i>0.50</i>	<i>0.50</i>	<i>0.11</i>	<i>0.39</i>	<i>6.4</i>	<i>0.18</i>	<i>0.10</i>	<i>0.51</i>	<i>1.0</i>
²³⁹ Pu	>>100%	>>100%	>>100%	>>100%	>>100%	>>100%	>>100%	>>100%	>>100%	>>100%	>>100%
²⁴⁰ Pu	>>100%	>>100%	>>100%	>>100%	>>100%	>>100%	>>100%	>>100%	>>100%	>>100%	>>100%
²⁴¹ Pu	>>100%	>>100%	>>100%	>>100%	>>100%	>>100%	>>100%	>>100%	>>100%	>>100%	>>100%
²⁴¹ Am	>>100%	>>100%	>>100%	>>100%	>>100%	>>100%	>>100%	>>100%	>>100%	>>100%	>>100%
⁹⁰ Sr	>100%	>>100%	>100%	>100%	>>100%	>>100%	63%	>>100%	>>100%	>100%	>100%
¹³⁷ Cs	>100%	>>100%	>100%	>100%	>>100%	>100%	22%	>100%	>>100%	>100%	>100%

Table 4-8: Critical release fraction under wet deposition conditions

	Bolshoi Kamen	Pavlovsk Bay				Cape Sysoeva				Reference Submarine	
Nuclide	PM-74	PM-80	PM-125	PM-133	K-610	Bldg 11	Bldg 30	Bldg 7	Bldg 31	One core	Both cores
<i>Sum of Fractions</i>	<i>110</i>	<i>12</i>	<i>50</i>	<i>50</i>	<i>11</i>	<i>39</i>	<i>640</i>	<i>18</i>	<i>10</i>	<i>51</i>	<i>100</i>
²³⁹ Pu	87%	>100%	>100%	>100%	>100%	>100%	16%	>100%	>100%	>100%	>100%
²⁴⁰ Pu	>100%	>>100%	>100%	>100%	>>100%	>>100%	68%	>>100%	>>100%	>100%	>100%
²⁴¹ Pu	>100%	>>100%	>100%	>100%	>>100%	>>100%	64%	>>100%	>>100%	>100%	76%
²⁴¹ Am	>>100%	>>100%	>>100%	>>100%	>>100%	>>100%	>100%	>>100%	>>100%	>100%	93%
⁹⁰ Sr	3%	32%	8%	8%	37%	10%	1%	22%	38%	8%	4%
¹³⁷ Cs	1%	12%	3%	3%	13%	4%	0.2%	8%	13%	3%	1%

between 1 and 10. The Sum of Fractions entry represents the computation of Equation 4.4, and allows the contribution from all nuclides to be combined for screening purposes. A sum of fractions of greater than one indicates that a sufficient inventory to exceed the critical deposition level *could* (but may not) exist in the facility.

It can immediately be seen that only three facilities (the floating workshop PM-74, both cores on a single submarine, or the spent fuel warehouse Building 30) contain sufficient inventories to cause lifetime doses exceeding one mSv under dry deposition conditions. The dose is primarily due to ⁹⁰Sr and ¹³⁷Cs. However, the inventories of the PM-74 and a single submarine are just at the limit. If an accident either affected only a single core or single tank, or if less than the full amount of all nuclides were released, the lifetime dose would be less than 1 mSv.

Table 4-9: Airborne Release Fractions under different accident conditions

Element	Chernobyl (<i>NEA, 1995</i>)	"Gap" Activity Loss (<i>DOE, 1994</i>)	High Temperature Fire	Low Temperature Fire
Pu	3.5%	0	0.0001%-1%	N/r
Sr	4-6%	0	0.2%	10 ⁻⁸
Cs	20-40%	5%	90%	10 ⁻⁶ - 10 ⁻⁸

When the critical release fractions are compared to the values in Table 4-9, it can be seen that only a major release from Building 30, the spent fuel storage facility at Cape Sysoeva, is capable of releasing sufficient material to result in lifetime doses above one mSv. Such an accident would have to be one that results in a high temperature fire or criticality accident affecting between a quarter to a half of the spent fuel assemblies in storage. A low-temperature fire or a gap release would not be expected to give rise to a sufficient release.

However, under wet deposition conditions, none of the facilities can be completely ruled out simply based on atmospheric dispersion alone. The critical release fraction must then be compared to the airborne release fractions as shown in Table 4-9 for plutonium, strontium, and cesium under a variety of accident conditions. It can be immediately seen that it would be extremely unlikely that transboundary plutonium contamination could occur at levels sufficient to cause a lifetime dose of greater than 1 mSv. The worst-case release fraction of plutonium, a Chernobyl-type reactor fire affecting all of the fuel stored in Building 30, is still considerably less than the critical release fraction. However, the fission products ¹³⁷Cs - and to a much lesser extent, ⁹⁰Sr - are present in sufficient (i.e., the lowest critical release fraction is lower than the largest feasible release fraction given by Table 4-9) quantities in several facilities. Damage to less than 10% of the fuel elements in Building 30 (or all of the fuel elements on board the floating workshops or in a single core) that resulted in loss of the "gap" activity of ¹³⁷Cs could result in areas of contamination above 6 kBq/m² in Japan, but only if a heavy rainfall event occurred during the passage of the cloud. Damage to

- 1) the majority of the the spent fuel assemblies on the two floating workshops, in a single submarine core, or in Building 11; or to
- 2) about a third of the fuel onboard the PM-74 or both submarine cores,

that resulted in a gap release could also just exceed the critical level in the event of heavy rainfall during cloud passage. A criticality accident or high temperature fire would also be sufficient and would require less fuel to be affected.

5 Conclusions and Recommendations

K. L. Compton, V. M. Novikov, F. L. Parker, Yu. V. Sivintsev

There have been extensive studies of the current and potential environmental impact of Russian Northern fleet activities. However, despite the fact that the total number of ships in both fleets are comparable, there have been very few studies published in the open literature of the impact of the Pacific fleet. This study of the Pacific fleet's impact on neighboring countries was undertaken to partially remedy this lack of analysis. This study is focused on an evaluation of the inventory of major sources of radioactive material associated with the decommissioning of nuclear submarines, and an evaluation of releases to the atmosphere and their long-range (>100km) transboundary transport. A logical next step would be an analysis of the effects within Russia.

The main bases of the Pacific fleet are located in southern Primorye Territory, near Vladivostok, and in Kamchatka Oblast, near Petropavlovsk. Information on the amount and type of radioactive material stored at both sites has been provided by collaborating Russian scientific institutes. The transport analyses carried out by the IIASA RAD project and presented in this report comprise two elements: 1) a set of trajectory analyses of the probability of contaminants reaching certain countries and during which times of the year, and 2) a case study to evaluate one of the more significant cases, namely, transport of radioactive material to Japan from an accident in Southern Primorye Territory. Finally, a description of an approach to identify high-priority facilities for remediation or further evaluation, based upon their potential for transboundary impact, was applied to evaluate the effect of an accident in southern Primorye Territory upon Japan.

The potential human health impact of these facilities is affected by a large number of variables: the type of accident; the height to which the contaminant cloud is driven into the atmosphere; the time of year, which will profoundly impact the path and dilution of the contaminants and the potential exposure pathways; the degree of deposition of the contaminant; and the human and environmental exposure.

It is important to note that because of the proximity of the facility in southern Primorye Territory to China and the Korean Peninsula, intermediate range atmospheric transport (<100km) might be also of transboundary nature, and may have serious impacts. However, apart from noting the potential for transboundary impacts to North China or North Korea resulting from intermediate range transport, the effects are not discussed further. Our ongoing work (*Brown et al., 2003*) is studying that problem.

5.1 Conclusions

5.1.1 Source Term

The report contains the details of the types of ships involved, the amount of radioactive material in the spent fuel and reactor components, problems in operation, storage of fuel and wastes and details of accidents that have occurred. The information was provided by Russian scientific institutions (Kurchatov Institute, CDB "Lazurit", and DalRAO),

and was evaluated by the IIASA RAD project. The following conclusions can be drawn with respect to the evaluation of sources:

- 1) Existing information about the source term in Russian Far East is limited and subject to considerable uncertainty.

Significantly fewer international projects deal with environmental issues in the Russian Far East, possibly because of significantly less attention of Western countries to that region. There are significant differences in the reported descriptions of the environmental situation in the Russian Far East. The task of developing a reliable source term is hampered by the variety of names used to refer to different facilities, the inconsistencies between reported inventories from different sources, and the omissions in available reports of important facilities. The reported inventory of 2200 TBq in Construction 19 at Kamchatka is a striking example of the problems involved in compiling a consistent source term from the available literature. There was no definite explanation why the official Russian data shows that the Pacific Fleet, having less than 70% of the capacity of Northern Fleet, produced twelve times more radioactive waste than the Northern Fleet. One possible explanation is that the infrastructure in the Far East is so poor that no transportation of radioactive waste to the storages in the central part of Russia took place in the past. However, this is only a conjecture.

- 2) Despite the problems, it has been possible to draw a general picture of the sources of radioactive contamination in the Russian Far East. It can be seen that there are a few large sources that contribute the vast majority of the radioactive inventory. Of all categories of radioactive material (liquid waste, solid waste, and spent fuel), spent fuel contributes the vast majority of the radioactive inventory, followed by solid radioactive waste. The majority of the radioactivity in liquid radioactive waste is associated with the wet storage of damaged spent fuel elements.

For spent fuel and solid radioactive waste, the inventories are dominated by the Cape Sysoeva facility. The largest single source of radioactivity in spent fuel is Building 30. For solid radioactive waste, the dominant sources are constructions 1-5, 7, 31, and 32, all of which contain more than 1,000 TBq and which together constitute 99% by activity (11,000 TBq) of the solid radioactive waste in the Russian Far East³². The vast majority (97.5%) of the reported radioactive inventory in liquid radioactive waste is onboard the two floating workshops containing damaged spent fuel, with most of this being onboard the PM-32 (210 TBq out of a total of 220 TBq, or 95%) (Danilyan et al. 2000b, Table 18).

- 3) Additional data necessary for a full risk analysis is beginning to be obtained, but is not yet complete.

These studies made the radiological picture clearer not only by specifying the radioactive inventory but also by making available data important for risk analysis, such as the conditions on ships for storage of spent nuclear fuel. It is clear from the description of the service ships that most of the ships are in extremely poor condition and are storing wastes for which they were not designed. However, critical information for properly evaluating potential releases is missing, particularly for land-based

³² Or 83% of a total inventory of 13,000 TBq, depending upon the true inventory of Construction 19 in Kamchatka. The inventory of Construction 19 in Kamchatka needs to be clarified, as the discrepancy has a significant impact on the results.

storages. Information on the design and construction of spent fuel storage facilities, such as the conditions of storage (the type of storage, the characteristics and condition of the fuel stored in the building, the availability and condition of the systems for fire protection and heat removal, the conditions of storage that would affect the ability of a fire to propagate throughout the facility, etc) is necessary to evaluate the risk posed by these facilities.

5.1.2 Transport and Consequence Analysis

The evaluation of long-range atmospheric transport and a review of potential consequences were carried out by the IIASA RAD Project based on the data provided by Russian scientific institutes and publicly available meteorological data. The following conclusions can be drawn with respect to airborne transport and the consequences following a major accident at a Russian Pacific Fleet facility near Vladivostok or Petropavlovsk:

1. Radioactive material released from either site could reach neighboring countries within a relatively short time (twelve hours to three days)

The results of the trajectory analysis show that releases from the facilities in southern Primorye Territory are most likely to pass over North China and North Japan. Transport time to North China and North Japan could occur in as little as 0.5 and 1.6 days, respectively. For releases at the Kamchatka sites, the Aleutian Islands and the Western Shore of Alaska are at the highest risk of impact. Because of their greater distance from the site, their average transport times are 3.0 and 5.1 days, respectively.

2. Although detectable amounts of radioactivity may reach neighboring countries, committed effective doses from inhalation and external irradiation as a result of exposure during passage of the contaminated cloud are expected to be several orders of magnitude below 1 mSv.

Using the computer code WSPEEDI together with meteorological data provided by JAERI, the impact on Korea and the Japanese islands from a hypothetical accident in southern Primorye Territory was evaluated under three typical winter weather patterns. A criticality accident similar to that which occurred in August 1985 in Chazhma Bay that resulted in a release of 2.5×10^{12} Bq of iodine (2.9×10^{10} Bq ^{131}I , 6.2×10^{11} Bq ^{133}I , and 1.8×10^{12} Bq ^{135}I) could result in a maximum dose in Japan of $\sim 4 \times 10^{-8}$ mSv under either strong or weak wind conditions. The maximum dose in Korea would be similar ($\sim 2 \times 10^{-8}$ mSv), but would occur as a result of a cyclonic wind condition. If the same accident were to release fission products (3.5×10^{14} Bq ^{137}Cs , 3.5×10^{13} Bq ^{134}Cs , and 7×10^{13} Bq ^{90}Sr), the maximum doses would be higher (up to $\sim 10^{-3}$ mSv in Japan, due to ^{137}Cs and ^{90}Sr , and $\sim 5 \times 10^{-4}$ mSv in Korea), but still quite low. It is worth noting that there have been three severe submarine reactor accidents in the past near Vladivostok, including one reactivity accident and two loss of coolant accidents. None of these accidents appear to have resulted in appreciable contamination in Japan.

3. The number of facilities with sufficient inventories of radioactive material to give rise to any significant transboundary contamination is very limited.³³

³³ As noted, we defined significant contamination as that giving rise to a lifetime dose of 1 mSv, corresponding to a lifetime risk of fatal cancer due to exposure to deposited radioactivity of 5×10^{-5} .

The lack of a probabilistic risk assessment of the sites in the Russian Far East available to us, coupled with a lack of data about the details of the facilities, forced us to use an inverse approach based on the critical value of radioactive deposition in the neighboring country as a result of accidental radioactive release from a nuclear risk site followed by atmospheric transfer to the country of interest. Application of a screening methodology to the inventories reported for Vladivostok to evaluate the risk to Japan indicates that only one source - Building 30, the storage facility for spent nuclear fuel at the Cape Sysoeva Waste Management Facility - might be capable of causing significant contamination in Japan due to dry deposition. A major accident at this facility releasing on the order of 10^{16} Bq (~300,000 Ci) of ^{137}Cs (~20% of the total inventory) could result in contamination due to dry deposition at levels of about 6 kBq/m², resulting in individual lifetime equivalent doses on the order of 1 mSv. However, such an accident would require either a criticality accident affecting all of the fuel at the facility or a high-temperature fire that propagated throughout the majority of the facility. Such an accident seems very unlikely, although it is not possible to evaluate the likelihood of such an accident without additional data on the facility and the conditions of storage. Although fallout from an accident at the other facilities - including the decommissioned submarines - cannot be ruled out, they are not expected to be capable of giving rise to widespread contamination. Deposition above the "critical" level (6 kBq/m²) in Japan would only be possible if rather heavy rainfall occurred during passage of the peak of the cloud resulting from a major accident. Transboundary plutonium contamination is not expected even under worst-case conditions, such as complete spent fuel melting combined with rainfall during plume passage over Japan.

5.2 Recommendations

- 1) The only significant source of transboundary risk to Japan is an accident involving severe damage to large amounts of spent fuel. Measures to improve spent fuel management in the Russian Far East and to ensure the integrity of the spent fuel could reduce the potential transboundary risks to Japan. Ensuring that criticality and fire protection systems are adequate may be particularly useful.
- 2) The number of facilities that warrant further investigation in regard to potential transboundary impacts to Japan are limited, and most are at the Cape Sysoeva Waste Management Facility. Better information at this site, including the details of construction, the condition of the facilities, and a fire safety assessment, would yield a better picture of the transboundary risks.
- 3) The generally lower inventories of radioactivity in storage near Petropavlovsk and the longer distances to the United States suggests that the transboundary risks to the United States are also expected to be low. However, this should be confirmed with a more detailed evaluation of the potential for atmospheric transport and a clearer inventory of radioactive material in storage in Kamchatka Oblast.

6 References

1. Alexander, C.A., and others (1984). "Actinide Release from Irradiated Fuel at High Temperatures", Proceedings of the ANS Topical Meeting on Fission Product and Source Term Research, Snowbird, UT, July 1984.
2. Baker, Wayman, ed. (1992). Research Highlights of the NMC Development Division: 1989-1991. National Oceanic and Atmospheric Administration, Washington, DC. 469 pp.
3. Baklanov A., A. Mahura, D. Jaffe, L. Thaning, R. Bergman, and R. Andres (2002). "Atmospheric Transport Patterns and Estimation of Consequences after the Nuclear Accident at the Russian North-West" *Journal of Environmental Radioactivity* **60**(23-48)
4. Banba, T. (2001). "Radionuclide release fractions from the spent nuclear fuel storage facilities under potential fire accident conditions in the Russian Far East Region" Internal RAD Project Report, IIASA, Laxenburg, Austria
5. Bellona (1996). The Russian Northern Fleet Report 2, Bellona Foundation, (available at <http://www.bellona.no/imaker?id=10090&sub=1>, accessed March 2001)
6. Bradley, D.J. (1997). Behind the Nuclear Curtain: Radioactive Waste Management in the Former Soviet Union, Battelle Press, Columbus, USA, 716 pp.
7. Brown, K.G., and others. (2003). Analysis of the Dose Commitments Resulting from Atmospheric Transport and Deposition from Nuclear Risk Sites in the Russian Far East. (IIASA interim report, in preparation). International Institute for Applied Systems Analysis, Laxenburg, Austria.
8. Chaikovskaya, E. L., V. L. Visotskii, and D.V. Gichev. (2001). "Characteristics of the Formation of the Radiation Situation on Territory of Primorskii Territory." *Russian Journal of Atomic Energy*, **91**:3(223-237)
9. Chino, M., H. Ishikawa, H. Yamazawa, H. Nagai, and S. Morinchi (1995). WSPEEDI (Worldwide Version of SPEEDI) A Computer Code System for Prediction of Radiological Impacts on Japanese due to Nuclear Accident in Foreign Countries. Japan Atomic Energy Research Institute, Japan.
10. Danielsen, E. (1961). "Trajectories: Isobaric, Isentropic and Actual" *Journal of Meteorology* **18**(479-486)
11. Danilyan V.A., V. L. Vysotsky, and A. A. Maksimov (2000a). "Radioecological Situation on territory of land-based technical bases of Far Eastern region" *Russian Journal of Atomic Energy* **89**:2(673-679)
12. Danilyan V. A., Vysotsky V. L., A. A. Maksimov., and Yu.V. Sivintsev (2000b) "Effect of the Utilization of Nuclear-Powered Submarines on the Radioecological Conditions in the Far-East Region" *Russian Journal of Atomic Energy* **89**:6(982-1003)
13. Davis, P. A., M. R. Avadhanula, D. Cancio, P. Carboneras, P. Coughtrey, G. Johansson, R. H. Little, G. M. Smith and B. M. Watkins (1998). "BIOMOVs II: An

- international test of the performance of environmental transfer models" *Journal of Environmental Radioactivity* **42**:2-3(117-130)
14. Desiato, F., D. Anfossi, S. T. Castelli, E. Ferrero and G. Tinarelli (1998). "The role of wind field, mixing height and horizontal diffusivity investigated through two Lagrangian particle models" *Atmospheric Environment*, **32**:24(4157-4165)
 15. DOE (1994). Airborne Release Fractions/Rates and Respirable Fractions for Nonreactor Nuclear Facilities (DOE-HDBK-3010-94) U.S. Department of Energy
 16. Draxler, R. (1987). "Sensitivity of the trajectory model to the spatial and temporal resolution of the meteorological data during CAPTEX" *Journal of Climatology and Applied Meteorology* **26**(1577-1588)
 17. Egorov, N.N., V. Novikov, F. L. Parker, and V. Popov, Eds. (2000). Radiation Legacy of the Soviet Nuclear Complex Earthscan Publications, London. 236 pp.
 18. Goriglejan, E.A. (1999). "Design Support to Minimize the Risk of Environmental Impact of Damaged Nuclear Steam Generating Plants of the Russian Nuclear Submarines During Their Long-Term Storage in Sarcophaguses". pp 291-302 in Analysis of Risks Associated with Nuclear Submarine Decommissioning, Dismantling, and Disposal, A. A. Sarkisov and A. Tournyol du Clos, eds. Kluwer Academic Publishers, The Netherlands.
 19. Guenther, et al. (1996). Initial Evaluation of Dry Storage Issues for Spent Nuclear Fuels in Wet Storage at the Idaho Chemical Processing Plant (INEL-96/0140)
 20. Handler, J. (1998). "The Lasting Legacy - Nuclear Submarine Disposal". *Janes Navy International*, **103**:1(12-20), Jan/Feb 1998
 21. Handler, J. (1995). "Russia's Pacific Fleet - Problems with Nuclear Waste". *Janes Intelligence Review*, 7:3(136-140), March 1995
 22. Handler, J. (1994a). Preliminary Report on Greenpeace Visit to Vladivostok and Areas around the Chazhma Bay and Bolshoi Kamen Submarine Repair and Refueling Facilities, Greenpeace, Washington, DC.
 23. Handler, J. (1994b). "Russia's Pacific Fleet - Submarine Bases and Facilities". *Janes Intelligence Review*, April 1994, pp.166-171
 24. Hanna, S.R., G.A. Briggs, and R. Hosker (1982). Handbook on Atmospheric Diffusion (DOE/TIC-11223) Office of Health and Environmental Research, US Department of Energy, Washington, DC.
 25. Harris, J. M. & Kahl, J. D. (1990). "A descriptive atmospheric transport climatology for Mauna Loa Observatory, using clustered trajectories" *Journal of Geophysical Research* (13651-13667)
 26. Harris, J.M. and Kahl, J.D. (1994). "Analysis of 10-day Isentropic Flow Patterns for Barrow, Alaska: 1985-1992" *Journal of Geophysical Research* **99**(25845-25855)
 27. ICRP (2000). Protection of the Public in Situations of Prolonged Radiation Exposure (ICRP Publication 82). International Commission on Radiation Protection, Elsevier Science Ltd.

28. Interfax (2002). "Fire breaks out in Russian Pacific Fleet's nuclear submarine", November 22, 2002 (cited in RANSAC Nuclear News, accessed 9 Dec 2002 from <http://www.ransac.org/new-web-site/pub/nuclearnews/11.22.02.html#1m>)
29. Ishikawa, H. (1995). "Evaluation of the Effect of Horizontal Diffusion on the Long-range Atmospheric Transport Simulation with Chernobyl data" *Journal of Applied Meteorology* **34**:7(1653-1665)
30. Ishikawa, H. (1994). "Development of Worldwide Version of system for Prediction of Environmental Emergency Dose Information, WSPEEDI (III)" *Journal of Nuclear Science and Technology (Japan)* **31**:9(969-978)
31. Jaffe, D., A. Mahura, and R. Andres (1997a). Atmospheric Transport Pathways to Alaska from Potential Radionuclide Sites in the Former Soviet Union (Research Report, UAF-ADEC Project 96-001) Fairbanks, AK. 71 pp.
32. Jaffe, D.A., A. Mahura, J. Kelley, J. Atkins, P. C. Novelli, and J. Merrill (1997b). "Impact of Asian Emissions on the Remote North Pacific Atmosphere: Interpretation of CO Data from Shemya, Guam, Midway and Mauna Loa" *Journal of Geophysical Research* **23**(28627-28636)
33. Jaffe, D., A. Mahura, R. Andres, A. Baklanov, L. Thaning, R. Bergman, and S. Morozov (1998). Atmospheric Transport from the Kola Nuclear Power Plant (Pilot Study Research Report, UAF-FOA-BECN Joint Project) 61 pp.
34. Kahl, J.D. (1996). "On the prediction of trajectory model error" *Atmospheric Environment* **30**(2945-2957)
35. Kirchner, G., S. R. Peterson, U. Bergström, S. Bushell, P. Davis, V. Filistovic, T. G. Hinton, P. Krajewski, T. Riesen and P. U. de Haag (1998). "Effect of user interpretation on uncertainty estimates: examples from the air-to-milk transfer of radiocesium" *Journal of Environmental Radioactivity* **42**:2-3(177-190)
36. Kobzev, V. I., and S. A. Lavkovsky (2001). "Collection, Processing and Submission of Information in Addition to the Existing Database of ISTC Project 101 on Radioactive Waste Resulting from the Russian Nuclear Fleet Activity at the Far East", Contractor Report to IIASA of July 30 2001, Lazurit Central Design Bureau, Nizhniy Novgorod, Russian Federation.
37. Kudrik, I. (1999). "Spent fuel storage barge on fire", (accessed 9 Dec 2002 from <http://www.bellona.no/en/international/russia/navy/pacific/incidents/13896.html>)
38. Kupca, S. and A. Natalizio (1999). "Accident Risk Associated with Fueled Decommissioned Nuclear Powered Submarines. pp 41-52 in Analysis of Risks Associated with Nuclear Submarine Decommissioning, Dismantling, and Disposal, A. A. Sarkisov and A. Tournyol du Clos, eds. Kluwer Academic Publishers, The Netherlands.
39. Kutcher V.A. et al. (1996). "Nuclear Submarines of Russia. First Generation (Vol.IV, Part 1)", "Rubin" Central Design Bureau of Marine Technologies, St. Petersburg (in Russian, cited in *Lavkovsky 2000*)
40. Kuzin, V.P. and V.N. Nikolsky (1996). "USSR Navy 1945-1991" Historical Marine Society, St. Petersburg (in Russian, cited in *Lavkovsky 2000*)

41. Lavkovsky, S. A. (2000). "Selection and Submission of Information from the Existing Database of ISTC Project 101 on Radioactive Wastes Resulting from the Russian Nuclear Fleet Activities at the Far East", Contractor Report to IIASA of December 9 2000, Lazurit Central Design Bureau, Nizhniy Novgorod, Russian Federation.
42. Lorenz, R.A., and M.F. Osborne (1995). A Summary of ORNL Fission Product Release Test With Recommended Release Rates and Diffusion Coefficients (NUREG/CR-6261) U. S. Nuclear Regulatory Commission, Washington, DC.
43. Lysenko, N. I., B. G. Pologich, and Yu. V. Sivintsev (2002). Radioecological consequences of accidental helicopter/airplane fall on a nuclear submarine during a removal of spent nuclear fuel (SNF) or on a shore storehouse of SNF (Paper Number 31/3-529-02), Russian Research Centre "Kurchatov Institute", Moscow, Russia.
44. Mahura, A. (2002) Assessment of Impact of Russian Nuclear Fleet Operations on Russian Far Eastern Coastal Regions (IR-02-004). International Institute for Applied Systems Analysis, Laxenburg, Austria.
45. Mahura, A., A. Baklanov, J.H. Sorensen, F. Parker, V. Novikov, Kevin Brown, and K.L. Compton. (2002) Probabilistic Analysis of Atmospheric Transport and Deposition Patterns from Nuclear Risk Sites in Russian Far East (Scientific Report 02-09), Danish Meteorological Institute, Copenhagen, Denmark/ International Institute for Applied Systems Analysis, Laxenburg, Austria. December 2002.
46. Mahura A., D.A. Jaffe, R.J. Andres, and J. T. Merrill (1999a). "Atmospheric transport pathways from the Bilibino nuclear power plant to Alaska" *Atmospheric Environment* **33**:30(5115-5122)
47. Mahura A., D. Jaffe and R. Andres (1999b). "Air Flow Patterns and Precipitation Probability Fields for the Kola NPP". pp. 87-93 in Abstracts of the International Conference "Nuclear Risks, Environmental and Development Cooperation in the North of Europe", held 19-23 June 1999 in Apatity, Murmansk Region, Russia.
48. Mahura, A., D. Jaffe, R. Andres, D. Dasher, and J. Merrill (1997a). "Atmospheric Transport Pathways to Alaska from Potential Radionuclide Sites in the Former Soviet Union" pp 173-174 in Volume 1 of Proceedings of American Nuclear Society Sixth Topical Meeting on Emergency Preparedness and Response, held April 1997 in San Francisco, CA.
49. Mahura, A., Jaffe D., Andres, R., Dasher, D., Merrill, J.(1997b). "Atmospheric Transport Pathways from the Kola Nuclear Power Plant" pp 52-54 in Volume 2 of Extended Abstracts of Intentional Symposium on Environmental Pollution of the Arctic and The Third International Conference on Environmental Radioactivity in the Arctic, held June 1-5 1997 in Tromso, Norway.
50. Merrill, J. (1994). "Isentropic Airflow Probability Analysis" *Journal of Geophysical Research* **99**(25881-25889)
51. Merrill, J., R. Bleck, and L. Avila (1985). "Modeling Atmospheric Transport to the Marshall Islands" *Journal of Geophysical Research* **90**(12927-12936)

52. Merrill, J., R. Bleck, and D.B. Boudra (1986). "Techniques of Lagrangian Trajectory Analysis in Isentropic Coordinates" *Monthly Weather Review* **114**(571-581)
53. Mordashev, V. and A. Pechkurov (2000). The Natural, Geographical and Climatic-Meteorological Characteristic of the Regions of the Far East of Russia Contractor Report to IIASA.
54. NATO (1998). NATO/CCMS Pilot Study: "Cross-Border Environmental Problems Emanating from Defence-Related Installations and Activities", Phase II: 1995-1998, Final Report, Vol. 4: "Environmental Risk Assessment for Two Defence-Related Problems" (Report No. 227), North Atlantic Treaty Organization, Brussels.
55. NEA (1995). Chernobyl: Ten Years On. Radiological And Health Impact: An Assessment By The NEA Committee On Radiation Protection And Public Health, OECD Nuclear Energy Agency, Paris.
56. OTA (1995). Nuclear Wastes in the Arctic (An Analysis of Arctic and Other Regional Impacts from Soviet Nuclear Contamination). Office of Technology Assessment. Congress of the United States. (OTA-ENV-623). Office of Technology Assessment, Washington. 239 pp.
57. Poirot R.L., and P.R. Wishinski (1984). "Visibility, sulfate and air mass history associated with the summertime aerosol in northern Vermont" *Atmospheric Environment* **20**(1457-1469)
58. Quade, Edward S. (1980) "Pitfalls in Formulation and Modeling." Chapter Three in Pitfalls of Analysis, Giandomenico Majone and Edward S. Quade, Eds. John Wiley and Sons, London.
59. Randel, William (1992) Global Atmospheric Circulation Statistics, 1000-1mb; NCAR Technical Note TN-366+STR. National Center for Atmospheric Research, Boulder, CO. 256 pp.
60. Restrepo, L. (1991). Building 771, Subteam 6 Report, Chapter 7, Criticality Assessment. EG&G Rocky Flats, Golden, CO (cited in *DOE (1994)*)
61. Romanov, V.I. (1993). "Hot particles near a nuclear object in case of explosive hypothetical accident" *Russian Journal of Atomic Energy* **75**:5(377 - 381) (In Russian, cited in *Sivintsev 2000a*)
62. Romanova, V., and M. Takano (2002). Atmospheric Transport of Radioactive Nuclides from Russia to Neighboring Countries (IR-02-010) International Institute for Applied Systems Analysis, Laxenburg, Austria.
63. Romesburg, C.H. (1984). Cluster Analysis for Researches Lifetime Learning, Belmont, CA. 334 pp.
64. Sailor, V.L., K.R. Perkins, J.R. Weeks, H.R. Connell (1987). Severe Accidents in Spent Fuel Pools in Support of Generic Safety Issue 82 (NUREG/CR-4982) U. S. Nuclear Regulatory Commission, Washington, DC.
65. Sarkisov, A. A (1999). "Analysis of current status and methods of resolving of the nuclear submarine decommissioning problem" pp. 4-41 in Nuclear Submarine Decommissioning and Related Problems" (Proceedings of the International

- Workshop held June 19-22 1995 in Moscow), "KomTech" Moscow. (In Russian, cited in *Sivintsev 2000a*).
66. Shilgan, Yu.P. "Issues of Nuclear and Radiation Safety in Nuclear Submarine Disposal", In Ecological Problems of Nuclear Submarine Disposal (Proceedings of an International Seminar held July 4-9 2001 in Severodvinsk, Russia.) (in Russian, cited in *Kobzev and Lavkovsky, 2001*)
 67. Sivintsev, Yu. (2000a). Assessment of Impact of Decommissioned and Utilized Russian Nuclear Submarines on the Environment of the Far Eastern Regions. Contractor Report to IIASA of November 2000.
 68. Sivintsev, Yu. (2000b). "Number of fission in the Chazhma Bay Accident in 1985" *Russian Journal of Atomic Energy* **89**:3(269)
 69. Sivintsev, Yu. and O. Kiknadze (1998a). "Inventory of Radionuclides in the Ship Nuclear Reactors Dumped in the Sea of Japan" *Radiation Protection Dosimetry* **75**:1-4(195-198).
 70. Sivintsev, Yu. and O. Kiknadze (1998b). Estimation of Radionuclide Inventories with Prediction of Release Rates for Dumped Radioactive Wastes in the Far Eastern Seas (RRC "Kurchatov Institute" Report 31/8104 in fulfilment of IAEA Technical Contract No. 9488), Russian Research Centre "Kurchatov Institute", Moscow.
 71. Sivintsev, Yu., V. Vysotsky, and V. Danilyan (1994a). "Radioecological Consequences of Radiation Accident on the Nuclear Submarine in Chazhma Bay" *Russian Journal of Atomic Energy* **76**:2(158-160), 1994 (In Russian, cited in *Sivintsev 2000a*).
 72. Sivintsev, Yu. (1994b). Study of the Radionuclides Inventory and Fuel Characteristics in the Dumped Reactors of Nuclear Submarines and Nuclear Icebreaker "Lenin" - Part 2 - Nuclear Submarines. Russian Research Centre "Kurchatov Institute", Moscow. (also available as IAEA-IASAP-5 from the International Atomic Energy Agency, Vienna.)
 73. Sørensen, J.H. (1998). "Sensitivity of the DERMA long-range Gaussian dispersion model to meteorological input and diffusion parameters" *Atmospheric Environment* **32**:24(4195-4206)
 74. Stohl, A. (1998). "Computation, accuracy and applications of trajectories - A review and bibliography" *Atmospheric Environment* **32**:6(947-966)
 75. Takano, M., V. Romanova, H. Yamazawa, Y. Sivintsev, K. L. Compton, V. Novikov, and F. L. Parker (2001). "Reactivity Accident of Nuclear Submarine near Vladivostok" *Journal of Nuclear Science and Technology (Japan)* **38**:2(143-157)
 76. Till, J. E. and H. R. Meyer, Eds. (1983). Radiological Assessment: A Textbook on Environmental Dose Analysis (NUREG/CR-3332), U. S. Nuclear Regulatory Commission, Washington, DC.
 77. Travis, R.J., R.E. Davis, E.J. Grove, M.A. Azarm (1997). A Safety and Regulatory Assessment of Generic BWR and PWR Permanently Shutdown Nuclear Power Plants (NUREG/CR-6451) U. S. Nuclear Regulatory Commission, Washington, DC.

78. Trenberth, Kevin & Olson, Jerry (1988). Evaluation of NMC Global Analyses: 1979-1987 (NCAR Technical Note TN-299+STR) National Center for Atmospheric Research, Boulder, CO. 82 pp.
79. UNSCEAR (1993). "Sources and Effects of Ionizing Radiation". UNSCEAR 1993 Report to the General Assembly (with Scientific Annexes). United Nations Scientific Committee on the Effects of Atomic Radiation, New York.
80. Van Dop, H., R. Addis, G. Fraser, F. Girardi, G. Graziani, Y. Inoue, N. Kelly, W. Klug, A. Kulmala, K. Nodop and J. Pretel (1998). "ETEX: A European tracer experiment; observations, dispersion modelling and emergency response" *Atmospheric Environment* **32**:24(4089-4094)
81. Yamazawa, H., Akiko Furuno, Masamichi Chino (1998). "Evaluation of a Long-range Lagrangian Dispersion Model with ETEX" *Atmospheric Environment* **32**:24(4343-4349)
82. Yu, C. et al. (1993). Manual for Implementing Residual Radioactive Material Guidelines Using RESRAD, Version 5.0 (ANL/EAD/LD-2), Environmental Assessment Division, Argonne National Laboratory, Argonne IL
83. Yu, C. et al. (2000). RESRAD 6.0 for Windows: A computer code for evaluating radioactively contaminated sites, Environmental Assessment Division, Argonne National Laboratory, Argonne IL
84. Zakharkin, B.S. (1995). "Chemical Basis of the Reprocessing of Spent Nuclear Fuel from Naval Reactors at RT-1" p. 174 in Summary of Workshop on Russian Naval Spent Nuclear Fuel and Waste Management. Office of Technology Assessment, Washington, D.C., April 1995. (cited in *Sivintsev 2000a*)